Study of infection induced alteration in *Drosophila* larval feeding behavior

Dissertation

zur

Erlangung des Doktorgrades (Dr. rer. nat.)

der

Mathematisch-Naturwissenschaftlichen Fakultät

der

Rheinischen Friedrich-Wilhelms-Universität Bonn

vorgelegt von

Sandya Surendran

aus

Kannur

Bonn 2018

i

Angefertigt mit Genehmigung der Mathematisch-Naturwissenschaftlichen Fakultät
der Rheinischen Friedrich-Wilhelms-Universität Bonn

1. Gutachter: Prof. Dr. Michael J. Pankratz
2. Gutachter: Dr. Reinhard Bauer

Tag der Promotion: 26.03.2018
Erscheinungsjahr: 2018

Abstract

Decision making ability is a key trait that can increase an organism's chances of survival. The animal has to constantly analyze its environment and modulate ones behavior to navigate through daily routine. This study aims at understanding the alteration of feeding behavior in *Drosophila* larvae when they are given a pathogenic food source. *Pseudomonas entomophila* (*Pe*), a Gram negative bacterium is orally given to the larvae, which in turn activates the larval immune system. Simultaneously, larvae alter its feeding preference and show evasion response. Changes in the gut (bacterial infection) lead to a change in feeding behavior. This modulation in the behavior helps larvae escape an otherwise lethal infection. Evasion response was diminished when hugin neurons were inactivated. Release of hugin neuropeptide is therefore necessary for evasion behavior, in addition to its role in bitter aversion. It was also found out that the internal nutritional state of the larvae has an effect on evasion response. Starved larvae showed a weaker response which is in line with the high hugin neuropeptide content in their soma. Thus peripheral information is integrated in the CNS for the animal to be able to generate a behavior or modulate one. Since generating a behavioral response involves CNS, this behavioral assay could be used a powerful assay to screen molecular messengers that can convey peripheral information to the brain.

Acknowledgement

First I would like to thank Professor Michael J. Pankratz for the opportunity given to me as a PhD student in his lab. He has always been an enthusiastic supervisor who let me work in an independent manner and provided me with insightful discussions whenever I needed them.

I would also like to thank Ingo who was no less than a guide to me, whom I could always run to during a crisis, both in and outside of academia. Same goes for all my fellow lab members Andreas, Sebastian, Philipp, Anton, Torsten and Susanne who were always supportive and provided a healthy working environment. Their suggestions and constructive criticism have helped me a great deal along the way. Special thanks to the two wonderful lab technicians, Tania and Sarah for maintaining the lab space and making sure everything in it works. I would also like to thank Jacqueline who has helped me a lot with the formal procedures during the admission process.

Above all, I thank my parents and my sister for their continuous support and belief in me. I am thankful to my husband Harish for keeping me motivated. Last but not the least; I thank all of my friends in Bonn for keeping me company and helped me get through my PhD days.

Author's Declaration

I, Sandya Surendran, hereby declare to be the sole author of this thesis and that the work has not been submitted for any other degree or professional qualification. I confirm that the work submitted is my own, except for work that was part of a jointly-authored publication, which has been included. Most part of this thesis has been published in Surendran *et al.*, 2017. My contribution and those of the other authors to this work have been explicitly indicated wherever necessary. I confirm that appropriate credit has been given within this thesis where references have been made to the work of others.

Signature   ……………………..   Date   ……………………

Table of Contents

x

1. INTRODUCTION

1.1 Understanding behavior during infection

When host encounter pathogens, there are few defense mechanisms that the host can put forward to limit the damage. It can either avoid, resist or tolerate (Medzhitov *et al.*, 2012; Curtis, 2014). Avoidance works mainly based on sensory cues such as olfactory or visual while resistance and tolerance requires the host's immune system to recognize and start up an immune reaction (Read, Graham and Råberg, 2008). Often one finds that an animal is lethargic, hypothermic, depressed or anorexic during the times of an infection. These behavioral symptoms that are generally observed in infected animals are collectively termed as sickness behavior (SB) or sickness syndrome. Contrary to earlier beliefs, sickness behavior is now understood to be an organized behavioral strategy to fight the infection better rather than just a maladaptive response due to the infection itself (Hart, 1988). These behaviors limit the growth of the pathogen inside the host, prioritizing the behavior, thereby preventing the spread of infection. However SB is often observed in higher animals and primates. It is the pro-inflammatory cytokines produced in the periphery, reaching the brain that results in sickness syndrome (Dantzer, 2001; Dantzer and Kelley, 2007). Nausea is one such commonly seen behavioral response seen in certain animals and humans that allow the body to expulse the ingested toxin (Rubio-Godoy, Aunger and Curtis, 2006). These behavioral responses are usually manifested after the infection has been established. However the biology of sickness behavior is poorly understood mainly because this can be hard to identify as these behaviors could be easily masked by stronger needs like nutrition.

Understanding behavior requires studying the underlying neuronal circuit and the molecular components that work together to generate it. Study of infection behavior sheds light to a whole different aspect of infection and immune system. Infection behavior can in part be just a secondary result due to the activation of immune system or an active choice made by the animal for a better survival.

Studies in mice have shown that pro-inflammatory cytokines that are released during infection when inhibited, blocks the generation of infection behavior (McCusker and Kelley, 2013). In mice, sickness behavior is assessed by their motivation for exploration. An infected or sick rodent would be less motivated to move around and search for food source. Depression is one such behavior observed in humans, that has been shown to be induced by pro-inflammatory cytokines (Dantzer *et al.*, 2008). It is often accompanied by conditions that lead to chronic inflammation. A balance between pro and anti-inflammatory cytokines is therefore very critical.
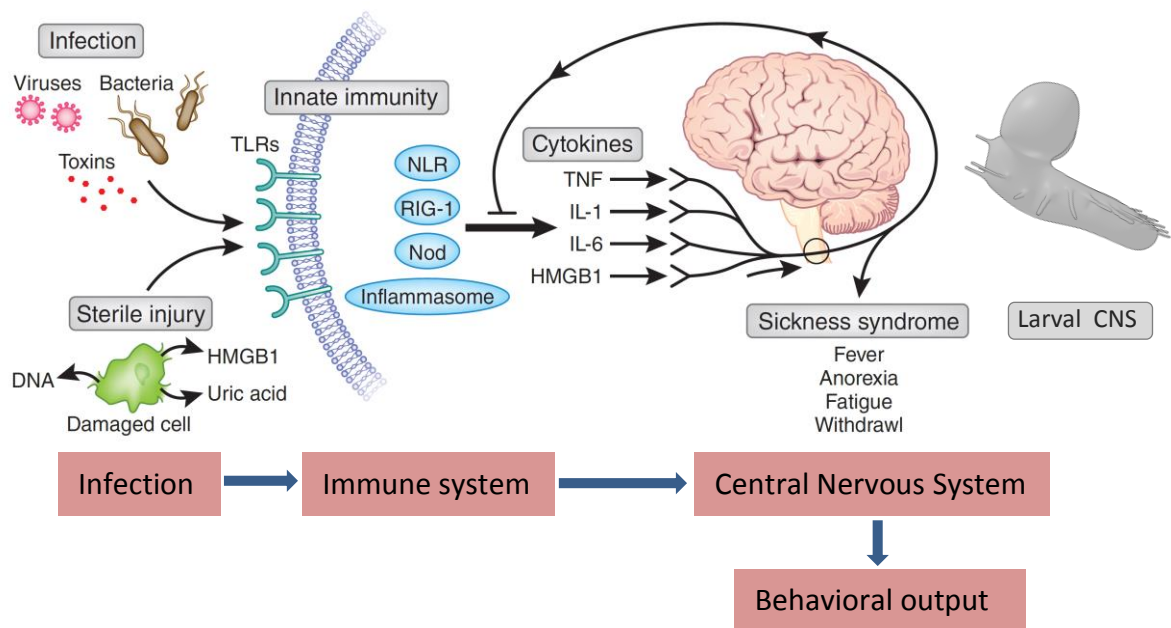
FIGURE 1.1: Sickness behavior or sickness syndrome. Pathogenic molecules or product of cell damage activate receptors of the innate immune system like Toll-like receptors (TLRs) leading to the production of cytokines and interleukins (ILs). These molecules relay the information to the CNS resulting in a set of behavior know as sickness syndrome and at the same time preventing excessive inflammatory reactions. This circuit that starts with an infection shows how activation of the immune system can modify behavior. NLR, Node-like receptor; RIG, retinoid acid inducible gene; Nod, nucleotide oligomerization domain protein; HMBG1, high-mobility group protein B1. Figure modified from (Tracey, 2010)

1.2 Immune – neural connection

Human body contains trillions of micro-organisms that are capable of being pathogenic but instead inhabit our body and help in daily functioning of the host (Lozupone *et al.*, 2013). However under certain change in the conditions, these microbes cause illness and turn deadly to the host (Shreiner, Kao and Young, 2015). This is true for many organisms that have a co-dependent mode of existence. On the other hand, certain micro-organisms start up an infection every time it comes in contact with a host. These pathogenic microbes are mostly identified by the animal's immune system which would then start up a detection and elimination process. The success of every pathogen lies in how effectively it masks itself in the host's environment and dodges every defense attempt executed by the host's multi-layered immune system. In case of higher animals, skin is the first line of defense on the outside and the epithelium when it comes to the gastrointestinal tract (Baganz and Blakely, 2013). Any damage in this physical barrier would signal the cells of the immune system resulting in inflammation and tissue damage. The activation and equally crucial inactivation of the immune system thus needs to be timely and precise. This is at large coordinated by the nervous system of the host that has both direct anatomical and hormonal routes. These neural network keeps a check on the inflammatory responses by activating the inhibitory circuits of the CNS, maintaining the host homeostasis (Sternberg, 2007). Imbalance in this critical relationship can lead to detrimental physiological or even emotional outcome. Studies over the past few decades have clearly shown that immune system play a role in the animal's behavior (Dantzer, 2001; McCusker and Kelley, 2013; Curtis, 2014; Shakhar and Shakhar, 2015). We have all observed how an infection can make us 'feel' sick. We experience fatigue, increased in body temperature, loss of appetite, alteration in sleep pattern, and even mood disorders. Even though it is not clear how several non-related pathogens lead to a similar set of symptoms, these responses help the host to conserve energy and fight the infection better. All of this requires a highly organized control of the information flow from the periphery to the CNS and back.

Information from the periphery can enter the brain/ CNS either directly via the neurons or through diffusible ligands such as cytokines. There are several

examples of neurons that span across one or more organ in the animal, thus allowing a direct flow of information from the periphery. One such example is the vagal nerve in humans which has innervations to the pharynx, stomach, pancreas and gut and that has been shown to be important for inducing fever responses after intraperitoneal IL-1 administration in mice (Watkins LR et al. 1995). A similar circuit has been identified in *Drosophila*, the antennal nerve projection that leaves the brain innervating the feeding apparatus, ring gland and mid gut which may be a functional analog of the vagus nerve (Schoofs, Hückesfeld, Surendran, *et al.*, 2014). Both these neurons innervate the gut which is one of the organs that encounters both pathogenic and non-pathogenic microbes on a routine basis.

1.3 *Drosophila* as a model system to study infection behavior

Studies in *Drosophila* immune system have contributed vastly to our understanding of innate immunity. The core signaling pathways are Toll and Imd that represent the major humoral reaction in *Drosophila* together with the JAK-STAT pathway that help in tissue renewal (Agaisse *et al.*, 2004) during bacterial infection. The end result is the production of anti-microbial peptides (AMPs) which are small cationic peptides that act mainly by damaging microbial cell membrane (Shai, 1999). They have a broad spectrum of activity directed against either Gram positive bacteria (defensin) or fungi (Drosomycin, Metchnikowin) and Gram negative bacteria (Attacin, Cecropin, Drosocin, Diptericin) (Hoffmann and Reichhart, 2002). The genes coding for these peptides have a promotor region similar to mammalian NF-kβ binding site (Kappler *et al.*, 1993). Cellular reactions involve phagocytosis where macrophage-like cells called plasmatocytes and lamellocytes encapsulate the invading microbe (Lanot *et al.*, 2001). These cells are a key part of the invertebrate immune system to defend them from invading pathogen. *Drosophila* comes in contact with a whole lot of microbes on a daily basis due to the nature of their living and feeding habits. Decaying fruits in the wild that are rich in yeast makes a strong attractive source of food for both flies and larvae. Female flies lay their eggs in and around these food sources. *Drosophila* being a holometabolous insect has a larval life and adult life. During

4

the larval phase, the animal spent most of its time feeding as they need a lot of nutrition to increase their body weight. Thus feeding is a strong innate behavior in them.
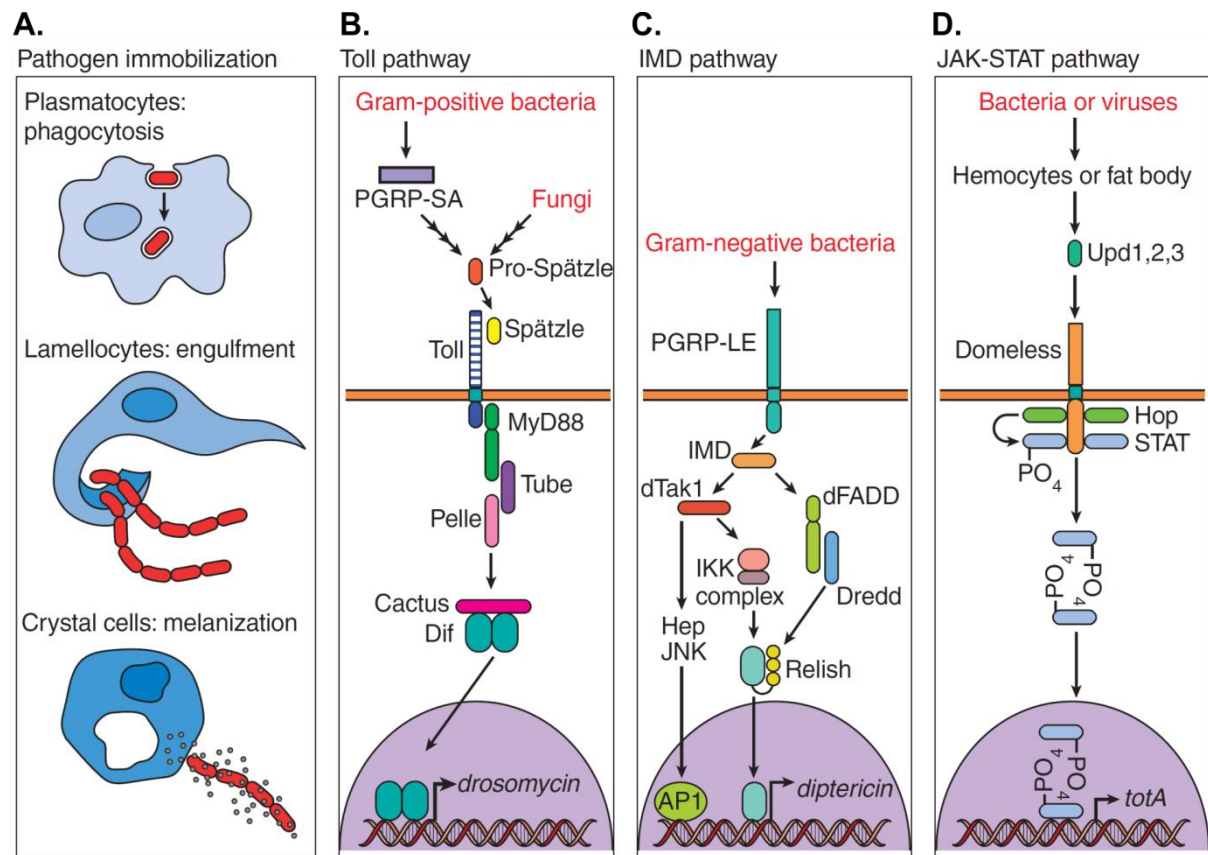
FIGURE 1.2: The above schematic represents different defense pathways seen in *Drosophila melanogaster* during infection. **A.** Plasmatocytes and lamellocytes engulf any foreign body while the crystal cells produce melanin to immobilize pathogen. **B.** Gram positive bacteria and fungi activate Toll pathway recruiting a complex of DEATH-domain proteins (MyD88, Tube, Pelle) which relieves the NF-kβ transcription factor, Dif from its inhibitor Cactus. Dif translocates to the nucleus and subsequently transcribing Toll responsive genes such as drosomycin. **C.** Gram negative bacteria bind to the transmembrane peptidoglycan recognition protein receptor (PGRP) activating the cytoplasmic IMD. IMD now binds to dTak1 and dFADD- Dredd complex activating the caspase activity of Dredd. dTak1 activates IKK complex which now together with Dredd cleaves and phosphorylates Relish. Matured Relish is translocated to the nucleus, leading to IMD responsive gene expression. **D.** Bacteria or viral infection leads to release of cytokines Upd 1,2, 3 which bind to the Domelss receptor activating the fly Janus Kinase (JAK) Hopscotch (Hop). This dimerises the the transcription factor STAT, which then translocates to the nucleus activating transcription of target genes such as totA. Modified from (Bier and Guichard, 2012)

5

Studies in the recent decades have made *Drosophila* a strong model for infection studies. It has been shown that upon damage due to infection or any form of stress, *Drosophila* gut undergo repair and renewal (Buchon *et al.*, 2009; Osman *et al.*, 2012; Zhou *et al.*, 2013). In addition to immune pathways, *Drosophila* gut lumen has special properties that make it hostile to invading microbes; the pH (high acidity), digestive enzymes and peristalsis. The pH of the gut lumen varies throughout the midgut, anterior and posterior midgut ranges from mild to highly alkaline pH whereas the middle midgut is acidic (Shanbhag and Tripathi, 2009). Infection studies in *Drosophila* have been carried out by performing septic injury as most of the microbes do not pose a threat nor activate the immune system upon ingestion. Thus infection studies focused on immune activation mostly circumvented the initial steps of infection that happens in the wild. The identification of few bacteria such as the Gram negative *Pseudomonas entomophila* or *Erwinia carotovora* 15 enabled researchers to orally infect the fly. *Ecc15* ingestion results in activation of the immune system and production of AMP unlike *Pe* which when ingested in high dose is lethal to the animal. However a transcriptome analysis showed both these infections activate expression of stress response genes and epithelial renewal (Vodovar *et al.*, 2005; Buchon *et al.*, 2009). While there are studies focusing on the effect of infection at the cellular level, this study addresses a different aspect of infection. How infection affects the behavior of *Drosophila* larvae. Since feeding and foraging are the two main behaviors seen in these animals, *Drosophila* larvae are ideal to study for change in feeding behavior. *Pe* provides the added advantage of orally infecting the animal opposed to septic injury. Behavioral studies in mice have been shown to be fruitful although it often comes with a certain complexity compared to simpler model such as *Drosophila* larvae. Hence we started out by investigating *Drosophila* larval feeding behavior and screening molecular players underlying the behavior.

1.3.1   The hugin neuropeptide

Drosophila has at least 42 genes that encode precursors of neuropeptide (Nässel and Winther, 2010). Many of them are highly conserved across other insects and

6

a few found even in mammals. The *Drosophila* hugin gene codes for a prepropeptide that is processed into two peptides, one with a structure similar to pyrokinins and the other to ecdysis-triggering hormone (Meng *et al.*, 2002). Hugin is expressed by a set of 20 neurons in the *Drosophila* brain with their cell body in the subesophaegal zone (SEZ). This is the region of the brain that is closely associated with feeding and sensory processing. Each neuron was projected to only one of the four major targets, namely ring gland, protocerebrum, pharynx and ventral nerve cord (VNC) (Melcher, Bader and Pankratz, 2007). Hugin gene was identified in a microarray analysis screen done in klumpfuss (klu) mutants, a zinc finger transcription factor coding gene. Klu mutant larvae showed a block in their food intake behavior and it was found that hugin was upregulated in those mutants (Melcher and Pankratz, 2005).
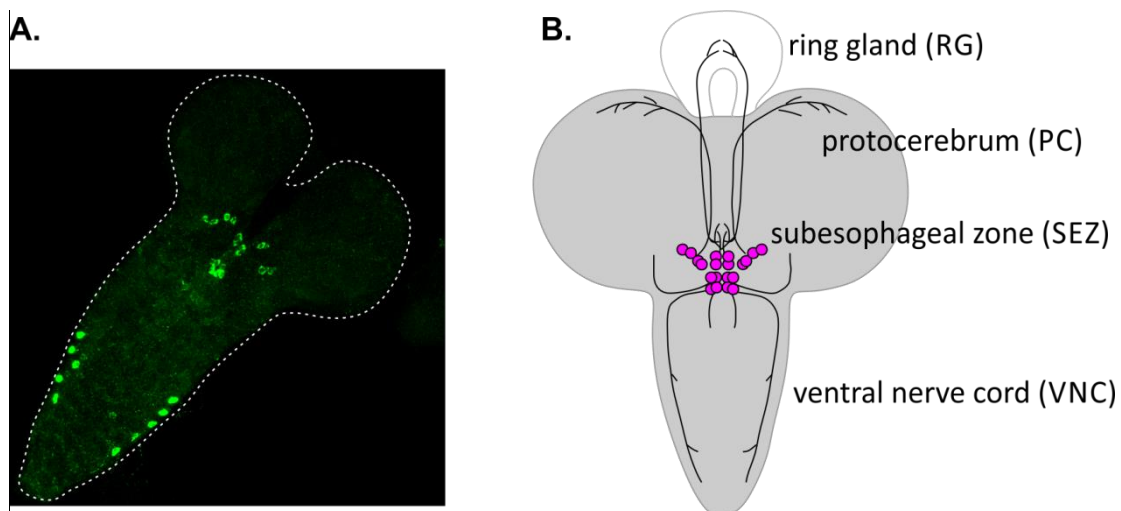
FIGURE 1.3: Hugin neurons in *Drosophila* larval brain. **A.** Larval brain is stained for hugin antibody and it shows a cluster of positive neurons in the subesophaegal zone together with few non-specific binding in the VNC. The cell bodies are represented in green false color. **B.** The image on the right is a schematic representation of a larval brain showing the positioning of the 20 hugin positive cell bodies and their respective neural projections (modified from Schlegel *et al.*, 2016).

Nmu, the mammalian homolog of hugin overexpression leads to hyperactivity in the animals and suppression of sleep. In mice, intra cerebroventricular (ICV) administration of neuromedin U lead to suppression of food intake while increasing gross locomotor activity (Nakazato *et al.*, 2000). It has also been recently shown to be involved in sleep/wake cycle in zebrafish (Chiu *et al.*, 2016). In *Drosophila*, activation of hugin expressing neurons leads to suppression of

feeding behavior in larvae combined with increase in wandering like behavior (Schoofs, Hückesfeld, Schlegel, *et al.*, 2014). These hugin interneurons were later shown to be important for conveying bitter taste to the larval brain resulting in bitter avoidance behavior (Hückesfeld, Peters and Pankratz, 2016). Latest work from the lab has worked on the complete reconstruction of the hugin neurons based on EM data (Schlegel *et al.*, 2016). The study also showed that hugin neurons have acetylcholine expressed in few of them and the effect on food intake and pharyngeal pumping requires both hugin and acetylcholine.

1.4   Aim of the study

This study looks into the feeding behavior of *Drosophila* larvae when they are given an infectious source of food. *Drosophila* larvae is known to be aversive towards bitter food source (L. Weiss, A. Dahanukar, 2011; Hückesfeld, Peters and Pankratz, 2016) and the neuropeptide hugin has been shown to be involved. This thesis mainly focuses on the alteration in larval feeding preference during an infection and the role of hugin in it. Hugin/ neuromedin U manipulation is known to be involved in affecting food intake and this study provides a biological context where such hugin dependent aversion would be important in the wild. The study also tries to find new neuropeptide/ neurotransmitter candidates that change their expression during infection leading to alteration in their feeding preference.

2.MATERIALS

2.1. Fly strains

All the flies listed were raised on standard fly food, kept at $25^{o}C$ or $18^{o}C$ with air humidity between 50% and 60% under 12h light and dark cycles.

Genotype	Fly names	Source
Oregon-R	Org-R	Bloom #4269
y^1 cv^1 $fs(1)M13^1$ v^1 f^1/FM0	W^{1118}	Bloom #4605
Rel^{E20}	Relish E20	Bloom #55714
w* ;; TPH-Gal4	TPH-Gal4	J. Chung
w* ;TRH-Gal4;	TRH-Gal4	S. Birman
w[*]; P{w[+mC]=Hug-GAL4.S3}3	HugS3- Gal4	Bloom #58769
w[*]; P{w[+mC]=UAS-Hsap\KCNJ2.EGFP}7	UAS-Kir2.1	Bloom #6595
UAS-rpr;; UAS-hid	UAS-rpr;; UAS-hid	S. Buch
w[*]; UAS-lacZ RNAi	UAS-lacZ RNAi	M. Jünger
w[*]; UAS-hugin RNAi	UAS-hugin RNAi	A. Schoofs
w[*] upd3[Delta]	w* $upd3^{\Delta}$	Bloom #55728
w[*] upd2[Delta]	w* $upd2^{\Delta}$	Bloom #55727
w[*] upd2[Delta] upd3[Delta]	w* $upd2^{\Delta}$ $upd3^{\Delta}$	Bloom #55729
w[*]; Upd3-Gal4, UAS-GFP	Upd3-Gal4, UAS-GFP	K. Woodcock
W; P (UAS-dome ΔCYT);+	UAS dome ΔCYT	J. Hombria
Domelss-Gal4;+;+	Domeless-Gal4	S. Noselli
W;;ilp2-Gal4	Dilp2-Gal4	EJ. Rulifson

2.2. Microorganisms

Name	Abbreviation	Source
Pseudomonas entomophila	*Pe*	Lemaitre lab
pvf P. entomophila	*pvf Pe*	Lemaitre lab
gacA P.entomophila	*gacA Pe*	Lemaitre lab
Erwinia carotovora 15	*Ecc15*	Lemaitre lab

2.3. Buffers and Media

Name	Composition
Standard fly food	13.3l H_2O, 330g beer yeast, 815g corn flour, 80g filamentous agar, 1l sugar beet syrup, 20g nipagin solved in 0.2 100% EtOH
Apple juice agar plates	8.5g agar, 100ml apple juice, 10g sucrose, 300ml VE-H_2O
PBS Phosphate buffered saline (10x)	2g KCL, 2g KH_2PO_4, 11.5g Na_2HPO_4, 80g NaCl, topped off with ddH2O to 1l. pH 7.4
PBT	0,1% or 0,5% Triton X-100 in 1X PBS
TAE buffer	40 mM Tris acetate (pH 8.0), 1mM EDTA
Agarose gel	1% agarose in 1x TAE
Yeast paste	42g live yeast, 7ml H2O
LB medium with rifampicin	10g LB in 400 ml VE-water, autoclaved and add 100µg/ml rifampicin

LB agar with rifampicin	10g LB, 8g agar in 400ml VE-water, autoclaved and add 100µg/ml rifampicin
Mowiol	12ml glycerine, 9.6g Mowiol 40-88, 24ml H_2O, 48ml 0.2M TrisHCl. pH 8,5

2.4.   Standard kits and reagents

Name	Manufacturer
Precellys Keramik-Kit 1,4 mm	Peqlab
DNA/RNA/protein purification reagent, peqGOLD TriFast	Peqlab
QuantiTect Reverse Transcription Kit	Qiagen
Taq-Polymerase, $MgCl_2$, Reaction Buffer	Bioline, Mango Taq DNA Polymerase, BIO-21078
2x SYBR-Green PCR-Mix	BioRad
SybrSafe	Invitrogen
Chloroform	Carl Roth, Karlsruhe
Isopropanol	Carl Roth, Karlsruhe
Ethanol	Carl Roth, Karlsruhe
Formaldehyde (37%)	Carl Roth, Karlsruhe
Triton X	Carl Roth, Karlsruhe
Agar-agar	Carl Roth, Karlsruhe

2.5. Real time PCR primers

Gene	Sequence
Allatostatin A (AstA)	F1_AGGACAACGAGATCGACTACAG
	R1_AGGCCAAAGTTGAAGGGTTG
Allatostatin B or Myoinhibiting peptide precursor (Mip)	F2_CTGTACGGCAACAATAAGCG
	R2_TTACCAGCGGAACAAAGTGG
Allatostatin C (Ast- C)	F1_TATTTGAGGAGTCCCACCTACG
	R1_AAAGTAGCACTGCCGGTATC
CCHamide1	F1_TGGTGGAGCAACTGTACAAC
	R1_TTCTGTTGCTGTCGTCATCG
CCHamide2	F1_TGATGGCGCCAAATGAACAG
	R1_GCGAGGTCGGTTAAACCATG
Choline acetyltransferase (ChAT)	Fwd-TTCCGGAAATCGCTGGTTTG
	Rev-TGGACAACAGCAATGCCTTC
Corazonin (Crz)	F_ACGGCAAGAGGTCCTTTAAC
	R_TGCTCCAATCCTGCAAATCG
Diuretic hormone 44 (Dh44)	F2_TCCCAAAGCAGTTGCAGTTG
	R2_TTGCCATCGTCGTTCTCATG
Diuretic hormone 31 (Dh31)	F1_TGGCTATAACGAACTGGAGGAG
	R1_AAAGTCCACGGTTCGTTT GG
Drosomycin (Drs)	ACCAAGCTCCGTGAGAACCTT
	TTGTATCTTCCGGACAGGCAG
Diptericin (Dpt)	AAAGTGGGAAGCACCTACAC

	GCTAGACTCGGATACCAATCG
Insulin-like peptide 2 (ilp)	F_CTGAGTATGGTGTGCGAGGA
	R_GCGGTTCCGATATCGAGTTA
Insulin-like peptide 3 (ilp3)	F_ACCCCGTGAACTTCAATCAG
	R_CGTCGAGTCTTGAGCATCTG
Myosuppressin (Ms)	F1_ACATCAACAACGAGGCATCC
	R1_TTTCCGAAACGCAGGAAGAC
Hugin (Hug)	F_CTACATCCTTGTTTGCAGTC
	R_GATAATGATCCTCTGGCAGAG
Limostatin (Lst)	F2_AACGATGACGACGACAATGG
	R2_TTGAACTGATTGGGCGTCTC
neuropeptide F (NPF)	Fwd-ATCGCTGATGGATATCCTGAGG
	Rev-AAACCGCGAGCAAATTCTCC
Painless (pain)	F2_AACGGAGCCATTTGCAGAAC
	R2_TCAAACGTTGGCAGATGCTG
Ribosomal protein L32 (RpL32)	F_GCTAAGCTGTCGCACAAATG
	R_GTTCGATCCGTAACCGATGT
short neuropeptide F precursor (sNPF)	F1_ TCAGTTCGAGGCAAACAACG
	R1_ TCCGGAATTTCGTACTGCTG
Tryptophan hydroxylase (Trh)	F_GGTGGTGGTCAGGATAATGG
	R_TGGTTACGCAGGGTGAAAAT
pale (ple)	F2-AGCCCGATTTGGACATGAAC
	R2-ATGCGATCTCGGCAATTTCC
upd1	F1_TTCAGCTCAGCATCCCAATC

	R1_AGTTGCTGTTCCGCTTTCTG
upd2	F1_ACCTCGAAAACTTGCGGAAC
	R1_TTCGGCAGGAACTTGTACTC
upd3	F1_ATTGAATGCCAGCAGTACGC
	R1_TCCTTTGGCGTTTCTTGCAG

2.6. Antibodies

Name	Host	Source
α-fitc-GFP	Goat	Abcam
α-hugin	Rabbit	Pankrtaz lab
α-Dilp2	Mouse	Pankrtaz lab
α-repo	Mouse	DSHB
α-prospero	Mouse	DSHB
α-Alexa Fluor 488	Rabbit	Thermofisher
α-Alexa Fluor 633	Mouse	Thermofisher

2.7. Consumables

Name	Source
Pipette tips w/ and w/o filter	Corning, NY
Cover slides	Carl Roth, Karlsruhe

Cell sieve	VWR International, Darmstadt
Glass slides	Carl Roth, Karlsruhe
Lab dishes	Schott, Mainz
Plastic vials	Greiner
1.5/ 2ml tubes	Eppendorf
Syringe disposable	Braun
PCR reaction tubes	

2.8. Devices

Name & Model	Manufacturer
Binocular, Stemi 2000	Carl Zeiss, Jena
Cold light source, CL 1500	Zeiss, Jena
Confocal microscope, LSM 780	Zeiss, Jena
Forceps	Fine Science Tools, Heidelberg
Pipettes 10/ 20/ 200/ 1000 µl	Gilson, Inc., USA

2.9. Softwares

All the immunostaining images were analysed and modified using Fiji/ ImageJ software. Graphs were plotted using GraphPad Prism6 and CorelDraw.

Evasion assays images were captured using iSpy.

3. METHODS

3.1.   Fly caretaking and egg collection

Flies were raised at 25°C in vials containing standard fly food. For setting up crosses, one week old flies were used. Virgin female were crossed to male flies in the ratio 3:1. The crosses were set in collection cages to enable age synchronised egg lay. Apple juice agar plates with a drop of yeast paste in the middle were used for egg collection. Typically 4 hours of egg collection was done to make sure enough larvae for the experiments. After the egg collection, the plates were kept in the 25°C incubator for 24 hours to hatch. Animals were left in the incubator till they reached the appropriate age for the experiment.

Once the required age was reached, larvae were collected using a brush and washed thoroughly using tap water to remove any food particles sticking onto its body. These larvae are now ready to be used for the experiments.

3.2.   Evasion assay

The assay was developed and established by a previous Masters student in the lab (Wäschle, 2014).

Preparation of bacterial culture: Bacterial cultures stored as glycerol stocks in -80°C freezers were first plated on to LB rifampicin plates. These LB plates also had 2% of milk powder mixed into it to also allow the selection of bacteria based on the presence of clearance zone around the colony. These plates were streaked with the required bacterial strain and kept at 29°C for at least 30 hours for the colonies to develop. Single colony was picked up using a pipette tip and dropped into a vial containing 4ml of LB rifampicin medium. This was then kept at 29°C, 250 rpm for 18 hours. The overnight culture was taken and OD600 measured. An OD of 10 was selected for the evasion assays. OD of the culture was also adjusted using 1x PBS if needed. A part of this culture was kept at 95°C for 10 minutes, followed by a cold

shock at -20°C for 5 minutes. This would kill the bacteria and was used as the dead bacteria/ heat killed bacteria food source.

Setting up the assay: Once the bacterial suspensions were ready, 350 µl of the appropriate suspension was mixed with 2g yeast to use as the food source for the evasion assays. Yeast mixed with 1x PBS was kept as the control food source. These food sources were filled into a syringe, which were later used to deposit the content onto apple agar plates. The plates were labelled appropriately as follows; yeast (PBS control)/ dead bacteria (yeast + heat-killed bacteria) and live bacteria (yeast + infectious bacteria). 50 first instar larvae (28±2 hours AEL) that were washed thoroughly were transferred onto each of these plates using a brush. The plates were then kept open inside the experiment chamber. The chamber was attached to a camera set up that took picture every half an hour for 12 hours, capturing the larval position at every half hour time point. iSpy software was used to take the images and ImageJ for analysis. For the analysis the number of larvae that were outside the food source was counted. This numbers were then used to plot a graph over time to analyse the trend of the behavior.

3.3 Isolation of whole RNA from larvae

For the RNA isolation from the whole larvae, 25 – 30 first instar larvae were picked after thorough washing. They were put in disposable polypropylene tubes containing glass beads and 700 µl of TriFast RNA/ DNA isolation solution was added. Homogenisation was done using a Precellys 24 homogeniser, 5500 rpm, 3 x 10 sec, 20 sec break. This homogenate was then kept at room temperature for 5 minutes followed by addition of 140 µl chloroform. This mixture was then shaken vigorously for 15 sec and then kept at room temperature for 3 minutes, after which it was centrifuged at 12000 g for 5 minutes at 4°C for phase separation. 350 µl of the upper aqueous phase was transferred to a 1.5 ml Eppendorf tube. To this an equal amount of ispropanol was added and vortexed. The tubes were then kept at -20°C for at least 10 minutes (or longer), followed by centrifugation at 12000 g for 10 minutes at 4°C. This would precipitate the RNA allowing removal of the supernatant. The pellet was then washed in 70% ethanol by spinning it again at 12000 g for 10 minutes at 4°C.

The supernatant was discarded carefully leaving the pellet intact. Depending on the pellet size, appropriate amount of RNase free water was used to dissolve it. The samples were kept on ice and taken to the nanodrop for concentration measurements.

3.4 cDNA synthesis

After measuring the RNA concentration per ml, the amount of sample that would make 500ng of the template RNA was calculated. In the meantime Quantiscript Reverse Transcription kit was left to thaw on ice. Each of the solution was vortexed and centrifuged to collect the liquid from the sides of the tubes. In a PCR tube, 500 ng of the RNA sample was taken and 1 µl of wipeout buffer added to eliminate genomic DNA. This was topped off with RNase free water to make it 7 µl, mixed well. This mixture was the incubated at $42^{o}C$ for 2 minutes and then immediately places on ice to stop the reaction. 2 μl Quantiscript RT Buffer, 0.5 μl RT Primer Mix and 0.5 μl Quantiscript Reverse Transcriptase was then added to each sample. If there were several reaction tubes, a master mix with a 10% higher volume was prepared and the distributed across the tubes containing the samples. The tubes were mixed well and stored on ice. Finally the tubes were incubated again at $42^{0}C$ for 20 minutes followed by $95^{o}C$ for 5 minutes to inactivate the reverse transcriptase enzyme. cDNA synthesized was then diluted 10 times using dd H2O.

To ensure the success of cDNA synthesis, reverse transcriptase PCR was also performed using actin primers. A master mix was prepared as follows:

Components	Volume (µl)	Final Concentration
Primer Mix (20 pM)	1,25	1 pM
dNTPs (10 mM)	0,5	0,2 mM
5x Reaction Buffer	5	1x
MgCl$_2$ (50 mM)	0,75	1,5 mM
Taq-Polymerase 5u/µl	0,25	0,625 u

H$_2$O ad 20	12,25	

20 µl of the master mix was transferred to 5 µl of the sample in a PCR reaction tube, mixed well and placed in a PCR cycler.

STEP	TEMPERATURE	TIME	
Initial Denaturation	95°C	5 min	
Denaturation	95°C	30 sec	
Annealing	56°C	30 sec	21 cycles
Extension (1 min/kb)	72°C	30 sec	
Final Extension	72°C	5 min	

The PCR product had to be loaded onto an agarose gel for electrophoresis. The gel was made in 1x TAE buffer. The Sybrsafe dye which is a less hazardous alternative for ethidium bromide was added to the agarose gel before it solidified. The samples were loaded and ran at 130 mV for 10 minutes and viewed under UV light for actin bands.
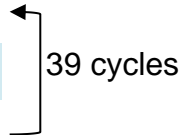
3.5 Quantitative Polymerase Chain Reaction (qPCR)

After successfully completing cDNA synthesis, the samples were taken for qPCR. A well clean 96 well plate was used to fill in the samples. Before pipetting out the reaction mixtures, 2 separate master mixes were prepared. One had the primer (1:4 dilution) and the other the cDNA samples. RpL32 was the reference gene used throughout and each sample was done in triplicate. Water controls for each primer was also included to look out for primer dimers.

Primer-Master Mix (1,1x)		cDNA-Master Mix (+1)	
SYBR-Green PCR-Mix	7,5 µl	cDNA	2 µl
Primer Mix	0,75 µl	ddH$_2$O	4,75 µl

After carefully pipetting out the master mixes, the plates were sealed with optical seal, and mixed by centrifuging at 4000g for 2 minutes. The plate was then placed into the qPCR machine; the right program was selected and allowed to run.

STEP	TEMPERATURE	TIME	
Activation	95°C	10 min	
Denaturation	95°C	10 sec	
Annealing	60°C	10 sec	39 cycles
Elongation	72°C	30 sec	

After the run was completed, the analysis was done using BioRad CFX Manager. The data was represented as log values.

3.6   Immunostaining

Larval brains or gut were carefully dissected in 1x PBS, transferred to Eppendorf tubes and stored on ice until all the animals were done. Then the brains were fixed in 4% para-formaldehyde solution for 20 minutes at room temperature on the rotating wheel. All the steps from now on were performed on the rotating wheel. The brains were washed with 0.5% PBT, 3 times, 20 minutes per wash. Followed by the washing steps, the samples were blocked using 5% normal goat serum (in 0.5% PBT) for 1 hour at room temperature. Primary antibodies were then added at appropriate dilutions. The antibody dilutions were made in 5% goat serum solution. After addition of the primary antibodies, the samples are stored at 4$^\text{o}$C for overnight incubation. On the second day, the antibodies added were removed and the samples washed using 0.1% PBT, 3 times, 20 minutes per wash. Following the wash, the samples are ready to add the secondary antibodies. Proper dilutions of the fluorophores were prepared and added to the brain samples. The tubes were then kept back at 4$^\text{o}$C for another overnight incubation. Finally on the third day, the antibodies were again removed and the samples washed with 0.1% PBT, 3 times, 20 minutes each. If required, before the final wash DAPI was applied in 1:1000 dilutions for 5 minutes. The samples were then mounted using mowiol on a glass slide.

3.7 Statistics

All the standard error bars represent standard error of the mean (SEM). Statistical significance was tested using GraphPad Prism6.

XY plot represents mean ± SEM values. Box plot was drawn by calculating the median, 25% percentile and 75% percentile. Whiskers represent the data range i.e., the minimum and the maximum value. Mann-Whitney Rank Sum test was used to compare the significance of the box plots. All the experiments were repeated at least 3 times independently.

For the qPCR assays, primer efficiencies were tested and verified. qPCR results were confirmed with 3 biological repeats. Significance was tested using t-test.

Asterisks indicate a p value of less than 0.05 (*), 0.01 (**) or 0.001 (***).

4. RESULTS

4.1. Developing *Drosophila* larval evasion assay

Drosophila larvae are continuous feeders, which makes it difficult to establish an assay to study food avoidance behavior. The strong innate liking for feeding overrides most of the aversive cues they confront. In the wild they feed on rotting fruits that are filled with microbes and mostly yeast. They are constantly being exposed to a wide range of pathogens on a daily basis. It is thus very important for their survival to distinguish between non-pathogenic and pathogenic ones. *Pseudomonas entomophila* is an entomopathogenic Gram negative bacterium that is lethal to both larvae and adult flies if used in high doses. Unlike other microbes used in the field so far, *Pe* can activate the *Drosophila* immune system when taken orally which was an advantage for establishing food avoidance/evasion assay.

An overnight culture of *Pe* was thus mixed with yeast and given to wild type Org-R larvae to feed. Appropriate controls were also done in parallel. Images taken during the 12 hours monitoring period were projected over time. The images show that larvae on the control yeast plate and heat-killed *Pe* plate have spent almost the entire period in or around the food source. On the other hand, larvae have moved out of the food source away from *Pe* infected yeast in the experimental plate. Fig 1B shows the behavior over time. The shape of the graph tells you how the behavior developed slowly and gradually. Up to 2 hour, larvae continue to feed in spite of *Pe* in the food. The behavior starts between 2.5 hours to 3 hours. By the end of 12 hours almost 80% of larvae have evaded the only pathogenic food source. The same data has been represented as a box plot in Fig 1C where each box represents 7 data points from 6 hours to 9 hours. The two control plates are comparable where almost all the larvae spend the entire time in the food source. On the other hand, the *Pe* plate has a significant percent of larvae moving out of the food source. Even though the immediate blockage of food uptake after high dose of *Pe* ingestion was previously reported (Vodovar et al, 2005), this is the first study that documents an active pathogen avoidance/ evasion behavior in *Drosophila* larvae (Wäschle, 2014).
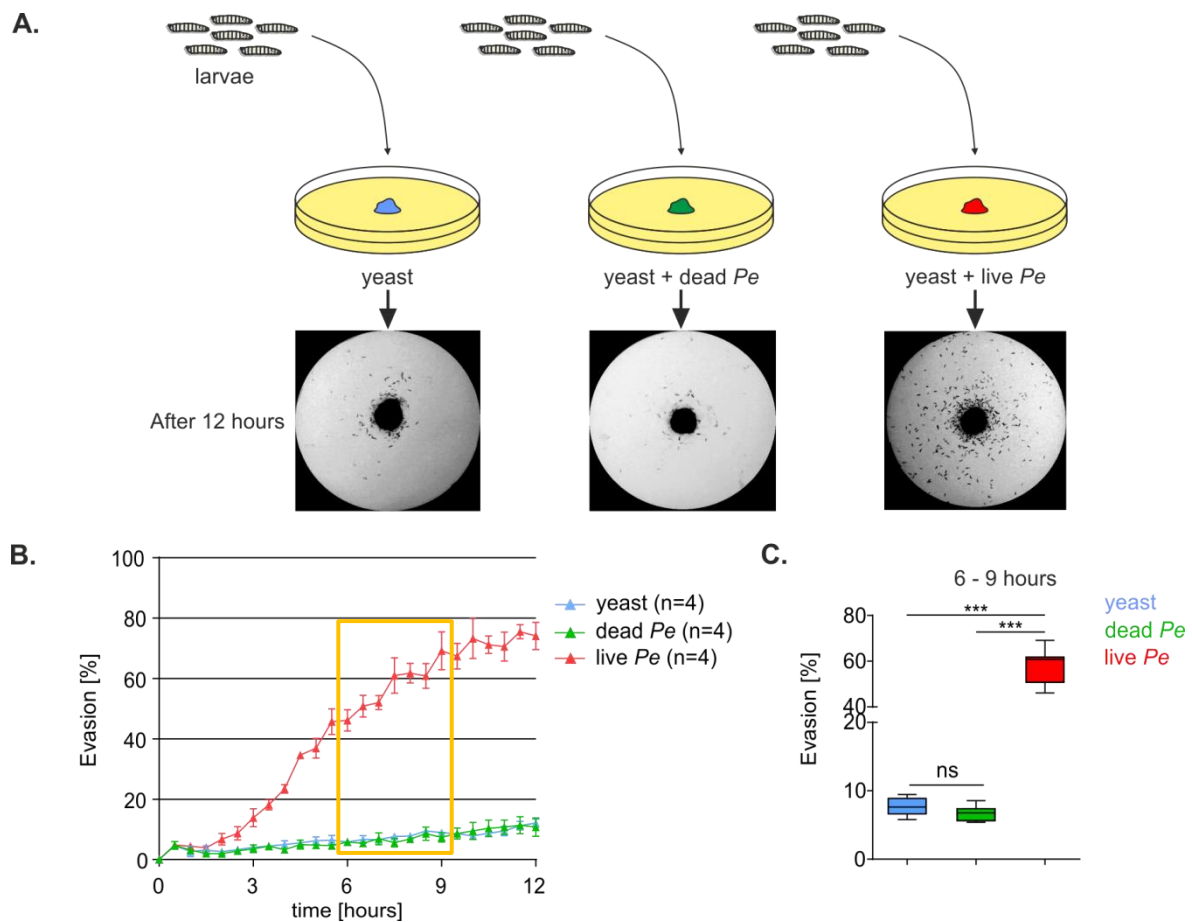
FIGURE 4.1: Evasion assay. **A.** Schematic representation of the behavioral assay. **B.** Evasion percentage plotted over time on Y axis. Larvae fed on yeast (n=4) and yeast+ dead *Pe* (n=4) do not move out while larvae on yeast + live *Pe* (n=4) does. See Table S1 for mean and SEM values. **C.** Box plot representing the cumulative data set between 6 hour to 9 hour time points as shown inside the rectangle in Fig 1B. Mann-Whitney-Rank-Sum test shows a significant difference. N=7. ***p ≤ 0.001. See Table S2 for the median and whisker values.

Next we wanted to check few *Pe* mutants that are known to have a compromised virulence. The pathogenicity of *Pe* is associated with several genes and so is multifactorial (Lemaitre, 2015). The *GacS/ GacA* two component system is the most critical component of them all. The *GacA* mutant is known to be completely avirulent to *Drosophila*. Then there is *pvf Pe* mutant that has an impaired virulence due to the 4 missing genes (*pvf*A, *pvf*B, *pvf*C and *pvf*D) together termed *Pseudomonas* virulence factors (*pvf*) (Lemaitre, 2015). This mutation makes the strain less persistent in the gut. The evasion assay was performed using these two mutant *Pe* strains and the wild type *Pe* in parallel. Fig 4.2 shows the behavioral response of larvae towards all the different *Pe* strains over time. Larvae showed evasion in the *Pe*

plate as expected while larvae stayed in the food in the control plate. The larvae were even more attracted to *gacA* containing yeast more than control food, which might be due to the non-virulent bacterial membrane. *pvf Pe* plate showed little evasion toward the end of the assay which fits well with its reduced pathogenicity.
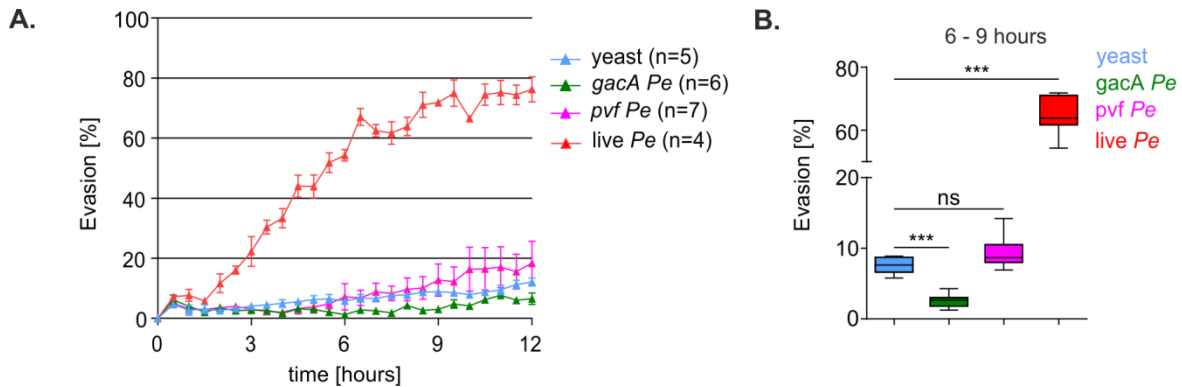
FIGURE 4.2: *Drosophila* larvae can differentiate between infectious and non- infectious food sources. **A**. Wild type *Pe* (red)(n=4) induces evasion behaviour while mutant *gacA Pe* (green)(n=6) and *pvf Pe* (magenta)(n=7) induced no significant change in behavior. See Tablbe S3 for mean ± SEM values. **B**. Box plot shows a significant evasion percentage only for *Pe* plate and not for *pvf Pe* when compared to the yeast control while there is a higher preference for *gacA Pe* containing food source. n=7. Mann-Whitney-Rank-Sum test shows a significant difference. ***p ≤ 0.001. See Table S4.

The evasion experiments were performed using first instar larvae. However, to test if the behavior was robust across later larval stages, second instar (L2) larvae were also tested. When second instar larvae were given food source containing Pe, OD_{600} 10 the larvae showed a comparatively weak evasion behavior (Fig 4.3). This could be due to the concentration of Pe in the food which might be too low for L2 larvae. Hence an OD_{600} of 130 was used and evasion assay was performed with a dead Pe control. L2 larvae showed a stronger evasion response comparable to earlier results with 1st instar.
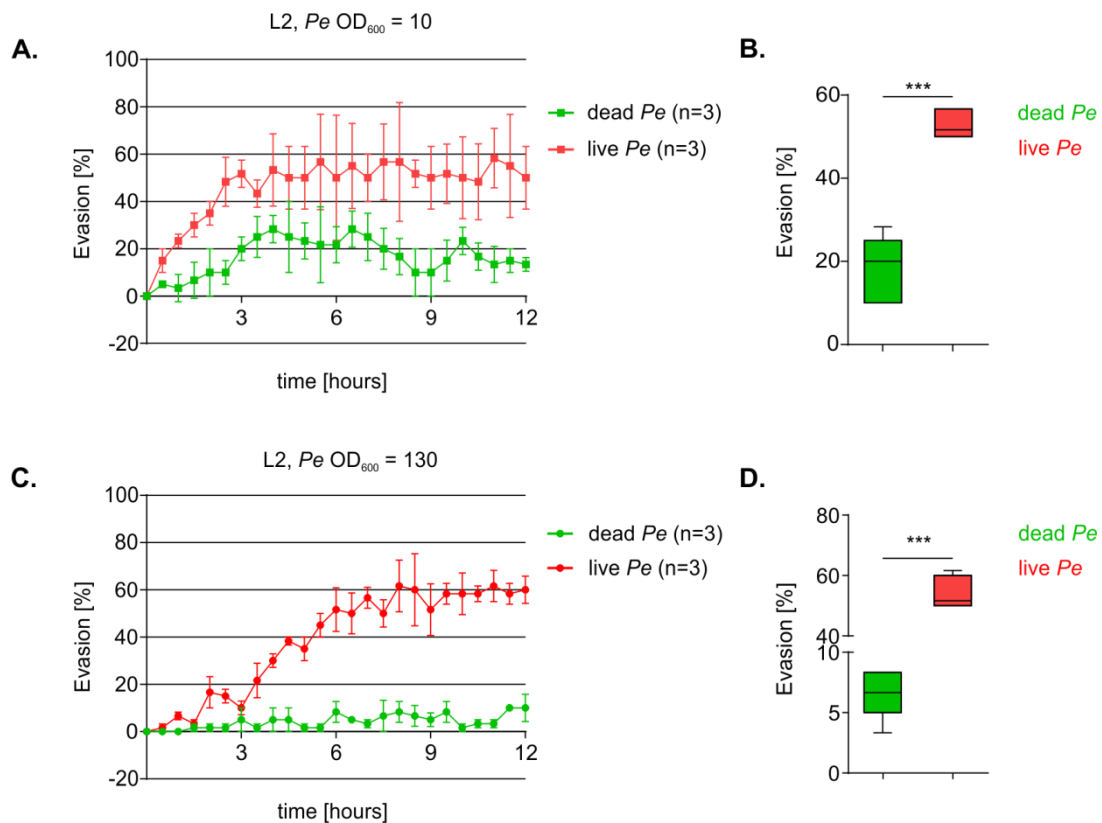
FIGURE 4.3: Evasion behavior in second instar larvae. **A.** The curve shows percentage of evasion over time with *Pe* of OD_{600} 10. As shown by the curves larvae tend to move away from the yeast containing infectious *Pe* more than yeast mixed with dead *Pe*. See table S5 for mean and SEM values. **B.** Box plots were generated using data points between 6 to 9 hours. Mann-Whitney-Rank-Sum test shows a significant difference. p value 0.0006. ***p $\leq$ 0.001. Also see Table S6. **C.** The curve shows evasion percentage of L2 larvae when tested using *Pe* of OD_{600} 130. See Fig S7 for mean $\pm$ SEM values. **D.** Box plots shows significant difference between yeast mixed with dead *Pe* fed larvae and yeast mixed with live *Pe* fed larvae. Mann-Whitney-Rank-Sum test shows a significant difference. ***p $\leq$ 0.001. See Table S8 for data points.

As mentioned already, *Pe* is a virulent bacterium that can naturally infect *Drosophila* without physical injury, unlike several other bacterial strains used for infection studies in *Drosophila*. To study if the evasion response is linked to the high virulence of *Pe*, we decided to test a second bacterial strain *Erwinia caratovora caratovora 15* (*Ecc15*) which can also naturally infect *Drosophila* and induce an AMP production but unlike *Pe*, *Ecc15* do not affect the larval viability (Basset et al. 2000). Thus evasion assay was performed as described before, with *Ecc15* (Fig 4.4). Interestingly,

infectious *Ecc15* could not induce an evasion response in larvae unlike *Pe* which suggests that the high virulence of *Pe* is a deciding factor for the alteration in larval feeding behavior.
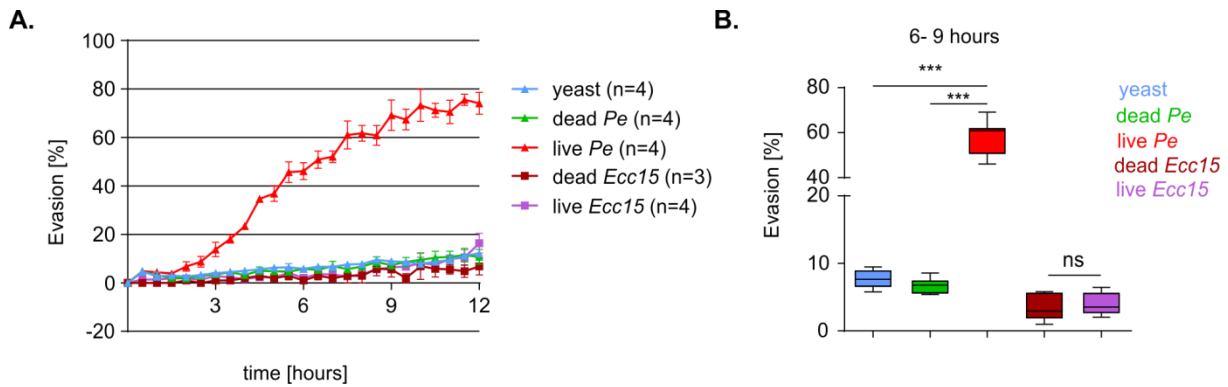
FIGURE 4.4: Non-pathogenic *Ecc15* do not affect larval feeding preference. **A.** *Drosophila* larvae do not show an evasion response to the non-virulent *Ecc15*. Neither dead *Ecc15* nor live *Ecc15* induced any evasion response in larvae. See table S9 for mean and SEM values **B.** Box plot showing the evasion percentage of *Ecc15* plates as compared to *Pe* plates. Mann-Whitney-Rank-Sum test don not shows any significant difference between the evasion percentages of dead and live *Ecc15* plates. n=7. ***p ≤ 0.001. See Table S10

4.2. Relish dependent anti-microbial peptide induction is not necessary for evasion behavior.

Drosophila is an invertebrate model organism that solely depends on innate immune system for its survival. There are two main immune pathways in *Drosophila* responsible for mounting anti-microbial peptide (AMP) production (De Gregorio *et al.*, 2002), the Toll pathway and the Imd pathway. Toll is responsive to fungal and Gram positive bacteria while Imd pathway is activated by Gram negative bacterial infection. To confirm the pathogenicity of the *Pe* strains that we had used for the assay or the absence of it, we performed real time PCR (qPCR) analysis and measured the level of AMPs produced in larvae after 6h of infection (Fig 4.5 A). Three AMPs were tested, *diptericin* (*Dpt*) a Gram negative specific AMP, *defensing* (*Def*) which is a

Gram positive specific peptide and *drosomycin (Drs),* an antifungal peptide. Only larvae infected with the wild type *Pe* showed a specific upregulation in *Dpt* mRNA level while larvae infected with *pvf Pe and gacA Pe* did not. Thus we understand that establishing an infection is important for generating evasion response.
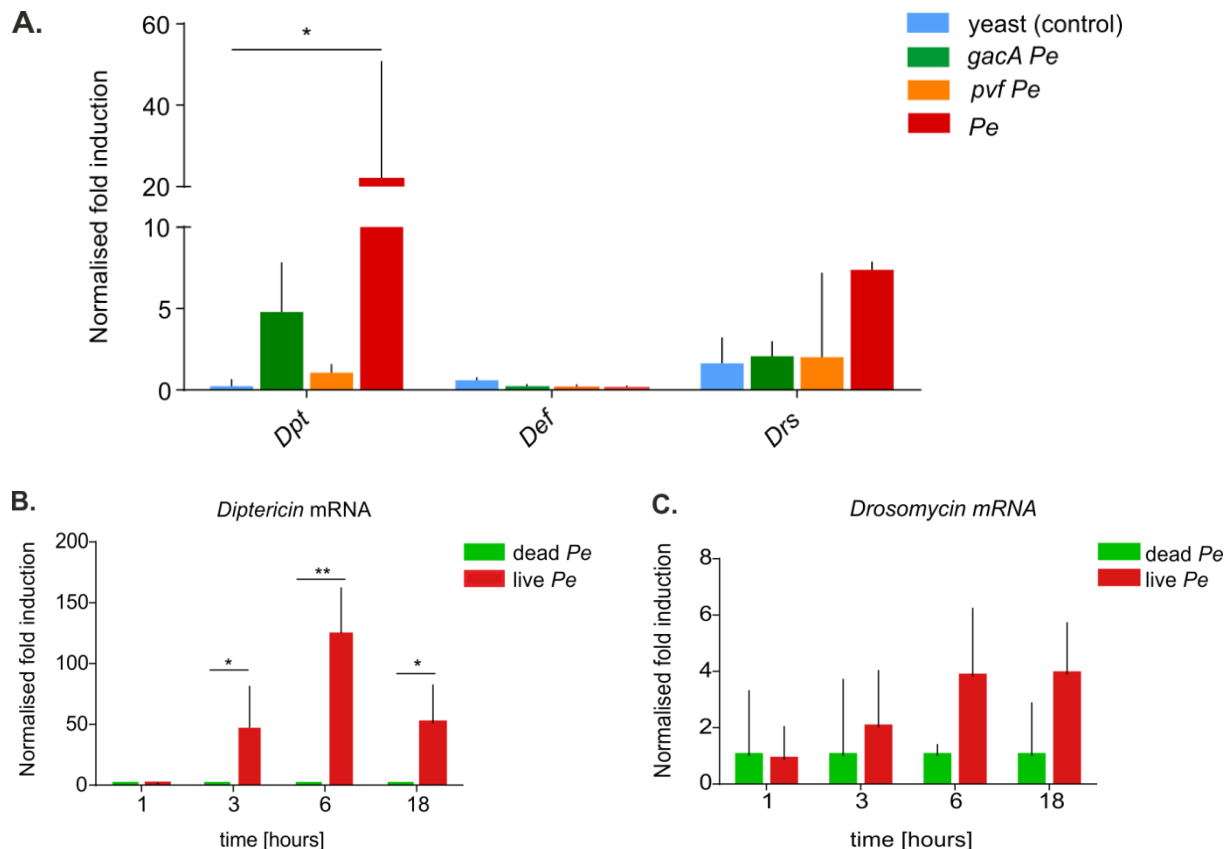
FIGURE 4.5: *Pe* infection specifically activates Imd pathway mediated AMP response. **A.** Real time PCR data shows significant *Dpt* induction only in the case of wild type *Pe* infection. Diptericin (*Dpt*), Defensin (*Def*), Drosomycin (*Drs*). n=3. Significance was tested using Unpaired t-test. *p< 0.05. **B.** qPCR data showing the kinetics of *Dpt* mRNA induction over different time points. n=3 repeats. *p< 0.05, **p< 0.01. **C**. qPCR data for *Drs* mRNA over 1h, 3h, 6h and 18h infection. Green bar represents fold induction in larvae fed on dead *Pe* and red represents larvae fed on live Pe. Significance was tested using unpaired t test. *p< 0.05, **p< 0.01. n=3 for each time point. See Tables S11 - S13 for mean and SEM values for each graph.

To understand the kinetics of immune activation during *Pe* infection, we performed qPCR of infected larvae and measured the level of anti-microbial peptides (AMPs)

mRNA over different time points of infection. The first peak of a significant AMP induction appeared only from 3h post infection. *Dpt* started showing an increase in its fold change mRNA level from 3h, continued to go up at 6h and subdued by 18 hours (Fig 4.5 B). On the other hand *Drs* mRNA which is an anti-fungal AMP did not show any change in its mRNA level at any time points tested (Fig 4.5 C).

The specific AMP induction in case of *Pe* infection in parallel to the evasion behavior forced us to ask if evasion behavior was a result of AMP induction in these infected larvae. An Imd pathway mutant Relish[E20] was chosen that is known to have an impaired AMP response. Relish is a key factor in the induction of Imd mediated humoral immune response (Hedengren *et al.*, 1999), so the mutant is impaired in its AMP production. Evasion assays were performed with relish homozygous mutant larvae (Fig 4.6). Heterozygous flies crossed to Org-R were used as the control genotype. The impairment in AMP induction in no way seemed to have an effect on the larval evasion behavior. The mutant larvae responded similar to the control genotype towards infectious food, showing evasion. There was no significant difference in the evasion percentage.
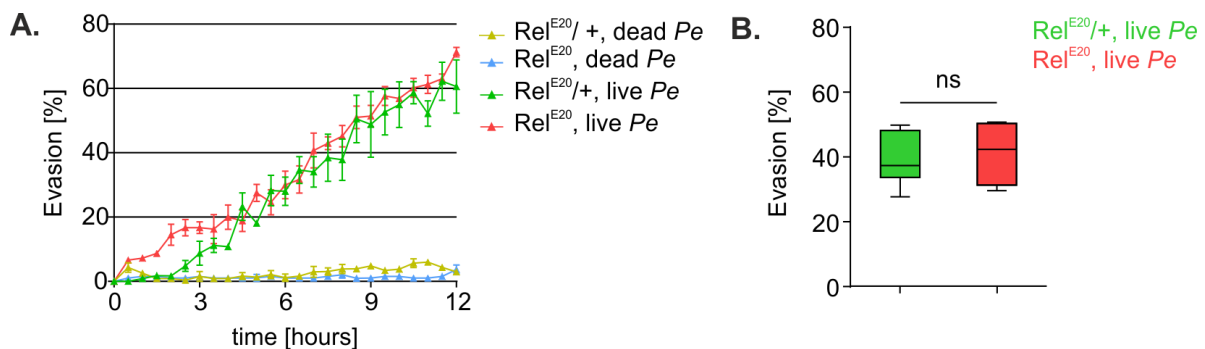
FIGURE 4.6: Relish dependent AMP production is not important for evasion behavior. **A.** Relish mutant larvae showed normal evasion response to *Pe* food compared to the control genotype. Each condition was repeated 3 times. **B.** Box plot shows no significant difference in the evasion percentage. Significance was tested using Mann-Whitney Rank sum test. P=0.3548. n=7. See Table S14 and S15 for data points.

4.3 Hugin is important for evasion behavior

Hugin is a neuropeptide expressed by a cluster of 20 neurons in the *Drosophila* larval and adult brain. Previous studies on from the lab have shown the importance of hugin neuropeptide in bitter avoidance (Hückesfeld, Peters and Pankratz, 2016). Upon activation of hugin neurons, larvae also exhibit a wandering-like behavior and decrease in feeding (Schoofs, Hückesfeld, Schlegel, *et al.*, 2014). This behavior is important when larvae come across aversive food sources. This prompted us to ask if hugin is also involved in larval evasion behavior.

The first experiment was to ablate the hugin neurons by expressing two pro-apoptotic genes reaper (rpr) and head involution defective (hid) using Hugin-Gal4 (Hug-Gal4) (Fig 4.7A & B). Hugin Gal4 drives expression in all 20 hugin positive neurons in both larvae and adults. The ablation was confirmed by immunostaining Hug> UAS-rpr;; UAS-hid larval brains using anti-hugin antibody (see Fig S1). Evasion assay was performed with these larvae and compared to the control genotypes. Ablation of hugin neurons lowered the percentage of evasion significantly. Larvae preferred to stay in the infected food for longer time when hugin neurons were ablated while the control genotypes showed normal evasion response. This could mean hugin neurons are important for generating an altered preference in larvae upon infection. This observation needed to be confirmed by reproducing the phenotype using another approach. Thus hugin neuronal inactivation was carried out by expressing the inward rectifier potassium channel UAS-Kir2.1 (Baines *et al.*, 2001). Inactivating hugin neurons also resulted in a significant decrease in evasion percentage (Fig 4.7C & D). This experiment also confirms that hugin neuronal circuit is important for generating evasion response.
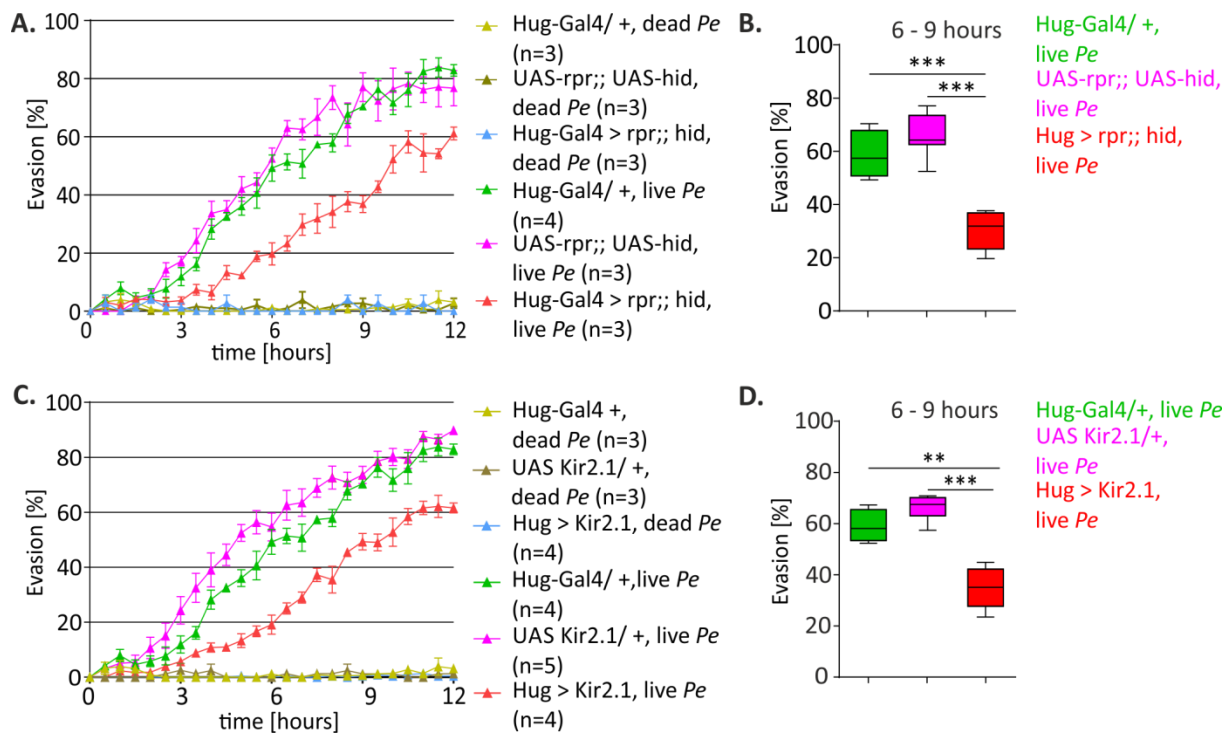
FIGURE 4.7: Hugin neuronal ablation/ inactivation lower evasion percentage. **A.** Ablating hugin neurons by expressing UAS-rpr;; UAS-hid (red) decreased the overall evasion percentage throughout the assay. Hug-Gal4 x OrgR (green) and UAS-rpr;; UAS-hid (magenta) are the control genotypes fed on live *Pe* and showed normal evasion behavior. **B.** Evasion percentage between 6 to 9 hours represented by box plots show a significant decrease in hugin ablated larvae when compared to both the control genotypes. ***P value 0.0006 **C.** Inactivating hugin neurons using UAS-Kir2.1 (red) also decreased the evasion percentage. **D.** Box plots show a significant drop in evasion percentage in Hug-Gal4 x UAS-Kir2.1 larvae as compared to the Hug-Gal4 x OrgR (green) and UAS-Kir2.1 x OrgR (magenta). Also see Table S16 – S19.

Finally to confirm the involvement of hugin neuropeptide specifically in this behavioral response, we decided to knockdown the level of hugin mRNA using RNAi. Hugin levels were downregulated in all 20 hugin neurons and evasion assay was performed (Fig 4.8). Knockdown of hugin neuropeptide alone was sufficient to recapitulate the effect on evasion behavior. The evasion percentage went down by 50% throughout the assay.
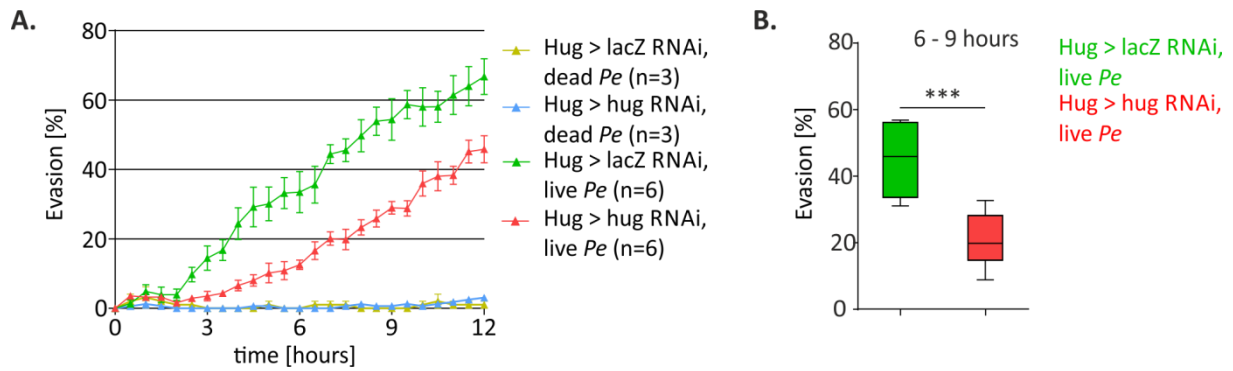
FIGURE 4.8 : Hugin neuropeptide knockdown lowered evasion percentage. **A.** Larvae expressing hugin RNAi (red) showed a lower evasion percentage to the infectious Pe food when compared to the control line Hug-Gal4 > UAS-lacZ RNAi (green). B. Decreasing hugin mRNA level resulted in a 50% decrease in the evasion percentage (red). See Table S20 and S21.

Evasion assays after hugin manipulation clearly shows that hugin neuropeptide is necessary for larval evasion behavior. Inactivation of hugin neurons/ decreasing the level of hugin mRNA brought down the larval evasion percentage. Larvae with lower hugin spent more time on infected food compared to its control genotype. This observation is in line with the previous study that has shown how hugin is necessary in larvae to avoid an aversive food source (Hückesfeld, Peters and Pankratz, 2016). Recently we have also shown by measuring calcium activity in hugin neurons that larvae in a suspension of live *Pe* showed an increase in its neuronal activity as compared to larvae given dead *Pe*. CaMPARI (Calcium Modulated Photoactivable Ratiometric Integrator) was used to measure calcium activity dependent photoconversion (Fosque *et al.*, 2015). Hugin-Gal4 animals were crossed to UAS CaMPARI and the larvae were placed in 96 well PCR plate with 50µl of PBS and dead/ live *Pe* suspension. All the CaMPARI, hugin antibody experiments and analysis were performed by Dr. Hückesfeld. Fig 4.9A-B shows Hugin-PC neurons (hugin cells that have projection to the protocerebrum) of larvae that were placed in dead Pe/live *Pe* suspension and PBS. Larvae incubated in live *Pe* had a high red to green ratio of photoconversion compared to PBS control and dead *Pe*. Quantitative analyses show a significant difference. Hugin antibody staining of larval brains exposed to dead or live Pe showed a high peptide concentration at the Hugin-PC release sites in larvae incubated in live Pe suspension. This would mean release of hugin-PC neurons respond to infectious *Pe*.
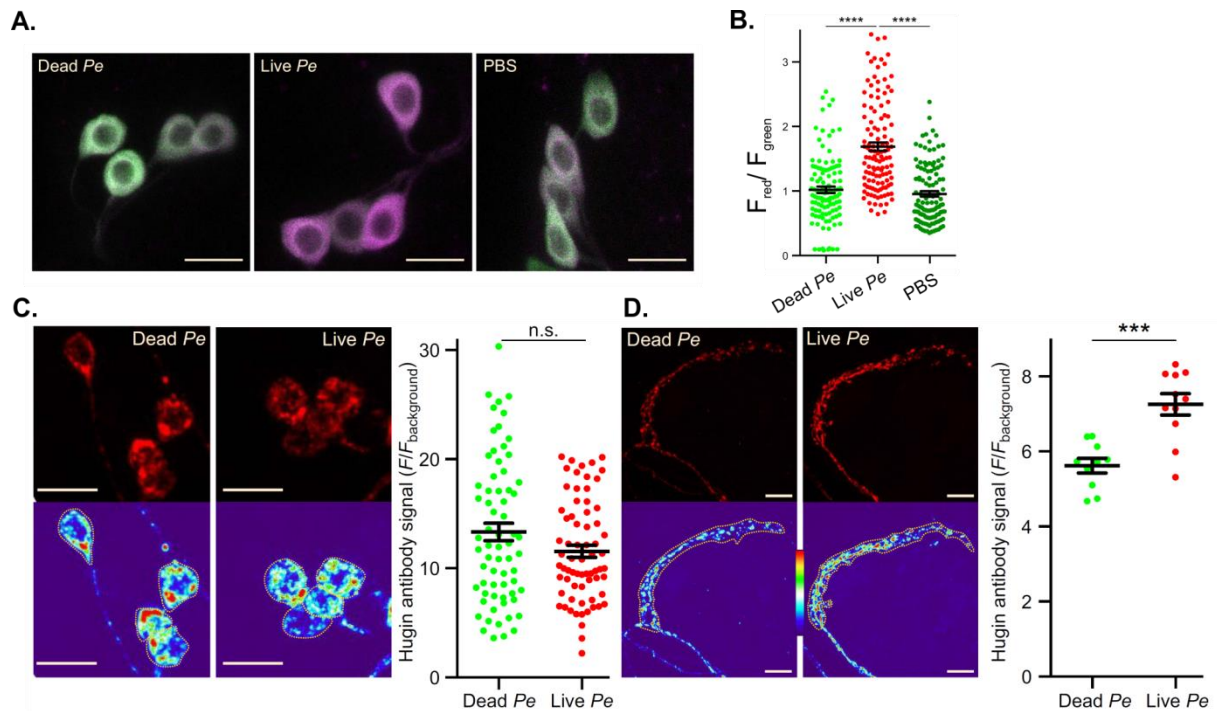
FIGURE 4.9: Hugin-PC neurons are activated by infectious Pe. **A.** Hug-Gal4 x UAS CaMPARI larvae were incubated in PBS/dead Pe/live Pe for 5 minutes and exposed to laser (405nm) for 30 sec. Images show high calcium dependent red to green fluorescence ratio in Hugin-PC neurons incubated in live *Pe* as compared to dead *Pe*/ PBS. n=15 larvae each. **B.** Quantitative analysis shows significant difference. ***p< 0.0001. **C.** OrgR larvae were incubated in dead *Pe*/ live *Pe* for 5 minutes and stained for hugin. Hugin-PC somas were analyzed and no significant difference was observed (P = 0.2123). **D.** However antibody signal in the Hugin-PC release sites in the protocerebrum showed a significantly high peptide concentration in the live *Pe* incubated larval brains than the control. ***p< 0.0001.

4.4 Starvation regulates hugin neuronal activity and evasion behavior.

As already mentioned before, *Drosophila* larvae being continuous feeders hardly stop feeding at any point during its larval life. Hence it was interesting to test if the internal nutritional state of the larvae would have an effect on evasion behavior. To test this, wild type first instar larvae were taken and starved for 6h on a filter paper soaked with 1x PBS. Fed larvae were used as the control genotype here. Evasion assay was performed and it was observed that starved larvae continued feeding on the infected *Pe* food for longer time period compared to the fed animals (Fig 4.10A & B). This

drop in evasion behavior is very similar to the hugin inactivation data. This prompted us to look into a possible connection between starvation and hugin level. Functional imaging as done by Dr. Hückesfeld using CaMPARI showed that there is time dependent inactivation of hugin neurons upon starvation (Surendran *et al.*, 2017). Longer starvation period resulted in lower CaMPARI signal in hugin neurons (Fig 4.11A & B).

FIGURE 4.10: Starvation decreases evasion response in wild type larvae. **A.** Fed larvae (green) show a normal evasion behavior while 6h of starvation resulted in a slower response (red). **B.** The box plot shows that starved larvae exhibits a 50% drop in the evasion percentage. Mann-Whitney-Rank-Sum test shows a significant difference. ***$p \leq 0.001$, n=7. See Table S22 and S23 for mean and median values.
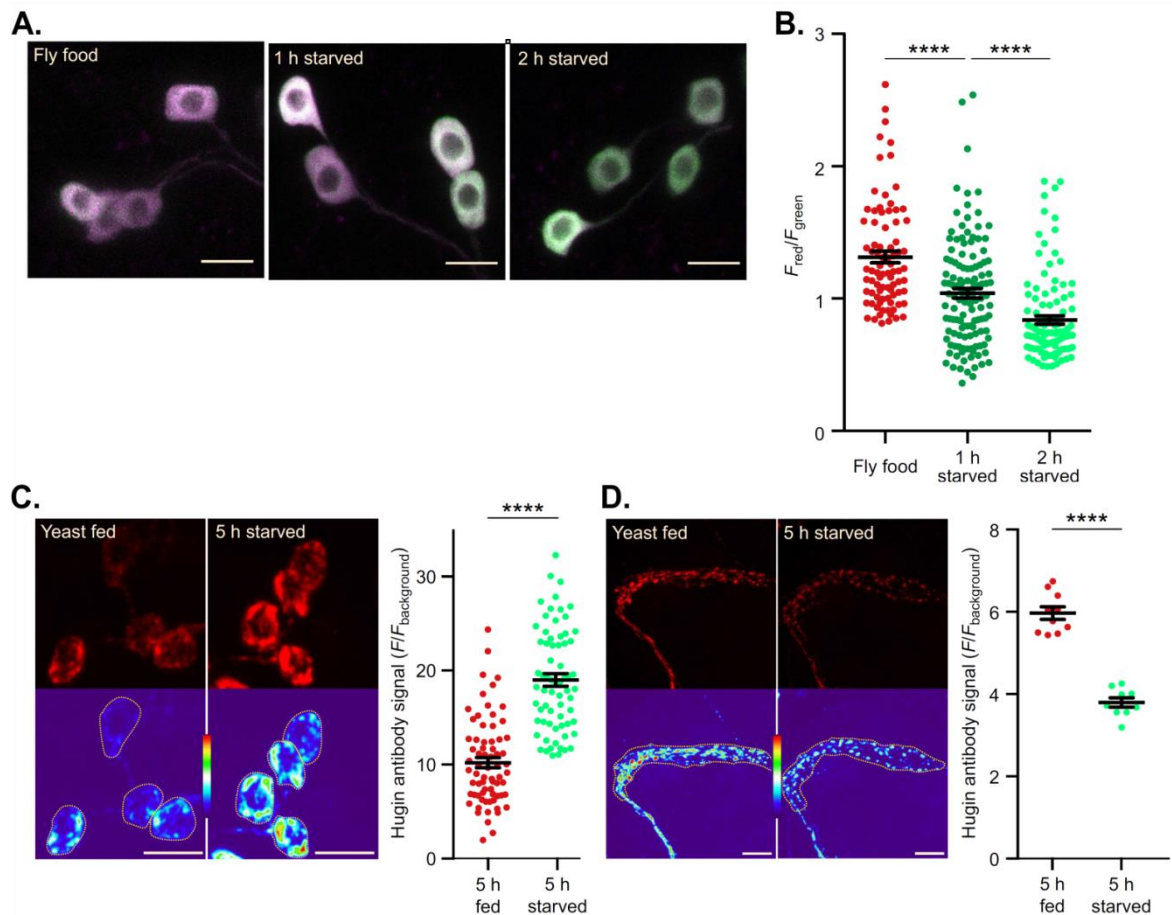
FIGURE 4.11: Hugin neural activity is affected by starvation. **A.** Hug-Gal4 x UAS CaMPARI larvae were either kept in fly food (n=14) or starved for 1 hour (n=18) or 2 hours (n=15). Images show that calcium activity dependent red to green ratio of photoconversion in fed, 1hour starved and 2 hours starved larvae. **B**. Quantitative analysis shows a significant drop in the CaMPARI signal when the larvae were starved. ***$p < 0.0001$. **C.** Wild type OrgR larvae were fed or starved for 5 hours and stained for hugin and quantified for the peptide content. Hugin-PC somas showed a higher peptide signal when the animals were starved compared to the fed larvae. **D.** On the other hand, Hugin-PC release sites, or the projections in the protocerebrum showed a significantly lower peptide content in the starved animals (n=9) compared to fed larvae (n=10). The experiments and analysis in this figure panel were performed by Dr. Hückesfeld.

This finding was also backed up by immunostaining data for hugin neuropeptide. Starvation significantly increased the hugin antibody signal in the hugin cell body and lowering the peptide content at the release site. While larvae that were fed has a

lower signal in hugin cell body and a higher content at the release site (Fig 4.11 C & D) (Surendran *et al.*, 2017). This once again confirms that hugin release/ hugin activity is regulated by starvation.

4.5 Role of other neurotransmitters/ neuropeptides in evasion behavior

Every organism continuously perceives changes in its external or internal environment and alternates its behavior accordingly. However this requires a strong coordination between the sensory pathway and the motor neurons, centrally controlled by the central nervous system (CNS). Neurotransmitters and neuropeptides are molecular messengers that transmit message from one neuron to the other in the form of information. The nature of the neurotransmitter can be either excitatory like glutamate or inhibitory like GABA (gamma-aminobutyric acid). Based on the sensory information, animals need to modulate and generate appropriate behavior to keep themselves away from danger. On the contrary, evasion response shown by larvae is generated due to a change in the animal's internal environment ie., an infection in the gut. Here the information is not entirely sensory as is clear from the timeline taken by the animal to generate an evasion response. We decided to test the classical neurotransmitters known in *Drosophila* and few neuropeptides that might have a role in signaling the CNS. We started out with candidates that looked promising based on studies done in either *Drosophila* or *C.elegans* with regard to aversion behavior (Zhang, Lu and Bargmann, 2005) and included neuropeptides that are known to have expression in the larval gut (Veenstra, 2009).

4.5.1 Effect of serotonergic neurons on evasion behavior

Serotonin is one of the most abundant neurotransmitter found in the intestine of all vertebrates. Studies in *C. elegans* have shown that this soil dwelling nematode can learn to associate the aversive odour of the pathogen after interacting with the pathogen and exhibit a avoidance response analogous to conditioned taste aversion (Zhang, Lu and Bargmann, 2005). Exposure to the pathogen led to an increase in

serotonin expression in one of the chemosensory neuron (ADF) in these animals which directly promoted the learning.

The evasion behavior in *Drosophila* larvae could very well share a similar circuit. In *Drosophila* larval CNS, there are about 96 5-HT neurons in total of which 84 are bilaterally symmetrical interneurons with intrasegmental arborizations (Huser *et al.*, 2012). Trh-Gal4 crossed to UAS-mcd8::GFP clearly marks almost all the serotonin positive neurons in the larval brain as shown in the images below where GFP positive neurons are co-stained with anti-5HT (serotonin) positive neurons. Additionally anti-Trh (tryptophan hydroxylase) antibody was also used which binds to the rate limiting enzyme of serotonin synthesis.
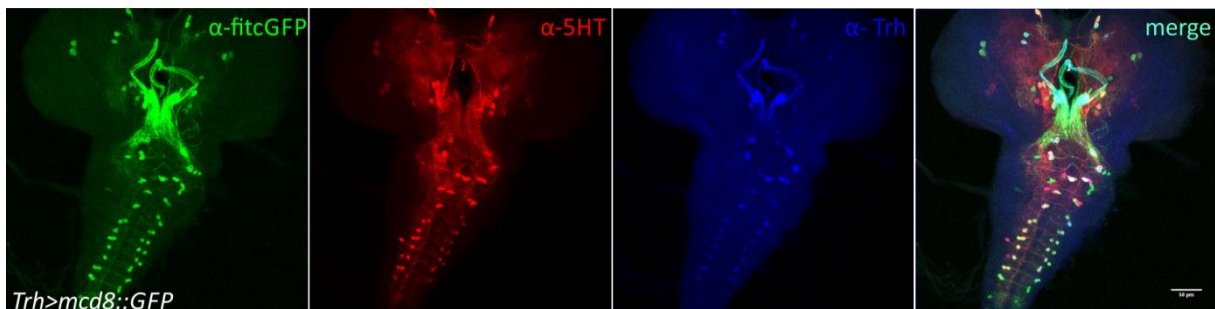
FIGURE 4.12: Serotonergic neurons of the larval CNS. Panel shows *Trh > mcd8::GFP* larval brains stained for anti- GFP (green), anti- 5HT (red) and anti-Trh (violet) shows co-localization.

To understand the role of serotonin in *Drosophila* larvae during infection, we decided to manipulate the serotonergic circuit in first instar larvae using two different Gal4 lines TRH-Gal4 (generated by Serge Birman) and TPH-Gal4 (Park *et al.*, 2006). Both these Gal4 drivers uses promotor fragment of the gene Tyrosine Hydroxylase (Trh) which is a rate limiting enzyme in serotonin synthesis. In addition, two different modes of manipulations were employed to disrupt the larval serotonergic circuit. TPH-Gal4 was used to express the pro-apoptotic genes *reaper (rpr) and head involution defect (hid)* (Fig 4.13A & B); ablating all serotonin positive neurons and evasion assay was carried out. The ablation was also confirmed by immunostaining serotonergic neurons (See Fig S2). Control genotypes used were TPH-Gal4 x OrgR and UAS-rpr;; UAS-hid. Ablation of serotonergic neurons did not affect the evasion behavior. There was however a slight increase in the evasion percentage when

36

compared to one of the control genotypes while the other did not. Consistent with this observation, inactivation of TRH positive neurons also did not affect evasion percentage (Fig 4.13C & D).
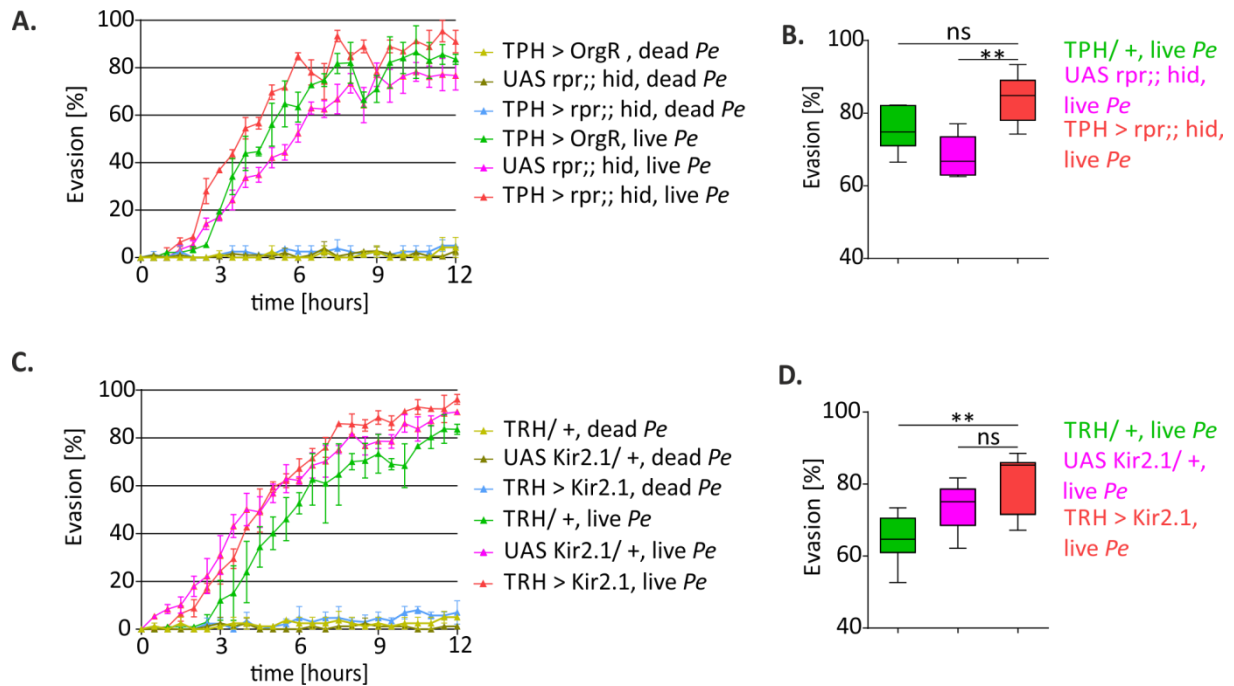
FIGURE 4.13: Manipulating serotonergic neurons did not affect evasion behavior. **A. & B.** show evasion percentage after ablation of TPH positive neurons (red). Even though there is a significant increase in evasion compared to the UAS rpr;; hid control (magenta), the TPH-Gal4 x Org-R (green) was comparable to the experimental genotype. Mann-Whitney-Rank-Sum test shows a significant difference. **p≤ 0.01. **C. & D.** show similar result where TRH-Gal4 is used to inactivate the serotonergic circuit by expressing UAS-Kir2,1. Larvae show a significantly higher evasion when compared to TRH-Gal4 x Org-R control but not UAS-Kir2.1 x Org-R control. Mann-Whitney-Rank-Sum test shows a significant difference. **p≤ 0.01. See Table S24 – S27 for mean ± SEM and median values.

4.5.2 Quantitative PCR screen for more candidates

To investigate the involvement of more signaling molecule in this infection induced feeding behavior, a small screen was performed. The strategy was to look for any change in the mRNA level of the candidate genes in whole larvae, after infection by performing qPCR. The selected candidates included genes indispensable in the synthesis of classical neurotransmitters in *Drosophila,* several neuropeptides known to have expression in larval gut, and cytokines as listed in the table below.

	GENE	NAME
1.	ChAT	Choline Acetyl Transferase
2.	TRH	Tryptophan Hydroxylase
3.	ple	Pale (Tyrosine Hydroxylase)
4.	AstA	Allatostatin A
5.	Mip	Myoinhibiting peptide precurosor
6.	AstC	Allatostatin C
7.	CCHa1	CCHamide- 1
8.	CCHa2	CCHamide- 2
9.	Crz	Corazonin
10.	Dh31	Diuretic hormone 31
11.	Dh44	Diuretic hormone 44
12.	Ilp2	*Drosophila* insulin-like peptide 2
13.	Ilp3	*Drosophila* insulin-like peptide 3
14.	Ms	Myosuppressin
15.	Hug	Hugin
16.	Lst	Limostatin
17.	NPF	Neuropeptide F
18.	sNPF	short neuropeptide F precursor
19.	pain	Painless
20.	upd1	Unpaired 1
21.	upd2	Unpaired 2
22.	upd3	Unpaired 3

Table 1: List of candidate genes selected for qPCR screen after *Pe* infection in whole larvae.

RNA isolation was done from whole larvae that were fed on dead *Pe* and live *Pe* for 3h and 6h. qPCR data were plotted as fold change normalized to RpL32 control gene. None of the 20 candidates out of the 22 tested had any significant change in their mRNA level after infection. However two genes coding for the *Drosophila* cytokines upd2 and upd3 showed a significant induction at 3h (Fig 4.14A). *Drosophila* cytokines upd 2 and 3 mediated Jak/Stat signaling have been shown to be important for gut regeneration and repair (Jiang *et al.*, 2009; Osman *et al.*, 2012). Any physical damage, enteric infection or even stress signaling causing enterocyte damage can induce this cytokine production by the enterocytes. Larvae infected for 6h were then checked for the same set of genes and a consistent induction of upd2 and upd3 could be observed (Fig 4.14B).
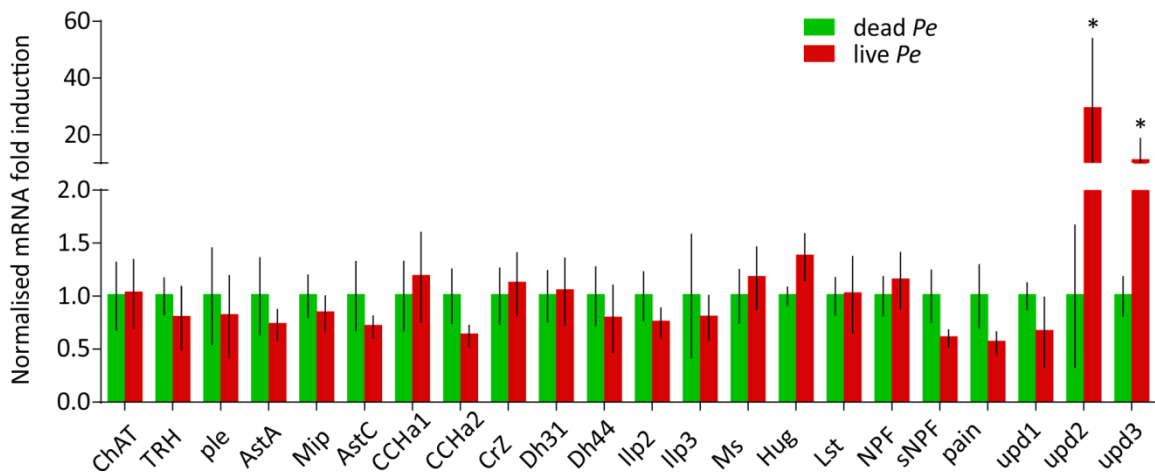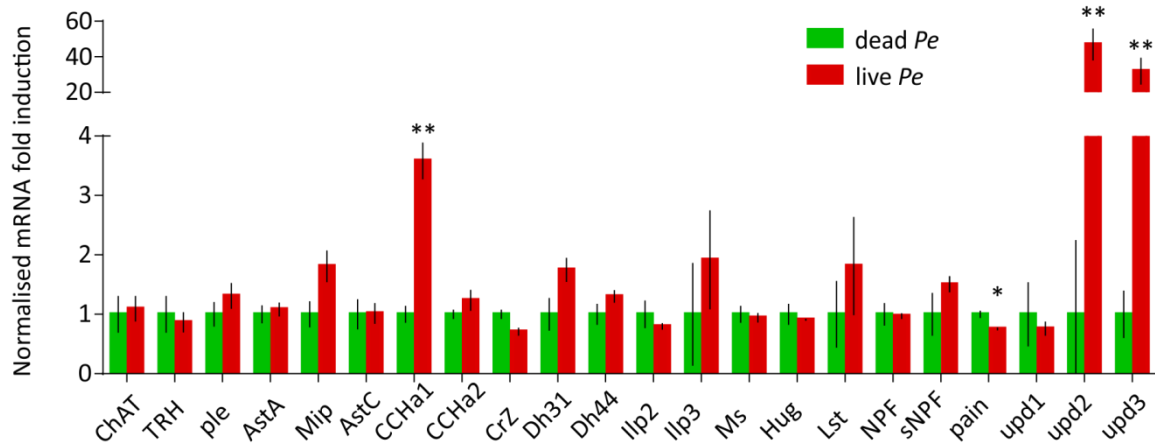
FIGURE 4.14: Real time PCR data showing mRNA expression in larvae after *Pe* infection. **A.** qPCR comparison of larvae after 3h infection with dead *Pe* (green bar) and live *Pe* (red bar) shows a significant induction in the level of upd2 and upd3 mRNA. **B.** qPCR data after 6h of infection shows consistent change in the fold level. Significance was tested using unpaired t test. *$p \leq 0.05$, **$p \leq 0.01$. See Table S28 and S29 for mean values.

Drosophila cytokines upd1, upd2 and upd3 are small molecules that act as the ligand for a single receptor *domeless*, the *Drosophila* receptor for JAK-Stat pathway (Agaisse *et al.*, 2003). While upd2 and upd3 is important for repair and maintenance of the damaged gut cells upd1 has a role during embryonic development (Harrison *et al.*, 1998) and maintaining intestinal stem cells (Osman *et al.*, 2012). The upregulation of upd2 and upd3 we observed upon *Pe* infection as early as 3h could be a part of this repair in the gut. To check if cytokine induction is partially or fully responsible for the behavioral response during infection, upd2 and upd3 null mutants (Osman *et al.*, 2012) were tested. The receptor for these cytokines, *domeless* in addition to gut and muscles is also expressed in the *Drosophila* brain which makes them a promising candidate for the current behavioral study. Evasion assay was done using the null mutants for upd2 and upd3 larvae with the appropriate genotype controls (Fig 4.15).
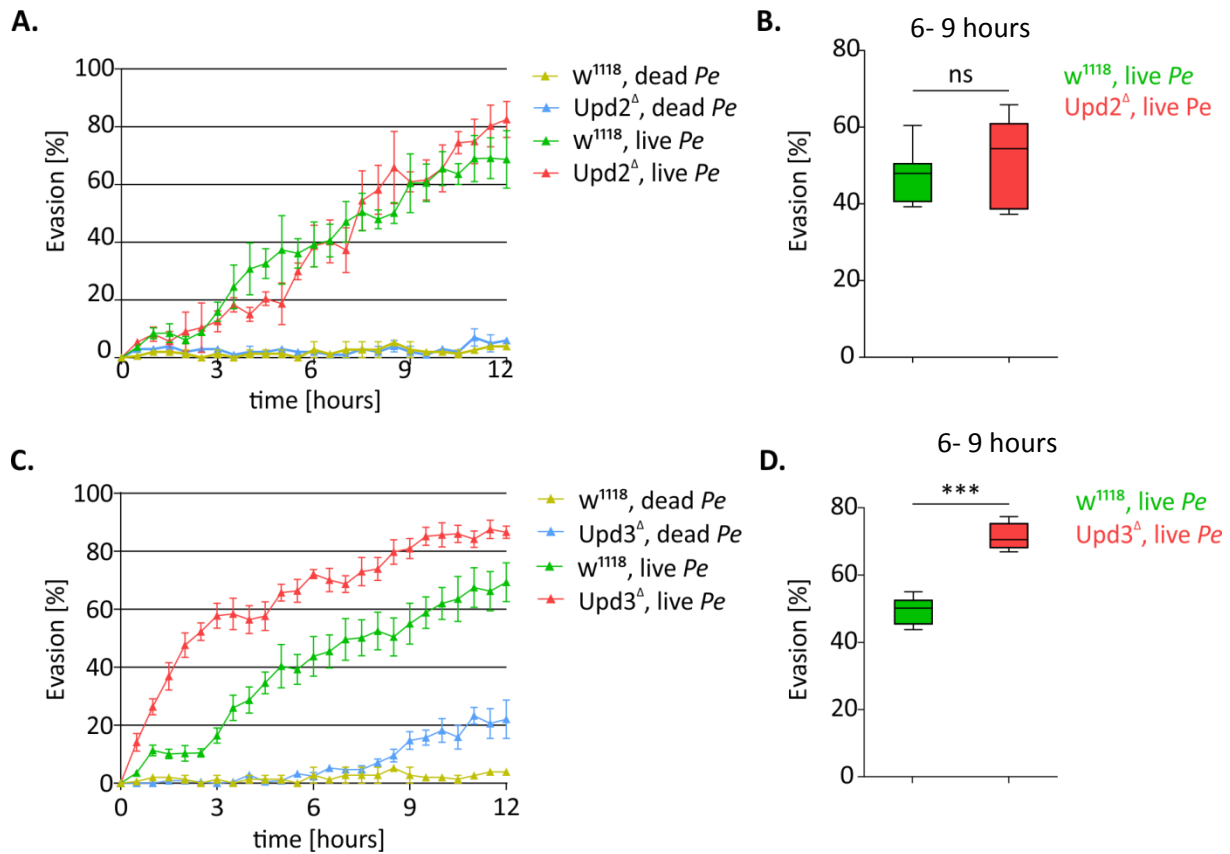
FIGURE 4.15: Upd3 mutant show a higher sensitivity to infectious food source. **A.** Upd2 null mutant (red) on *Pe* food showed a normal evasion pattern compared to the control genotype w[1118] (green). **B.** The evasion percentage of the experimental genotype was not significantly different from the control. P=0.7791. **C.** Upd3 null mutant larvae showed a faster response and an overall higher evasion compared to the control on *Pe* food. **D.** The evasion percentage of upd3 null mutant was significantly higher than the control. ***p ≤ 0.001. See table S31 – S34 for mean and SEM values.

Upd2 null mutant showed a normal evasion behavior compared to its control when presented with an infectious food source (Fig 4.15 A & B). Absence of upd2 cytokines did not affect evasion response of the larvae. On the other hand, Upd3 null mutants upon exposure to *Pe* food started moving away from the source of infection very early on. Almost 60% of the larvae showed evasion within the first 3 hours of the assay (Fig 4.15B & C). The heightened sensitivity shown by Upd3 null mutant was a rather interesting phenotype because none of the genotypes tested so far showed had shown such a high percentage of evasion within the first 3 hours. To make this point more apparent, few of the lines tested previously was plotted together with upd3 null focusing on the initial 3 hours (Fig 4.16).
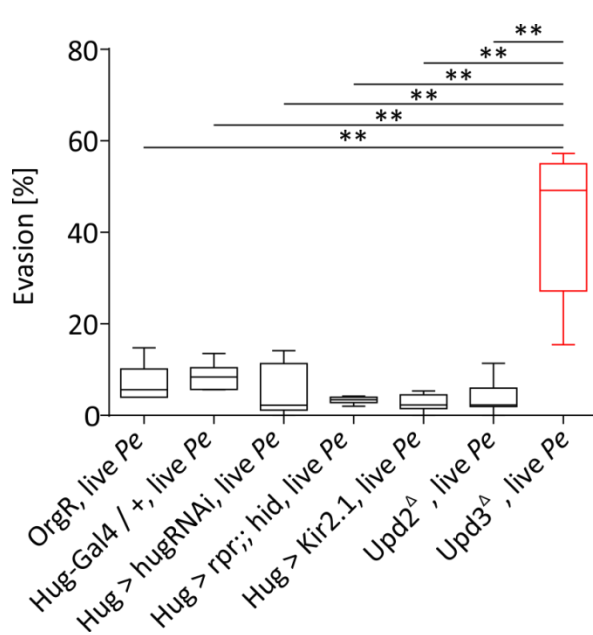
FIGURE 4.16: Upd3 null mutant has a significantly higher evasion percentage compared to all the other genotypes tested. Box plot compares upd3 null mutant to the following; wild type (OrgR), Hug-Gal4 x OrgR (Hug-Gal4/+), Hug-Gal4 x hugin RNAi (Hug> hug RNAi), Hug-Gal4 x UAS rpr;; UAS hid (HugS3> UAS-rpr;; hid), Hug-Gal4 x UAS-Kir2.1 (Hug> Kir2.1), and Upd2 null mutant. Plot represents the cumulative data point between 1- 3 hours of evasion assay. Mann-Whitney-Rank-Sum test shows a significant difference. **p ≤ 0.01

To further understand the role of Upd3 release in the context of infection, the source of release had to be identified. Hence histological staining was carried out on larval brain and gut after infection. Upd3 Gal4 crossed to UAS GFP homozygous lines was provided by Katie Woodcock, Giessmann lab. These larvae were fed dead/ live *Pe* for 6 hours and guts were dissected and stained with antibodies. Co-labelling was done with anti-prospero, a marker for the enteroendocrine (EE) cells of *Drosophila* gut. Both larvae fed dead *Pe* and live *Pe* showed areas of Upd3 expression in their midgut. However, preliminary observation shows live *Pe* fed larvae had a higher level of Upd3 induction in the posterior mid gut region when compared to the dead *Pe* fed larvae as shown by the GFP signal (Fig 4.17A-C). This result has not been quantified. Prospero staining shows no co-localization with the Upd3 positive cells (Fig 4.17D-F) in the gut confirming that cytokine release is by enterocytes in the larval gut and not enteroendocrine cells.
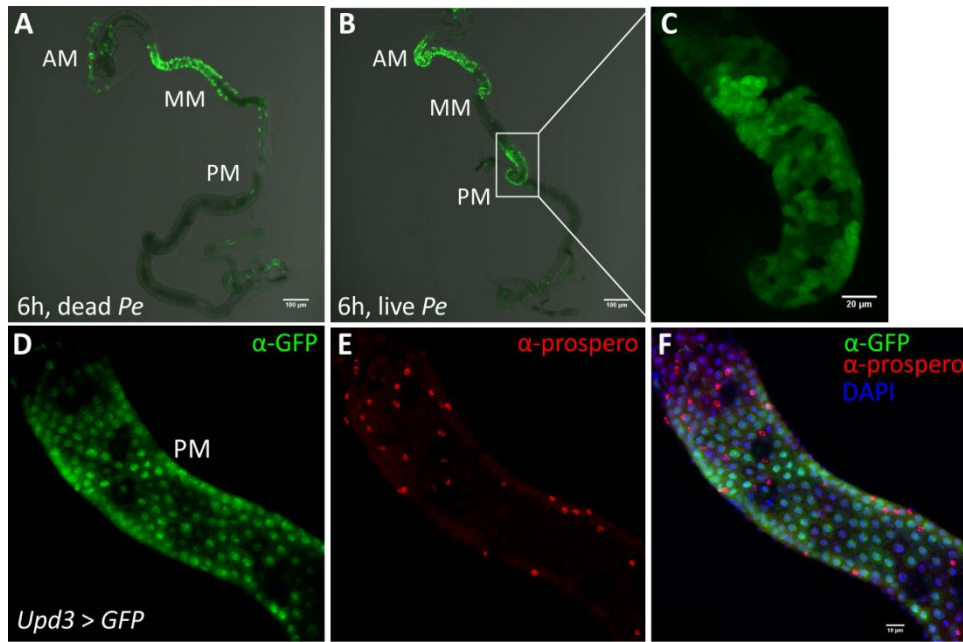
FIGURE 4.17: Upd3 is released by enterocytes in the larval gut upon *Pe* infection. *Upd3* > UAS *GFP* larvae were fed dead *Pe*/ live *Pe* for 6 hours and gut stained for anti-GFP. **A.** Anterior midgut (AM) and mid midgut (MM) region show GFP signal in the dead *Pe* fed larval gut **B.** An induction of GFP signal in the posterior midgut (PM) was seen in live *Pe* fed larval gut, **C.** Enlarged area shows Upd3 positive cells in the PM. **D. E. & F.** *Upd3* > *GFP* larvae were fed live *Pe* and gut stained for anti-GFP (green), anti-propsero (red) and DAPI (violet). No co-localization was observed.

Additionally, I also wanted to check the expression of *upd3* in the larval CNS. Larval brains were dissected and stained to find that other than few artefacts, larval CNS did not show any sign of *upd3* expression, anti-repo was used as background staining (Fig 4.18).
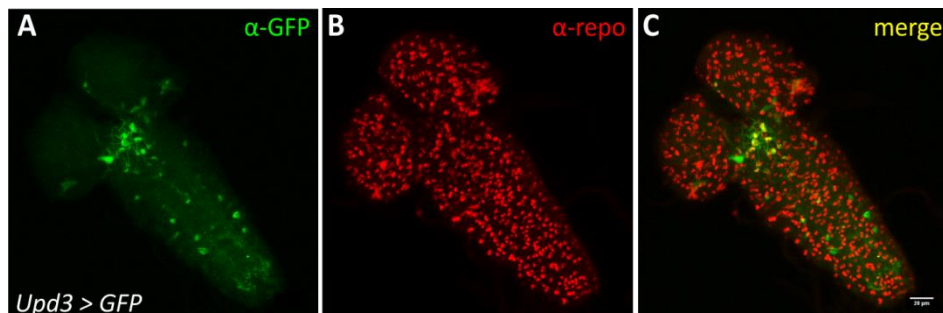
FIGURE 4.18: *Upd3* is not expressed in the larval CNS. **A- C,** show *Upd3* > *GFP* larval brains were stained for anti-GFP (green) and anti-repo (red) shows random, non-specific GFP staining across samples. Also see fig S4, n = 3

Absence of Upd3 expression in the brain meant the induction during infection is entirely peripheral. However the receptor for Upd3, *domeless* was reported to be widely expressed in the adult brain (Rajan and Perrimon, 2012). The larval expression of the receptor was tested by performing antibody staining on *Domeless-*Gal4 > UAS *mcd8::GFP* larval brains (Fig 4.19). Similar to the adult brain expression, dome-Gal4 showed wide expression in the larval brain including the optic lobe. Co-labelling was done with anti-hugin and anti-dilp2 to check for co-localization. Few of the *domeless* expressing neurons showed a co-localization with at least 6 hugin neurons.
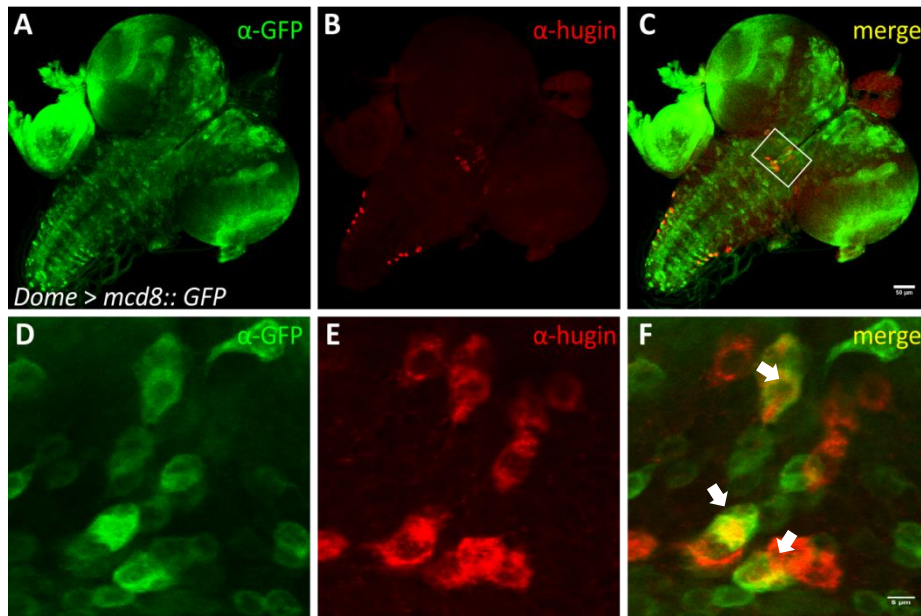
FIGURE 4.19: Hugin neurons show co-localization with domeless receptor expression. **A-C,** *Domeless > mcd8::GFP* larval brains were stained for anti-GFP (green) and anti-hugin (red) and the merge showing domelss co-localization with hugin. **D-F.** Single slice zoom of the ROI white arrows show co-localization. N=2

Domeless receptor expression in hugin neurons suggests a functional JAK/STAT pathway in these neurons. The question was if *domeless* signaling in hugin neurons has any role in the infection induced evasion response. To test this, *domeless* signaling in hugin neurons was blocked by expressing a dominant negative form of the *domeless* receptor in them. *Hug*-Gal4 > UAS-*domeΔCYT* larvae were generated and evasion assay was carried out. Evasion behavior was not affected when *domeless* mediated JAK/STAT pathway was inhibited in hugin neurons (Fig 4.20A).

Evasion percentage of the experimental genotype was comparable to the control (Fig 4.20B).
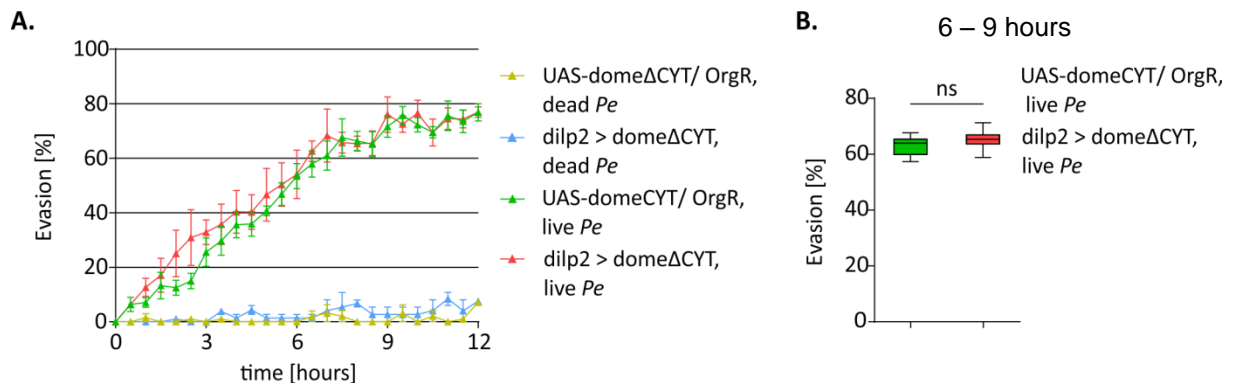
FIGURE 4.20: Domeless mediated signaling in hugin neurons is not important for evasion behavior. **A.** Blocking domeless signaling in hugin neurons by expressing dominant negative form of the receptor UAS-domeΔCYT did not affect evasion behavior. Each condition was repeated 3 times. **B.** Box plot shows no significant difference in the evasion percentage. Mann-Whitney-Rank-Sum test was used for comparison. P= 0.9656. n=7.

Domeless receptor expression analysis in adult brain had also shown some expression in the neurosecretory cells (mNSCs). In flies, this receptor mediated JAK/STAT signaling was shown to have an inhibitory effect on the neuronal activity of the mNSCs resulting in an increase in Dilp2 accumulation and reduced fat storage (Rajan and Perrimon, 2012). Co-immunolabeling of the receptor with anti-dilp2 showed a similar expression pattern in the larval brain. Out of the 20 mNSCs in larvae, 14 are the ilp2 positive Insulin Producing Cells (IPCs) (Nässel *et al*., 2013) and all 14 showed co-localization with *domeless* receptor expression (Fig 4.21 A-F).
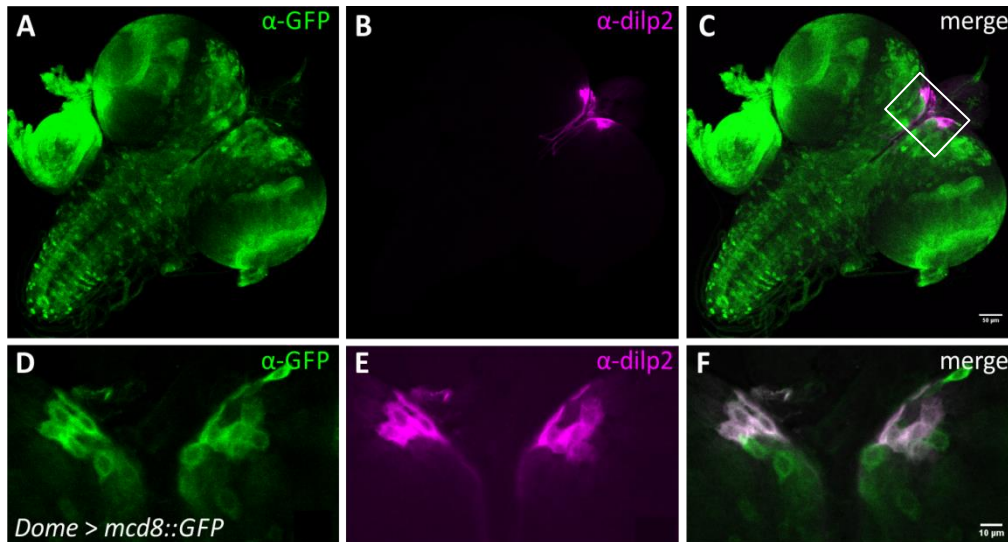
FIGURE 4.21: Domeless receptor is expressed by the IPCs in the larval brain. **A-C** shows Immunolabeling of dome> mcd8::GFP larvae shows domeless expression (green), co-localizes with dilp2 (magenta) staining as shown by the merge. **D-F** shows the single slice zoom of the ROI.

Co-expression of domeless receptor on IPCs in larval brain similar to the adult lead us to ask if the JAK/STAT pathway mediated inhibition of dilp2 neuronal activity has any role during evasion behavior. Dilp2-Gal4 was used to express the dominant negative form of the receptor and JAK/STAT pathway was blocked in the IPCs. Evasion assay was performed with these larvae and it was found that they showed normal evasion compared to its control (Fig 4.22A & B)
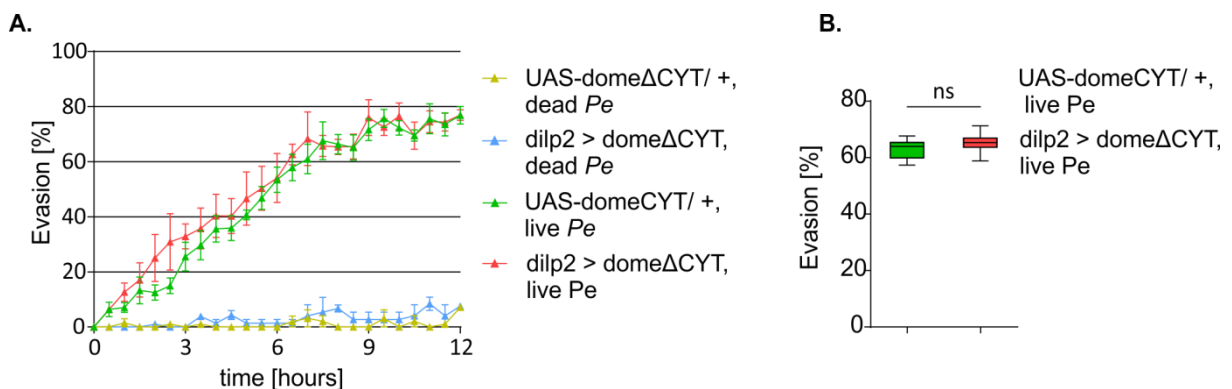
FIGURE 4.22: Domeless mediated JAK/STAT signaling in IPCs is not important for evasion behavior. **A,** Graph shows dilp2-Gal4 x UAS-dome ΔCYT larvae (red) showing evasion behavior comparable to the control genotype UAS-dome ΔCYT x OrgR (green). **B,** No significant difference was observed in the evasion percentage between the control and experiment. Mann-Whitney-Rank-Sum test was used to test the significance. See Table S38 and S39 for data points.

While it is clear that while there is an induction of Upd3 in the gut during infection, the signaling to the CNS has yet to be identified. However, manipulation of domeless receptor on hugin and IPCs suggest that Upd3 mediated JAK-STAT signaling do not act upstream of hugin neurons or the IPCs.

5. DISCUSSION

5.1.   *Drosophila* larvae can evade pathogenic food source

The study aimed at understanding the biology of feeding behavior in *Drosophila* larvae during infection. We have shown that *Drosophila* larvae can recognize and avoid pathogenic food source upon infection. A novel behavioral set up was successfully developed in the process, which can now be used for further screens. Infected larvae developed aversion to the pathogen containing food source after a certain period of exposure. This has not been reported before in *Drosophila* larvae. On the other hand, adult *Drosophila* has been earlier shown to recognize a specific microbial odorant known as geosmin that activates a specific circuitry for aversion (Stensmyr *et al.*, 2012). In larvae, such studies have been difficult mainly due to their strong preference for feeding, which generally overrides most of the aversive cues. This study offers a novel approach to understand the behavior. In *C.elegans*, chemosensory neurons were shown to be important in learning olfactory avoidance and exhibit an aversive behavior towards pathogenic bacteria (Zhang, Lu and Bargmann, 2005; Zhang and Zhang, 2012). A similar underlying mechanism could be in place in *Drosophila* which still needs to be identified. This is important as it would help us understand how information from the periphery (gut) reaches the brain and the molecular players involved in subsequently modulate the behavior.
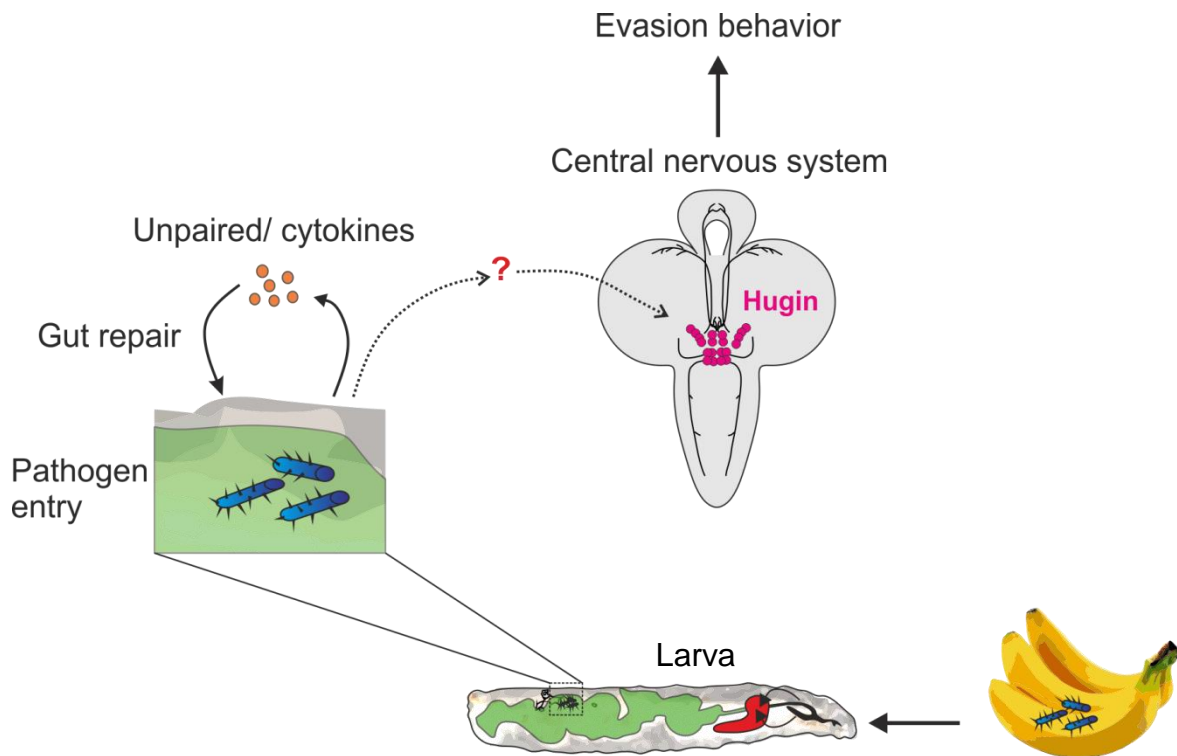
FIGURE 5.1: Gut-brain axis in evasion behavior. The model shows how ingestion of food source containing pathogenic microbes leads to gut infection in larva. The larval gut undergoes tissue damage leading to release of cytokines which is necessary for the repair. Simultaneously a signal from the periphery (red question mark) that yet needs to be identified reaches the brain and activates the hugin circuitry (magenta) leading to larval evasion response.

As represented in the schematic (Fig 5.1), the study started out by asking if *Drosophila* larvae can respond to a pathogenic food source and how. The answer was yes, however the second part of the question is still open. While there is a lot of research studying how cues from the environment are sensed and conveyed to the CNS leading to a behavioural output, there is not much known on how internal information reaches the brain. Gut- brain axis is a bidirectional communication route where information from the gut is continuously sent to and received by the brain through neuronal and hormonal means. Studies done on patients suffering from obesity to depression and projects have repeatedly helped us understand the importance of this homeostasis and how variation in the gut microbiome has a major effect on this axis (Mayer, 2013). Larval feeding behavior proved to be one of the simplest yet powerful assays to study how an infection in the gut can change feeding preference in larvae. An infection can kick start immune response in any animal. This is true even for larvae as shown by the AMP induction after infection, as early as 3

hours. Gram negative bacteria specific AMP was identified to be induced consistently during the infection, interestingly this was found out to be independent of the behavioural response. Mutant larvae defective in relish mediated AMP production still showed an evasion response that was comparable to the control animals. Thus evasion response was revealed to be independent of AMP dependent immune activation.

5.2. *Drosophila* neuropeptide hugin plays a major role in changing larval feeding preference during infection.

A role for neuropeptide hugin was discovered to be important for the evasion behavior. Hugin was already reported to be responsible for bitter aversion in larvae (Hückesfeld, Peters and Pankratz, 2016). Manipulating hugin neurons or decreasing the level of hugin neuropeptide alone, lowered the percentage of evasion response in the larvae. With its earlier reported role in bitter aversion, hugin neurons now seem to have a general role in conveying stress/danger signal to the larval CNS. Hugin in *Drosophila* and Nmu in mice have an inhibitory effect on feeding while increasing motor activity (Nakazato *et al.*, 2000; Schoofs, Hückesfeld, Schlegel, *et al.*, 2014). Thus the role of hugin seems to be conserved across species. It is interesting to note that a simple organism like *Drosophila* have the ability to recognize and actively avoid a source of infection thereby preventing further damage. This decision making ability is key for survival in the wild.

Recent work has shown that hugin positive neurons co-express the neurotransmitter acetylcholine (Schlegel *et al.*, 2016), which was not addressed in this study. Earlier reports have shown using in situ hybridisation how hugin level goes down when the animal is starved (Melcher and Pankratz, 2005). We observed that starvation also had an effect on evasion response. Starved larvae behaved similar to larvae with inactivated/ ablated hugin neurons. Functional imaging and immunohistochemical analysis revealed that this was indeed the case. It was observed by several others before that starved animal lower their sensitivity towards food sources which are otherwise aversive. This study helped us identify hugin to be one of the several players responsible.

5.3.　　Receptors for pathogen recognition

If we look at mammalian models, it has been shown that the receptors of the host's innate immune system can directly recognize the microbes in the gut through microbial associated molecular patterns (MAMPs) (Akira, Uematsu and Takeuchi, 2006) or via microbial metabolites which are be taken up by the circulating system, thus conveying the information to the whole body (Wikoff *et al.*, 2009). In some cases the gut microbiome helps in priming the host's immune system and thereby facilitating a less disruptive immune reaction (Clarke *et al.*, 2010; Kim *et al.*, 2016). In flies, receptors of the PGRP family (peptidoglycan recognition protein) sense Gram negative bacteria and activates the IMD pathway (Lemaitre and Hoffmann, 2007). Experiment with relish mutants showed that IMD mediated pathogen recognition is not important for evasion behavior. One of the aspects that were left unexplored in this particular study was the role of taste receptors in evasion behavior. There are around 68 gustatory receptors in *Drosophila* which are distributed across the body of the animal (Montell, 2009). Recent studies have shown that like in mammals, the enteroendocrine cells of the *Drosophila* midgut express a few of these gustatory receptors (Park and Kwon, 2011). This could mean that any substance that makes its way into the gut of the larvae could still serve as a cue for the gustatory receptors expressed in the gut. One such mammalian bitter taste receptor T2R38 was detected on neutrophils and shown to be able to recognize a bacteria quorum sensing molecule (Maurer *et al.*, 2015). It would be very interesting to look out for *Drosophila* gustatory receptors that show expression in the gut with similar properties. Additionally the enteroendocrine cells of the *Drosophila* gut are capable of releasing regulatory peptides, most of which has their receptors expressed in various regions of the gut or even the enteric nervous system which are yet to be identified. These neuropeptides are thus capable of conveying the information to the nearby regions of the gut or all the way up the brain generating behavioral response.

5.4.　　Gut – brain axis and behavior

Evasion response could be also seen as a primitive form of sickness syndrome which can be clearly observed in case of patients with chronic inflammation. In their cases,

pro-inflammatory cytokines play a major role which induces interleukin production signaling the vagus nerve (Tracey, 2009). Vagus nerve has projections to several lymphatic tissues (Baganz and Blakely, 2013) and immune organs. These projections are highly sensitive to the presence of any inflammatory agents and are capable of initiating an efficient response. Vagal nerves in humans and mice that innervate the gastrointestinal tract respond to a variety of intrinsic and extrinsic factors like nutrient, hormones and stress. Mouse vagus nerve contains approximately 2,300 sensory neurons. Recent studies on these sensory neurons using optogenetics, in vivo imaging and genetical mapping revealed how different set of vagal afferent (sensory) neurons is in charge of detecting intestinal nutrients and controlling gut motility. Vagal nerves that express the receptor for gut hormone GLP1 respond to mechanical distension of stomach and intestine while GPR65 expressing neurons detect intestinal nutrients (Williams *et al.*, 2016). A structurally similar serotonergic nervous system which has innervation to pharynx, esophagus, proventrivculus and ring gland was identified in larvae (Schoofs, Hückesfeld, Surendran, *et al.*, 2014). However when serotonin positive neurons were ablated, no effect was observed in the larval evasion behavior. A more targeted approach might still yield us a result.

Analysis of real time PCR data showed a consistent induction in *Drosophila* cytokines unpaired 2 and unpaired 3 after infection. Upd3 proteins have α-helix structure similar to human interleukin-6 (Oldefest *et al.*, 2013) and Upd2 is suggested to be the functional homolog of leptin (Rajan and Perrimon, 2012). Cytokine upd3 mediated gut repair has been well studied in the field (Jiang *et al.*, 2009; Zhou *et al.*, 2013), but we could not find a role for upd3 mediated Jak-STAT signaling in evasion behavior. A molecular messenger like the pro-inflammatory cytokines which link the periphery and the central nervous system is still a likely possibility in *Drosophila* that need to be identified.

Another interesting observation was the influence of starvation on larval feeding behavior. Starvation lowered the animals' sensitivity towards infectious food source and larvae were less aversive to them. Internal nutrient status of the animal sends a stronger signal to the brain which clearly overrides cues such as aversion. In adult flies, starvation has been shown to alter olfactory sensitivity (Farhan *et al.*, 2013). Even though the role of hugin in evasion has been established in this study, we know that it do not single handedly integrate and execute the change in behavior. More

players that are activated during infection and have the ability to act on neurons need to be screened for in the future.

5.5.   Host- microbe interaction

Maintaining a balance between commensal microbiome and carefully responding to pathogenic microbe is crucial for a healthy animal. In this study we have shown how introducing a pathogen in the food source made the food less attractive for the larvae. Several studies have shown the significance of maintaining a normal microbiota in animals. Inspite of their role in many gastrointestinal diseases, gut microbiome is crucial to host digestion and proper nutrient utilization (Woting and Blaut, 2016). Compared to mammals, flies have a simple and restricted microbiome consisting of mainly four bacterial families which greatly depend on the host diet (Chandler *et al.*, 2011). Axenic flies have been shown to have reduced metabolic rate and longer larval growth period (Ridley *et al.*, 2012). Certain microbes help in producing nutrients from substrates that are otherwise indigestible components to the host. Thus they have a major role in energy breakdown and absorption which when disrupted is possibly leading to conditions such as obesity and type II diabetes (Kootte *et al.*, 2012).

Another interesting example of the host-microbiota interaction was recently demonstrated by Yano et al, which showed how an indigenous gut microbiota was crucial for serotonin synthesis in the host. Serotonin produced by the enterochromaffin (EC) cells of the gut contributes to 95% of the total production in human and mice. It is released in response to the shearing forces that activate the mechanosensitive cation channels on the microvilli (Mayer, 2013). The serotonin in the blood now reaches various regions of the body and is also taken up by the platelets to the site of inflammation (Baganz and Blakely, 2013). Serotonin in the gut is important for its sensorimotor function (Gershon and Tack, 2007). The study showed that the level of peripheral serotonin in the germ free mice was significantly lower effecting gastrointestinal motility compared to the conventionally colonized control animals. This deficit could be restored postnatally by introducing spore forming microbes from healthy mice to the germ free mice (Yano *et al.*, 2015). With

the help of powerful genetics and more tools being developed, it becomes more and more clear that the relationship between the host and the microbiota is not a simple one. It is not always the microbes that exploit the host as their energy source and hence has several gray areas which could be unveiled in the years to come.

6. APPENDIX

Time [hours]	Yeast		Yeast + Dead *Pe*		Yeast + Live *Pe*	
	Mean	SEM	Mean	SEM	Mean	SEM
0.00	0.00	0.00	0.00	0.00	0.00	0.00
0.50	4.59	0.60	4.67	1.26	4.81	1.18
1.00	2.74	1.73	3.14	0.47	4.38	0.97
1.50	3.04	1.50	2.03	0.56	3.88	0.87
2.00	2.61	1.10	1.92	0.32	6.76	1.92
2.50	3.29	1.14	2.83	0.65	8.73	2.21
3.00	4.02	0.93	3.54	1.27	13.87	2.98
3.50	4.47	1.01	4.42	0.83	18.12	1.73
4.00	4.98	1.29	3.26	0.67	23.43	1.40
4.50	5.56	1.04	4.97	1.48	34.63	0.29
5.00	6.25	1.25	4.77	1.19	36.87	3.24
5.50	6.42	1.53	4.61	1.06	45.67	4.21
6.00	5.78	0.58	5.78	0.87	46.11	3.51
6.50	6.67	1.28	5.38	0.79	50.81	3.60
7.00	6.62	1.22	6.89	2.01	52.06	2.37
7.50	7.63	0.86	5.63	1.43	61.00	5.83
8.00	7.77	0.87	6.76	1.09	61.75	3.23
8.50	9.47	1.02	8.56	2.19	60.82	4.15
9.00	8.88	0.41	7.38	1.58	69.14	6.30
9.50	8.59	0.77	8.60	1.86	67.38	4.26
10.00	7.89	1.04	9.47	2.84	73.25	6.62
10.50	8.68	0.52	10.37	2.68	71.18	2.91
11.00	9.48	1.52	10.74	2.31	70.56	4.84
11.50	11.27	1.43	11.39	2.82	75.54	2.32
12.00	12.09	1.34	10.72	3.04	74.10	4.53

Table S1: Table shows mean ± SEM values of evasion percentage for each condition and time point.

	Yeast	Yeast + Dead *Pe*	Yeast + Live *Pe*
Minimum	5.788	5.388	46.11
25% Percentile	6.620	5.630	50.82
Median	7.633	6.768	60.82
75% Percentile	8.888	7.383	61.75
Maximum	9.470	8.563	69.15
P value	0.0006	0.0006	

Table S2: Table shows median and data range values represented as box plot in Fig 4.1

Time [hours]	Yeast		Yeast + gacA *Pe*		Yeast + Pvf *Pe*		Yeast + Live *Pe*	
	Mean	SEM	Mean	SEM	Mean	SEM	Mean	SEM
0.00	0.00	0.00	0.00	0.00	0.00	0.00	0.00	0.00
0.50	4.59	0.60	6.09	1.64	4.88	0.96	7.19	0.73
1.00	2.74	1.73	3.96	1.03	3.21	1.09	7.64	1.99
1.50	3.04	1.50	2.10	1.04	2.95	0.62	5.75	1.04
2.00	2.61	1.10	3.45	0.96	3.56	0.90	11.67	3.10
2.50	3.29	1.14	2.59	1.20	3.96	0.94	16.02	1.36
3.00	4.02	0.93	2.71	0.87	3.05	1.24	22.28	4.96
3.50	4.47	1.01	2.67	0.66	2.26	0.67	30.40	2.25
4.00	4.98	1.29	1.62	0.86	2.04	0.77	33.37	3.19
4.50	5.56	1.04	3.11	0.72	3.29	1.83	44.01	3.65
5.00	6.25	1.25	2.92	1.10	3.75	1.51	43.91	3.86
5.50	6.42	1.53	2.08	1.01	4.84	1.65	51.84	3.22
6.00	5.78	0.58	1.23	0.82	7.15	4.41	54.28	1.95
6.50	6.67	1.28	2.81	1.12	6.78	2.57	67.06	2.86
7.00	6.62	1.22	2.52	0.97	8.80	2.92	62.50	2.03
7.50	7.63	0.86	1.80	0.88	8.30	2.44	61.68	3.80
8.00	7.77	0.87	4.27	0.99	9.65	3.81	63.87	3.08
8.50	8.72	0.97	2.64	0.65	10.15	3.75	71.09	4.20
9.00	8.88	0.41	3.03	0.95	12.75	5.38	71.84	0.4

9.50	8.59	0.77	4.77	1.40	12.22	4.87	75.00	4.38
10.00	7.89	1.04	4.15	1.23	16.32	7.33	66.56	0.42
10.50	8.68	0.52	6.22	0.96	16.44	7.09	74.48	3.54
11.00	9.48	1.52	7.68	0.91	17.02	6.82	75.22	4.07
11.50	11.27	1.43	6.04	1.09	15.54	5.83	74.39	3.25
12.00	12.09	1.34	6.53	1.93	18.41	7.30	76.26	4.14

Table S3: Table shows mean ± SEM values of evasion percentage for each condition and every time point.

	Yeast	Yeast + gac *Pe*	Yeast + pvf *Pe*	Yeast + live *Pe*
Minimum	5.788	1.238	6.910	54.29
25% Percentile	6.620	1.800	8.010	61.68
Median	7.633	2.645	8.688	63.87
75% Percentile	8.720	3.030	10.52	71.09
Maximum	8.888	4.272	14.22	71.85

Table S4: Table shows median and data range values represented as box plot in Fig 4.2B

Time [hours]	Yeast + Dead *Pe*		Yeast + Live *Pe*	
	Mean	SEM	Mean	SEM
0.00	0.00	0.00	0.00	0.00
0.50	5.00	0.00	15.00	2.88
1.00	3.33	3.33	23.33	1.66
1.50	6.66	4.40	30.00	2.88
2.00	10.00	5.77	35.00	2.88
2.50	10.00	2.88	48.33	6.00
3.00	20.00	2.88	51.66	3.33
3.50	25.00	5.00	43.33	3.33
4.00	28.33	3.33	53.33	8.81
4.50	25.00	8.66	50.00	7.63

5.00	23.33	4.40	50.00	7.63
5.50	21.66	9.27	56.66	11.66
6.00	21.66	4.40	50.00	15.27
6.50	28.33	4.40	55.00	10.40
7.00	25.00	5.77	50.00	5.77
7.50	20.00	5.00	56.66	9.27
8.00	16.66	4.40	56.66	14.52
8.50	10.00	5.77	51.66	3.33
9.00	10.00	5.77	50.00	7.63
9.50	15.00	5.00	51.66	7.26
10.00	23.33	3.33	50.00	10.00
10.50	16.66	3.33	48.33	9.27
11.00	13.33	4.40	58.33	7.26
11.50	15.00	2.88	55.00	12.58
12.00	13.33	1.66	50.00	7.63

Table S5: Table shows mean ± SEM values of evasion percentage for each condition and every time point.

	Yeast + Dead *Pe*, n=7	**Yeast + Live *Pe*, n=7**
Minimum	10.00	50.00
25% Percentile	10.00	50.00
Median	20.00	51.67
75% Percentile	25.00	56.67
Maximum	28.33	56.67

Table S6: Table shows median and data range values represented as box plot in Fig 4.3B

Time [hours]	Yeast + Dead *Pe*		Yeast + Live *Pe*	
	Mean	SEM	Mean	SEM
0.00	0.00	0.00	0.00	0.00
0.50	0.00	0.00	1.66	1.66
1.00	0.00	0.00	6.66	1.66
1.50	1.66	1.66	3.33	1.66
2.00	1.66	1.66	16.66	6.66
2.50	1.66	1.66	15.00	2.88
3.00	5.00	5.00	10.00	2.88
3.50	1.66	1.66	21.66	7.26
4.00	5.00	5.00	30.00	2.88
4.50	5.00	5.00	38.33	1.66
5.00	1.66	1.66	35.00	5.00
5.50	1.66	1.66	45.00	5.00
6.00	8.33	4.40	51.66	9.27
6.50	5.00	0.00	50.00	8.66
7.00	3.33	1.66	56.66	4.40
7.50	6.66	6.66	50.00	5.77
8.00	8.33	4.40	61.66	10.92
8.50	6.66	4.40	60.00	15.27
9.00	5.00	2.88	51.66	10.92
9.50	8.33	4.40	58.33	4.40
10.00	1.66	1.66	58.33	8.81
10.50	3.33	1.66	58.33	3.33
11.00	3.33	1.66	61.66	6.66
11.50	10.00	0.00	58.33	4.40
12.00	10.00	5.77	60.00	5.77

Table S7: Table shows mean ± SEM values of evasion percentage for each condition and every time point.

	Yeast + Dead *Pe*	Yeast + Live *Pe*
Minimum	3.333	50.00
25% Percentile	5.000	50.00
Median	6.667	51.67
75% Percentile	8.333	60.00
Maximum	8.333	61.67

Table S8: Table shows median and data range values represented as box plot in Fig 4.3D.

Time [hours]	Yeast		Yeast + dead *Pe*		Yeast + live *Pe*		Yeast + dead *Ecc15*		Yeast + live *Ecc15*	
	Mean	SEM	Mean	SEM	Mean	SEM	Mean	SEM	Mean	SEM
0.00	0.00	0.00	0.00	0.00	0.00	0.00	0.00	0.00	0.00	0.00
0.50	4.59	0.60	4.67	1.26	4.81	1.18	0.00	0.00	1.43	0.90
1.00	2.74	1.73	3.14	0.47	4.38	0.97	0.00	0.00	1.33	0.83
1.50	3.04	1.50	2.03	0.56	3.88	0.87	0.00	0.00	1.88	0.80
2.00	2.61	1.10	1.92	0.32	6.76	1.92	0.98	0.98	1.86	0.77
2.50	3.29	1.14	2.83	0.65	8.73	2.21	0.00	0.00	1.33	0.83
3.00	4.02	0.93	3.54	1.27	13.82	2.98	0.98	0.98	2.89	1.45
3.50	4.47	1.01	4.42	0.83	18.12	1.73	0.98	0.98	2.29	0.86
4.00	4.98	1.29	3.26	0.67	23.43	1.40	1.93	0.96	1.55	0.90
4.50	5.56	1.04	4.97	1.48	34.63	0.29	2.91	1.69	2.31	0.88
5.00	6.25	1.25	4.77	1.19	36.87	3.24	1.93	0.96	2.29	0.86
5.50	6.42	1.53	4.61	1.06	45.67	4.21	2.91	1.69	4.16	1.57
6.00	5.78	0.58	5.78	0.87	46.11	3.51	0.98	0.98	2.03	0.74
6.50	6.67	1.28	5.38	0.79	50.81	3.60	2.91	1.69	3.72	1.73
7.00	6.62	1.22	6.89	2.01	52.06	2.37	1.93	0.96	3.40	1.29
7.50	7.63	0.86	5.63	1.43	61.00	5.83	2.94	2.94	2.72	1.12
8.00	7.77	0.87	6.76	1.09	61.75	3.23	2.94	2.94	3.52	0.84
8.50	9.47	1.02	8.56	2.19	60.82	4.15	5.79	2.89	5.52	0.65
9.00	8.88	0.41	7.38	1.58	69.14	6.30	5.56	3.10	6.45	1.16
9.50	8.59	0.77	8.60	1.86	67.38	4.26	1.90	1.90	6.69	0.60

10.00	7.89	1.04	9.47	2.84	73.25	6.62	6.83	5.46	8.12	2.49
10.50	8.68	0.52	10.37	2.68	71.18	2.91	5.82	3.39	7.51	1.50
11.00	9.48	1.52	10.74	2.31	70.56	4.84	5.53	1.94	9.82	1.70
11.50	11.27	1.43	11.39	2.82	75.54	2.32	4.84	2.58	10.45	3.28
12.00	12.09	1.34	10.72	3.04	74.10	4.53	6.75	3.45	16.30	4.07

Table S9: Table shows mean evasion percentage ± SEM values for each condition and every time point.

	Yeast	Yeast + Dead *Pe*	Yeast + Live *Pe*	Yeast + Dead *Ecc15*	Yeast + Live *Ecc15*
Minimum	5.78	5.38	46.11	0.98	2.03
25% Percentile	6.62	5.63	50.82	1.93	2.72
Median	7.63	6.76	60.82	2.94	3.52
75% Percentile	8.88	7.38	61.75	5.56	5.52
Maximum	9.47	8.56	69.15	5.79	6.45

Table S10: Table shows median and data range values represented as box plot in Fig 4.4B.

Gene Name	Mean	SEM	Mean	SEM
Diptericin	1.000	0.8336	47.253	34.456
Defensin	1.000	0.1792	0.9653	0.1294
Drosomycin	1.000	2.7334	2.0183	2.0291

Table S11: Table shows mean ± SEM values for RNA expression of each gene.

	Yeast + dead *Pe*		Yeast + live *Pe*	
Time point	Mean	SEM	Mean	SEM
1hr	1.0000	0.2982	0.8875	0.2832
3hr	1.0000	0.2682	6.1301	1.6782
6hr	1.0000	0.1883	122.2747	17.4711
18hr	1.0000	0.1876	48.2250	7.1474

Table S12: Table shows mean ± SEM values for *Diptericin* mRNA expression at different time points after infection.

Time point	Yeast + dead *Pe*		Yeast + live *Pe*	
	Mean	SEM	Mean	SEM
1hr	1.0000	0.1533	0.8704	0.1171
3hr	1.0000	0.2299	0.4826	0.1254
6hr	1.0000	0.1108	5.9528	0.6216
18hr	1.0000	0.3176	3.9677	1.2546

Table S13: Table shows mean ± SEM values for *Drosomycin* mRNA expression at different time points after infection.

Time [hours]	$Rel^{E20}/+$, dead *Pe*		$Rel^{E20}/+$, live *Pe*		Rel^{E20}, dead *Pe*		Rel^{E20}, live *Pe*	
	Mean	SEM	Mean	SEM	Mean	SEM	Mean	SEM
0.00	0.00	0.00	0.00	0.00	0.00	0.00	0.00	0.00
0.50	4.28	1.50	0.00	0.00	1.03	0.51	6.64	0.88
1.00	2.50	0.42	0.90	0.90	1.56	0.03	7.23	0.54
1.50	0.86	0.86	1.74	0.47	1.56	0.03	8.72	0.98
2.00	0.85	0.49	1.74	0.87	1.03	0.51	14.52	3.28
2.50	0.39	0.39	4.81	1.68	1.03	0.51	16.68	2.55
3.00	1.56	1.56	8.78	3.72	1.53	0.86	16.69	1.83
3.50	0.85	0.49	11.19	2.20	1.03	0.51	16.23	4.52
4.00	0.85	0.49	10.80	0.67	1.03	0.51	19.99	3.79
4.50	1.63	1.10	23.21	4.28	1.03	0.51	18.83	3.31
5.00	1.31	0.87	18.09	0.45	1.07	1.07	27.52	2.66
5.50	2.09	1.22	28.27	4.75	1.57	0.93	24.60	3.91
6.00	1.17	1.17	28.02	4.38	1.03	0.51	29.97	4.30
6.50	1.64	0.95	34.61	4.16	1.03	0.51	31.67	4.26
7.00	2.95	1.71	34.07	4.77	1.03	0.51	40.67	5.41
7.50	3.09	1.15	38.46	7.34	1.53	0.86	42.93	1.97
8.00	3.87	1.40	37.81	6.43	2.07	1.03	45.16	3.31
8.50	3.88	0.80	50.48	7.39	0.99	0.99	51.00	3.49
9.00	4.81	0.49	48.81	10.28	1.03	0.51	53.47	3.42

9.50	3.42	0.58	52.64	7.07	1.53	0.86	59.53	3.05
10.00	3.81	0.91	54.98	7.12	1.57	0.93	61.19	4.36
10.50	5.66	1.35	58.66	3.45	1.02	0.51	64.80	5.21
11.00	5.99	0.89	52.22	3.98	1.06	0.53	63.96	3.57
11.50	4.35	0.48	62.24	5.94	1.56	0.03	67.16	4.32
12.00	2.96	0.68	60.58	8.31	3.67	1.44	72.35	1.60

Table S14: Table shows mean evasion percentage ± SEM values at each time point for each condition.

	Rel^{E20}/ +, live *Pe*	**Rel ^{E20},live *Pe***
Minimum	28.02	29.97
25% Percentile	34.08	31.67
Median	37.81	42.93
75% Percentile	48.82	51.01
Maximum	50.48	51.41

Table S15: Table shows median and data range values represented as box plot in Fig 4.6B.
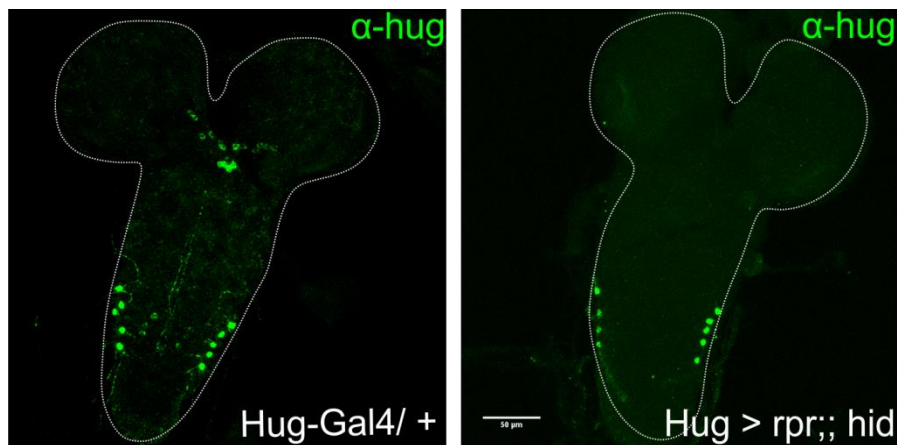
Figure S1: Hugin ablation using UAS rpr;; UAS hid.

Time [hours]	Hug-Gal4/ +, dead *Pe*		UAS rpr;; UAS hid, dead *Pe*		Hug > UAS rpr;; UAS hid, dead *Pe*	
	Mean	SEM	Mean	SEM	Mean	SEM
0.00	0.00	0.00	0.00	0.00	0.00	0.00
0.50	3.21	2.23	1.50	0.76	2.78	2.78
1.00	3.92	2.17	0.00	0.00	0.00	0.00
1.50	3.09	1.56	0.74	0.74	1.35	1.35
2.00	0.83	0.83	0.00	0.00	4.13	1.43
2.50	0.00	0.00	0.00	0.00	1.35	1.35
3.00	0.00	0.00	0.33	0.33	1.35	1.35
3.50	0.00	0.00	1.07	0.64	0.00	0.00
4.00	0.00	0.00	0.67	0.67	0.00	0.00
4.50	0.00	0.00	1.50	0.76	2.78	2.78
5.00	0.00	0.00	0.33	0.33	0.00	0.00
5.50	0.00	0.00	1.33	1.33	0.00	0.00
6.00	1.24	0.64	0.00	0.00	0.00	0.00
6.50	0.00	0.00	1.50	0.76	0.00	0.00
7.00	0.00	0.00	2.56	2.08	0.00	0.00
7.50	0.83	0.83	0.33	0.33	0.00	0.00
8.00	0.53	0.53	1.91	0.46	0.00	0.00
8.50	0.53	0.53	5.07	2.47	4.13	1.43
9.00	0.71	0.71	1.81	1.34	0.00	0.00
9.50	1.24	0.64	2.74	1.18	2.78	2.78
10.00	1.36	0.73	0.83	0.83	0.00	0.00
10.50	2.72	1.46	3.07	0.97	0.00	0.00
11.00	1.36	0.73	2.00	1.53	2.78	2.78
11.50	3.86	3.10	2.00	1.53	0.00	0.00
12.00	3.13	0.82	2.65	1.00	0.00	0.00

Time [hours]	Hug-Gal4/ +, live *Pe*		UAS rpr;; UAS hid, live *Pe*		Hug> UAS rpr;; UAS hid, live *Pe*	
	Mean	SEM	Mean	SEM	Mean	SEM
0.00	0.00	0.00	0.00	0.00	0.00	0.00
0.50	4.20	1.45	0.00	0.00	3.05	1.67
1.00	7.85	2.22	0.00	0.00	2.03	0.25
1.50	4.60	1.69	3.34	1.81	4.19	0.31
2.00	5.79	1.95	5.42	1.72	3.88	0.88
2.50	7.73	3.29	14.24	2.41	3.19	1.55
3.00	11.89	3.12	17.14	1.64	3.60	1.33
3.50	16.16	2.30	24.27	4.14	7.38	1.84
4.00	28.23	3.47	33.66	4.14	6.41	2.52
4.50	32.59	1.33	34.90	3.11	13.27	2.38
5.00	36.08	3.08	42.06	4.24	12.32	0.70
5.50	40.61	5.26	44.34	3.23	18.82	1.76
6.00	49.25	4.54	52.43	3.76	19.69	3.78
6.50	51.36	2.79	62.98	2.58	23.29	2.59
7.00	50.74	4.95	62.55	3.60	29.79	3.67
7.50	57.36	0.90	66.79	6.27	31.87	5.08
8.00	57.90	3.11	73.47	4.12	34.14	5.38
8.50	67.87	3.37	64.26	7.46	37.67	3.46
9.00	70.40	1.04	77.09	4.99	36.84	2.90
9.50	76.35	3.63	72.37	6.96	42.80	2.01
10.00	71.69	4.13	76.41	7.21	52.26	4.74
10.50	76.05	5.73	78.30	3.97	58.27	3.84
11.00	82.51	4.11	76.20	4.49	54.43	6.55
11.50	83.82	3.31	77.11	6.85	54.13	1.70
12.00	82.87	1.99	76.73	6.11	61.15	2.20

Table S17: Mean evasion percentage ± SEM values at each time point for each condition.

	Hug-Gal4/ +, live *Pe*	UAS rpr;; UAS hid, live *Pe*	Hug> UAS rpr;; hid, live *Pe*
Minimum	49.25	52.43	19.69
25% Percentile	50.74	62.55	23.29
Median	57.36	64.26	31.87
75% Percentile	67.87	73.47	36.84
Maximum	70.40	77.09	37.67

Table S18: Table shows median and data range values represented as box plot in Fig 4.7B

Time [hours]	Hug-Gal4/ +, dead *Pe*		UAS Kir2.1/ +, dead *Pe*		Hug> Kir2.1, dead *Pe*	
	Mean	SEM	Mean	SEM	Mean	SEM
0.00	0.00	0.00	0.00	0.00	0.00	0.00
0.50	3.21	2.23	0.00	0.00	0.00	0.00
1.00	3.92	2.17	0.00	0.00	0.00	0.00
1.50	3.09	1.56	0.00	0.00	0.00	0.00
2.00	0.83	0.83	0.00	0.00	0.00	0.00
2.50	0.00	0.00	1.19	1.19	0.00	0.00
3.00	0.00	0.00	2.50	2.50	0.00	0.00
3.50	0.00	0.00	1.25	1.25	0.00	0.00
4.00	0.00	0.00	2.38	2.38	0.00	0.00
4.50	0.00	0.00	0.00	0.00	0.00	0.00
5.00	0.00	0.00	0.00	0.00	0.46	0.46
5.50	0.00	0.00	0.00	0.00	0.00	0.00
6.00	1.24	0.64	0.00	0.00	0.00	0.00
6.50	0.00	0.00	1.25	1.25	0.46	0.46
7.00	0.00	0.00	0.00	0.00	0.00	0.00
7.50	0.83	0.83	1.25	1.25	0.00	0.00
8.00	0.53	0.53	1.25	1.25	0.44	0.44
8.50	0.53	0.53	2.38	2.38	0.00	0.00
9.00	0.71	0.71	1.19	1.19	0.44	0.44
9.50	1.24	0.64	1.19	1.19	0.89	0.89

Time [hours]						
10.00	1.36	0.73	1.25	1.25	0.44	0.44
10.50	2.72	1.46	0.00	0.00	0.91	0.45
11.00	1.36	0.73	0.00	0.00	1.33	1.33
11.50	3.86	3.10	1.19	1.19	0.44	0.44
12.00	3.13	0.82	1.25	1.25	0.46	0.46

Time [hours]	Hug-Gal4/ +, live *Pe*		UAS Kir2.1/ +, live *Pe*		Hug> Kir2.1, live *Pe*	
	Mean	SEM	Mean	SEM	Mean	SEM
0.00	0.00	0.00	0.00	0.00	0.00	0.00
0.50	4.20	1.45	3.13	1.16	0.00	0.00
1.00	7.85	2.22	5.01	1.80	2.32	0.80
1.50	4.60	1.69	5.43	2.61	1.67	0.97
2.00	5.79	1.95	10.64	3.91	1.75	0.75
2.50	7.73	3.29	15.12	4.61	3.99	0.95
3.00	11.89	3.12	24.36	5.02	5.70	0.72
3.50	16.16	2.30	32.53	5.30	8.88	1.57
4.00	28.23	3.47	39.02	6.18	10.79	1.69
4.50	32.59	1.33	44.54	3.90	10.99	1.38
5.00	36.08	3.08	52.51	3.03	13.31	2.53
5.50	40.61	5.26	56.40	4.26	16.67	1.99
6.00	49.25	4.54	54.65	5.07	19.12	3.48
6.50	51.36	2.79	62.60	5.43	25.02	2.02
7.00	50.74	4.95	63.55	5.00	28.98	2.00
7.50	57.36	0.90	68.89	3.40	37.26	2.47
8.00	57.90	3.11	72.64	4.21	35.52	4.91
8.50	67.87	3.37	70.90	3.68	45.49	1.11
9.00	70.40	1.04	73.60	3.09	49.28	3.04
9.50	76.35	3.63	78.59	3.59	49.04	3.10
10.00	71.69	4.13	80.15	3.13	52.80	5.15
10.50	76.05	5.73	79.33	3.46	58.47	2.90
11.00	82.51	4.11	87.55	1.91	61.59	2.42

11.50	83.82	3.31	86.59	1.84	62.17	4.05
12.00	82.87	1.99	89.81	0.68	61.60	1.83

Table S19: Mean evasion percentage ± SEM values at each time point for each condition.

	Hug-Gal4/ +, live *Pe*	UAS Kir2.1/ +, live *Pe*	Hug> Kir2.1, live *Pe*
Minimum	49.25	54.65	19.12
25% Percentile	50.74	62.60	25.02
Median	57.36	68.89	35.52
75% Percentile	67.87	72.64	45.49
Maximum	70.40	73.59	49.28

Table S20: Table shows median and data range values represented as box plot in Fig 4.7D.

Time [hours]	HugS3> lacZ RNAi, dead *Pe*		HugS3> lacZ RNAi, live *Pe*		HugS3> hug RNAi, dead *Pe*		HugS3> hug RNAi, live *Pe*	
	Mean	SEM	Mean	SEM	Mean	SEM	Mean	SEM
0.00	0.00	0.00	0.00	0.00	0.00	0.00	0.00	0.00
0.50	2.09	2.09	1.41	1.05	0.58	0.58	3.60	0.76
1.00	3.13	3.13	4.89	1.91	1.28	1.28	3.23	0.77
1.50	2.08	0.00	3.90	2.24	0.64	0.64	3.23	0.77
2.00	1.04	1.04	3.94	1.68	0.00	0.00	1.61	0.88
2.50	1.04	1.04	9.74	2.09	0.00	0.00	2.91	0.81
3.00	0.00	0.00	14.46	3.51	0.00	0.00	3.51	1.39
3.50	0.00	0.00	16.78	2.98	0.00	0.00	4.39	0.98
4.00	0.00	0.00	24.41	4.61	0.00	0.00	6.59	1.52
4.50	0.00	0.00	29.18	5.73	0.64	0.64	8.07	1.67
5.00	1.04	1.04	30.08	4.86	0.64	0.64	10.20	2.81
5.50	0.00	0.00	33.23	4.50	0.00	0.00	10.84	2.63
6.00	0.00	0.00	33.48	5.93	0.00	0.00	12.57	1.34
6.50	1.04	1.04	35.61	5.34	0.00	0.00	16.62	2.55
7.00	1.04	1.04	44.45	2.75	0.00	0.00	20.11	1.95
7.50	1.04	1.04	45.55	3.30	0.64	0.64	19.83	2.91
8.00	0.00	0.00	49.72	4.62	1.22	0.61	23.35	2.22
8.50	0.00	0.00	53.89	4.09	0.64	0.64	25.86	2.44

9.00	0.00	0.00	54.44	6.01	0.64	0.64	28.99	1.85
9.50	0.00	0.00	58.69	4.06	1.27	0.64	28.80	2.18
10.00	1.04	1.04	58.02	5.51	0.64	0.64	35.99	3.61
10.50	2.09	2.09	58.10	4.49	1.27	0.64	38.04	4.19
11.00	1.04	1.04	61.47	5.59	1.85	0.05	38.33	2.59
11.50	1.04	1.04	63.98	5.65	2.50	0.68	45.14	3.29
12.00	1.04	1.04	66.76	5.13	3.08	0.60	45.83	3.91

Table S20: Mean evasion percentage ± SEM values at each time point for each condition.

	HugS3> lacZ RNAi, live *Pe* n = 7	HugS3> hug RNAi, live *Pe* n =7
Minimum	33.48	12.57
25% Percentile	35.61	16.62
Median	45.55	20.11
75% Percentile	53.89	25.86
Maximum	54.44	28.99

Table S21: Table shows median and data range values represented as box plot in Fig 4.8B.

Time [hours]	OrgR, dead *Pe*		OrgR, live *Pe*		OrgR- 6 hr starved, dead *Pe*		OrgR- 6hr starved, live *Pe*	
	Mean	SEM	Mean	SEM	Mean	SEM	Mean	SEM
0.00	0.00	0.00	0.00	0.00	0.00	0.00	0.00	0.00
0.50	5.72	0.64	6.41	3.88	0.67	0.67	3.88	0.87
1.00	2.81	0.49	4.31	7.34	0.67	0.67	7.34	1.87
1.50	1.15	1.15	3.62	3.06	0.00	0.00	3.06	0.84
2.00	0.52	0.52	8.14	5.79	0.67	0.67	5.79	2.74
2.50	0.52	0.52	12.29	6.72	0.00	0.00	6.72	2.21
3.00	2.08	2.08	26.60	7.51	0.33	0.33	7.51	2.77
3.50	0.52	0.52	29.80	9.11	1.00	0.58	9.11	2.08
4.00	0.52	0.52	30.59	6.62	1.33	0.67	6.62	1.22
4.50	1.56	1.56	38.24	9.11	0.67	0.67	9.11	2.08
5.00	0.52	0.52	44.82	8.44	2.33	0.88	8.44	2.81
5.50	1.56	1.56	50.93	13.41	2.67	0.67	13.41	6.04
6.00	1.56	1.56	55.08	13.63	2.67	1.33	13.63	5.33
6.50	2.19	1.10	59.35	23.17	3.33	0.67	23.17	5.00
7.00	2.08	2.08	58.31	27.36	1.67	1.20	27.36	9.11

7.50	2.90	1.61	67.78	21.30	1.67	1.20	21.30	6.19
8.00	3.32	1.81	69.84	27.08	1.67	1.20	27.08	7.68
8.50	3.33	0.82	72.80	37.35	2.67	0.33	37.35	8.33
9.00	4.57	0.61	74.79	34.23	1.00	0.58	34.23	6.20
9.50	3.95	0.38	75.64	39.80	2.00	0.58	39.80	10.20
10.00	3.85	1.29	79.06	37.85	2.67	1.33	37.85	7.84
10.50	4.47	0.89	74.50	44.34	2.67	0.67	44.34	6.52
11.00	6.14	1.25	78.74	44.67	3.67	1.45	44.67	6.89
11.50	4.57	0.61	79.59	43.61	3.00	1.53	43.61	6.24
12.00	3.33	0.82	81.40	46.55	1.67	0.33	46.55	4.13

Table S22: Mean evasion percentage ± SEM values at each time point for each condition.

	OrgR, live *Pe*, n=7	OrgR- starved, live *Pe*, n=7
Minimum	56.42	13.63
25% Percentile	57.15	21.30
Median	65.84	27.08
75% Percentile	71.63	34.23
Maximum	76.82	37.35

Table S23: Table shows median and data range values represented as box plot in Fig 4.10B.
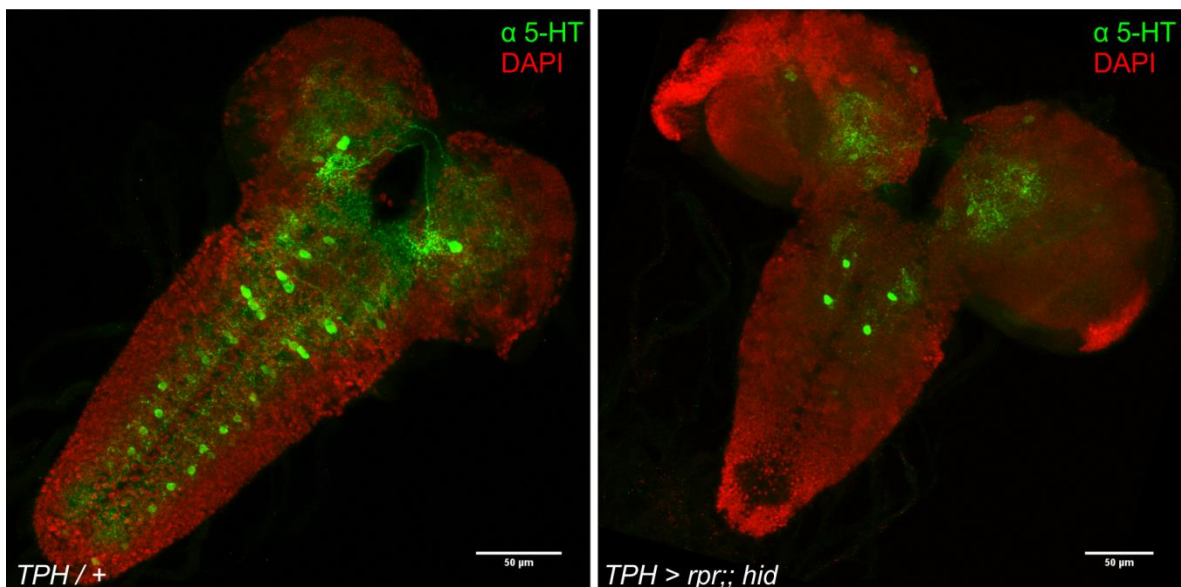
Figure S2: Ablation of serotonin (5-HT) positive cells using UAS-rpr;;UAS-hid.

Time [hours]	TPH > OrgR , dead Pe		UAS rpr;; UAS hid, dead Pe		TPH > RH , dead Pe	
0.00	0.00	0.00	0.00	0.00	0.00	0.00
0.50	0.00	0.00	1.00	1.00	1.28	1.28
1.00	0.00	0.00	0.00	0.00	0.00	0.00
1.50	0.00	0.00	1.11	1.11	2.50	2.50
2.00	0.00	0.00	0.00	0.00	0.00	0.00
2.50	0.00	0.00	0.00	0.00	0.00	0.00
3.00	1.43	1.43	0.50	0.50	1.25	1.25
3.50	0.00	0.00	1.61	0.61	2.50	2.50
4.00	0.00	0.00	1.00	1.00	2.50	2.50
4.50	0.00	0.00	1.00	1.00	1.25	1.25
5.00	2.50	2.50	0.50	0.50	1.25	1.25
5.50	0.00	0.00	2.00	2.00	3.78	1.22
6.00	0.00	0.00	0.00	0.00	2.50	2.50
6.50	0.00	0.00	1.00	1.00	2.50	2.50
7.00	2.50	2.50	3.84	2.84	2.50	2.50
7.50	0.00	0.00	0.50	0.50	3.75	3.75
8.00	0.00	0.00	1.61	0.61	2.50	2.50
8.50	1.43	1.43	2.61	0.39	1.25	1.25
9.00	2.50	2.50	2.72	1.72	2.50	2.50
9.50	0.00	0.00	1.61	0.61	1.25	1.25
10.00	1.43	1.43	0.00	0.00	2.50	2.50
10.50	0.00	0.00	2.11	0.11	2.50	2.50
11.00	0.00	0.00	0.50	0.50	2.50	2.50
11.50	4.29	4.29	0.50	0.50	5.03	2.47
12.00	4.29	4.29	2.72	1.72	5.07	0.07

Time [hours]	TPH > OrgR ,live Pe		UAS rpr;; hid, live Pe		TPH > rpr;; hid , live Pe	
	Mean	SEM	Mean	SEM	Mean	SEM
0.00	0.00	0.00	0.00	0.00	0.00	0.00
0.50	0.00	0.00	0.00	0.00	0.00	0.00
1.00	2.19	0.15	0.00	0.00	2.09	2.09
1.50	2.19	0.15	3.34	1.81	6.44	1.89
2.00	3.35	1.31	5.42	1.72	8.71	0.38
2.50	5.39	0.73	14.24	2.41	28.03	5.30
3.00	19.51	0.90	17.14	1.64	36.93	0.57
3.50	34.20	7.67	24.27	4.14	43.56	1.89
4.00	43.95	7.22	33.66	4.14	54.55	4.55

4.50	44.69	1.82	34.90	3.11	56.63	2.46
5.00	56.03	9.09	42.06	4.24	69.70	3.03
5.50	64.76	9.66	44.34	3.23	71.78	0.95
6.00	63.46	6.31	52.43	3.76	84.85	1.52
6.50	72.78	0.69	62.98	2.58	78.03	5.30
7.00	74.82	2.73	62.55	3.60	74.25	7.58
7.50	81.80	4.25	66.79	6.27	93.37	2.46
8.00	82.09	8.61	73.47	4.12	84.85	1.52
8.50	66.52	3.25	64.26	7.46	89.02	2.65
9.00	71.02	5.72	77.09	4.99	78.22	0.95
9.50	82.23	10.80	72.37	6.96	89.02	2.65
10.00	84.13	6.57	76.41	7.21	86.93	0.57
10.50	86.59	11.08	78.30	3.97	91.29	0.38
11.00	83.11	7.59	76.20	4.49	88.83	7.01
11.50	85.60	4.20	77.11	6.85	95.46	4.54
12.00	83.56	2.15	76.73	6.11	91.10	4.74

Table S24: Mean evasion percentage ± SEM values at each time point for each condition.

	TPH > OrgR, live *Pe*	UAS rpr;; UAS hid, live *Pe*	TPH > rpr;; hid, live *Pe*
Minimum	66.52	62.55	74.25
25% Percentile	71.02	62.98	78.03
Median	74.82	66.79	84.85
75% Percentile	82.09	73.47	89.02
Maximum	82.23	77.09	93.37

Table S25: Table shows median and data range values represented as box plot in Fig 4.13B.

Time [hours]	TRH/ +, dead *Pe*		UAS-Kir2.1/ +, dead *Pe*		TRH > Kir2.1, dead *Pe*	
	Mean	SEM	Mean	SEM	Mean	SEM
0.00	0.00	0.00	0.00	0.00	0.00	0.00
0.50	1.28	1.28	0.00	0.00	1.09	1.09
1.00	0.00	0.00	0.00	0.00	0.00	0.00
1.50	2.50	2.50	0.00	0.00	2.28	0.11
2.00	0.00	0.00	0.00	0.00	0.00	0.00
2.50	0.00	0.00	1.19	1.19	2.38	2.38
3.00	1.25	1.25	2.50	2.50	2.38	2.38

3.50	2.50	2.50	1.25	1.25	0.00	0.00
4.00	2.50	2.50	2.38	2.38	3.57	3.57
4.50	1.25	1.25	0.00	0.00	0.00	0.00
5.00	1.25	1.25	0.00	0.00	1.09	1.09
5.50	3.78	1.22	0.00	0.00	2.18	2.18
6.00	2.50	2.50	0.00	0.00	4.76	4.76
6.50	2.50	2.50	1.25	1.25	3.09	0.91
7.00	2.50	2.50	0.00	0.00	4.66	2.49
7.50	3.75	3.75	1.25	1.25	4.76	4.76
8.00	2.50	2.50	1.25	1.25	3.47	1.30
8.50	1.25	1.25	2.38	2.38	3.00	3.00
9.00	2.50	2.50	1.19	1.19	4.66	2.49
9.50	1.25	1.25	1.19	1.19	3.47	1.30
10.00	2.50	2.50	1.25	1.25	6.94	2.59
10.50	2.50	2.50	0.00	0.00	8.02	1.50
11.00	2.50	2.50	0.00	0.00	5.75	1.40
11.50	5.03	2.47	1.19	1.19	5.75	1.40
12.00	5.07	0.07	1.25	1.25	7.04	4.87

Table S26: Mean evasion percentage ± SEM values at each time point for each condition.

	TRH-Gal4/ +, live *Pe*	UAS Kir2.1/ +, live *Pe*	TRH > Kir2.1, live *Pe*
Minimum	52.65	62.19	67.17
25% Percentile	61.00	68.52	71.60
Median	64.70	75.12	85.26
75% Percentile	70.53	78.63	85.95
Maximum	73.40	81.72	88.54

Table S27: Table shows median and data range values represented as box plot in Fig 4.11D

	Yeast + Dead *Pe*		Yeast + Live *Pe*		
Gene Name	Geo Mean	SEM	Geo Mean	SEM	p value
ChAT	1.0000	0.3107	1.0925	0.2154	0.8159
TRH	1.0000	0.3104	0.8655	0.1718	0.7044
ple	1.0000	0.2056	1.3106	0.2171	0.3619
Ast A	1.0000	0.1527	1.0814	0.1156	0.6961
Mip	1.0000	0.2214	1.8092	0.2676	0.1089
Ast C	1.0000	0.2563	1.0140	0.1749	0.9696
CCHa1	1.0000	0.1442	3.5819	0.3087	0.0017
CCHa2	1.0000	0.0777	1.2355	0.1783	0.2851
Crz	1.0000	0.0796	0.7074	0.0685	0.0522
Dh31	1.0000	0.2760	1.7499	0.2029	0.1681
Dh44	1.0000	0.1791	1.3010	0.1050	0.2334
Dilp2	1.0000	0.2338	0.7980	0.0550	0.3592
Dilp3	1.0000	0.8651	1.9155	0.8337	0.5629
Dms	1.0000	0.1443	0.9410	0.0804	0.7468
Hug	1.0000	0.1792	0.9077	0.0181	0.6499
Lst	1.0000	0.5619	1.8125	0.8274	0.4562
NPF	1.0000	0.1881	0.9703	0.0506	0.8747
sNPF	1.0000	0.3599	1.5072	0.1356	0.2652
Painless	1.0000	0.0610	0.7535	0.0253	0.0146
upd1	1.0000	0.5404	0.7582	0.1197	0.6875
upd2	1.0000	1.2492	46.9250	8.9597	0.0069
upd3	1.0000	0.3995	31.9470	7.5961	0.0011

Table S29: Mean ± SEM values of mRNA expression of candidate genes after 3 hours of infection

	Yeast + dead *Pe*		Yeast + live *Pe*		
Gene Name	Geo Mean	SEM	Geo Mean	SEM	p value
ChAT	1.0000	0.3253	1.0221	0.32950	0.9672
TRH	1.0000	0.1787	0.7935	0.30380	0.5672
ple	1.0000	0.4610	0.8081	0.39240	0.7851
AstA	1.0000	0.3687	0.7255	0.15440	0.5250
Mip	1.0000	0.2059	0.8345	0.17410	0.5942
AstC	1.0000	0.3338	0.7085	0.11120	0.4160
CCHa1	1.0000	0.3355	1.1793	0.42920	0.7277
CCHa2	1.0000	0.2622	0.6260	0.10510	0.2036
Crz	1.0000	0.2714	1.1153	0.30080	0.8035
Dh31	1.0000	0.2479	1.0427	0.32430	0.9290
Dh44	1.0000	0.2843	0.7866	0.32350	0.6936
Dilp2	1.0000	0.2359	0.7479	0.14750	0.4075
Dilp3	1.0000	0.5885	0.7942	0.21910	0.6948
Dms	1.0000	0.2564	1.1692	0.30210	0.6763
Hug	1.0000	0.0920	1.3706	0.22650	0.1871
Lst	1.0000	0.1824	1.0145	0.36660	0.9761
NPF	1.0000	0.1918	1.1454	0.27280	0.6664
sNPF	1.0000	0.2535	0.6015	0.08710	0.1593
Painless	1.0000	0.3014	0.5580	0.11240	0.1738
upd1	1.0000	0.1312	0.6606	0.33595	0.3809
upd2	1.0000	0.6760	28.900	25.2840	0.0120
upd3	1.0000	0.1902	10.571	8.36630	0.0186

Table S30: Mean ± SEM values of mRNA expression of candidate genes after 6 hours of infection.

Time [hours]	W^{1118}, dead *Pe*		W^{1118}, live *Pe*		upd2$^{\Delta}$, dead *Pe*		upd2$^{\Delta}$, live *Pe*	
	Mean	SEM	Mean	SEM	Mean	SEM	Mean	SEM
0.00	0.00	0.00	0.00	0.00	0.00	0.00	0.00	0.00
0.50	0.63	0.63	3.69	1.10	3.00	1.00	5.39	0.22
1.00	2.02	0.77	8.41	1.92	3.00	1.00	8.15	2.50
1.50	2.02	0.77	8.54	3.25	4.00	2.00	5.71	3.40
2.00	1.39	1.39	6.10	1.29	2.00	0.00	9.04	6.73
2.50	0.00	0.00	8.88	0.72	3.00	1.00	10.45	8.60
3.00	1.39	1.39	15.90	3.33	3.00	1.00	12.57	3.64
3.50	0.00	0.00	24.54	7.58	1.00	1.00	18.36	2.49
4.00	1.39	1.39	30.78	9.01	2.00	2.00	15.01	2.43
4.50	1.39	1.39	32.61	5.18	2.00	0.00	20.41	2.34
5.00	1.39	1.39	37.31	11.87	3.00	1.00	18.66	7.23
5.50	0.00	0.00	36.09	5.13	2.00	0.00	29.91	2.89
6.00	2.78	2.78	39.24	7.76	2.00	0.00	38.68	7.24
6.50	1.25	1.25	40.60	5.69	1.00	1.00	40.30	7.46
7.00	2.78	2.78	47.04	7.01	1.00	1.00	37.28	7.77
7.50	2.78	2.78	50.47	6.48	3.00	1.00	54.42	10.34
8.00	2.78	2.78	47.92	3.27	2.00	2.00	58.14	8.48
8.50	5.28	0.28	50.13	3.64	4.00	2.00	65.85	12.52
9.00	2.78	2.78	60.43	10.21	2.00	2.00	60.91	3.46
9.50	2.02	0.77	60.55	6.47	1.00	1.00	61.54	6.95
10.00	2.02	0.77	65.52	5.87	3.00	1.00	65.59	8.11
10.50	1.39	1.39	63.58	3.64	2.00	0.00	74.45	3.82
11.00	2.64	0.14	68.96	7.98	7.00	3.00	74.88	7.71
11.50	3.89	1.11	69.11	7.06	5.00	3.00	80.28	7.20
12.00	3.89	1.11	68.70	9.98	6.00	0.00	82.53	6.24

Table S31: Table shows mean ± SEM evasion values for each time point.

	W[1118], live *Pe*	upd2[Δ], live *Pe*
Minimum	39.24	37.28
25% Percentile	40.60	38.68
Median	47.92	54.42
75% Percentile	50.47	60.91
Maximum	60.43	65.85

Table S32: Shows median and data range represented by box plot in Fig 4.15B

Time [hour]	W[1118], dead *Pe*		W[1118], live *Pe*		upd3[Δ], dead *Pe*		upd3[Δ], live *Pe*	
	Mean	SEM	Mean	SEM	Mean	SEM	Mean	SEM
0.00	0.00	0.00	0.00	0.00	0.00	0.00	0.00	0.00
0.50	0.63	0.63	3.57	0.71	0.00	0.00	14.10	3.02
1.00	2.02	0.77	11.29	1.85	0.00	0.00	26.40	2.74
1.50	2.02	0.77	10.09	1.67	0.91	0.91	36.85	4.73
2.00	1.39	1.39	10.30	2.69	0.91	0.53	47.63	4.26
2.50	0.00	0.00	10.43	1.45	0.46	0.46	52.30	3.03
3.00	1.39	1.39	16.48	2.63	0.00	0.00	57.81	4.29
3.50	0.00	0.00	26.05	4.39	0.46	0.46	58.43	5.41
4.00	1.39	1.39	28.72	4.50	2.85	0.57	56.46	4.78
4.50	1.39	1.39	34.61	3.74	0.50	0.50	57.65	4.94
5.00	1.39	1.39	40.37	7.51	0.91	0.53	65.71	2.95
5.50	0.00	0.00	39.29	5.13	3.25	0.83	66.41	3.99
6.00	2.78	2.78	43.74	6.84	2.41	1.27	72.12	1.57
6.50	1.25	1.25	45.45	5.73	5.24	0.99	70.14	4.08
7.00	2.78	2.78	49.59	7.19	4.67	1.16	68.73	2.93
7.50	2.78	2.78	50.15	6.21	4.75	1.30	73.00	4.86
8.00	2.78	2.78	52.47	6.52	7.10	1.26	73.93	3.99
8.50	5.28	0.28	50.44	6.56	9.57	2.22	79.78	4.25
9.00	2.78	2.78	55.00	7.10	14.77	3.07	80.95	3.44
9.50	2.02	0.77	58.83	5.43	15.71	2.64	85.15	3.11
10.00	2.02	0.77	62.02	5.53	18.19	4.08	85.64	4.17
10.50	1.39	1.39	63.53	7.77	15.85	4.14	86.01	2.96
11.00	2.64	0.14	67.48	6.88	23.29	2.92	84.22	2.84
11.50	3.89	1.11	66.24	6.76	20.60	5.17	87.60	3.19
12.00	3.89	1.11	69.32	6.73	22.05	6.69	86.59	2.14

Table S33: Shows mean ± SEM evasion values for each time point.

	W^{1118}, live *Pe*	Upd3$^{\Delta}$, live *Pe*
Minimum	43.74	66.88
25% Percentile	45.45	68.13
Median	50.15	70.54
75% Percentile	52.47	75.25
Maximum	55.00	77.35

Table S34: Shows median and data range represented by box plot in Fig 4.15D

	OrgR, live *Pe*	Hug-Gal4/ +, live *Pe*	Hug > hug RNAi, live *Pe*	Hug > UAS RH, live *Pe*	Hug > Kir2.1, live *Pe*	upd2$^{\Delta}$, live *Pe*	upd3$^{\Delta}$, live *Pe*
Minimum	3.963	5.597	0.0	2.033	0.0	0.0	15.43
25% Percentile	4.008	5.654	1.135	2.793	1.473	1.925	27.22
Median	5.598	8.395	2.250	3.395	2.280	2.310	49.18
75% Percentile	10.16	10.42	11.31	3.957	4.480	5.980	54.97
Maximum	14.80	13.54	14.15	4.187	5.340	11.36	57.24
P values	0.0022	0.0022	0.0022	0.0022	0.0022	0.0012	

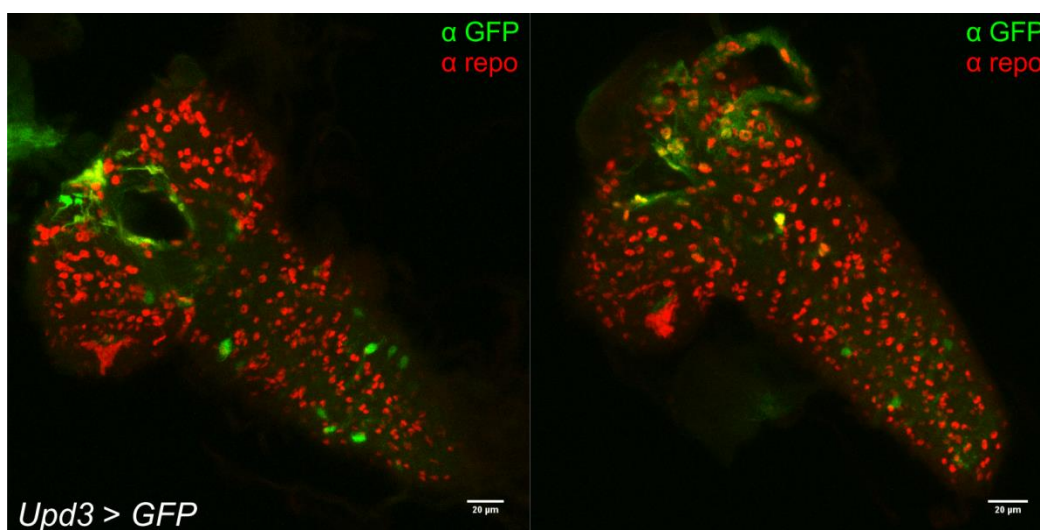Table S35: Shows median and data range represented by box plot in Fig 4.16

Figure S4: Upd3-Gal4 expressing UAS-mcd8::GFP larval brains were stained for GFP and repo. Images show non-specific and random binding of GFP on the brain samples.
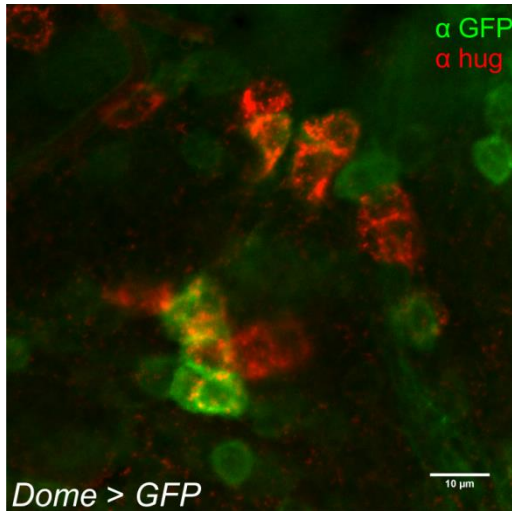
Figure S5: Dome-Gal4 x UAS-mcd8::GFP larval brains were stained for anti GFP and anti hugin.

Time [hours]	Hug-Gal4/ +, dead *Pe*		Hug-Gal4/ +, live *Pe*		Hug > dome$^\Delta$CYT, dead *Pe*		Hug > dome$^\Delta$CYT, live *Pe*	
	Mean	SEM	Mean	SEM	Mean	SEM	Mean	SEM
0.00	0.00	0.00	0.00	0.00	0.00	0.00	0.00	0.00
0.50	3.21	2.23	4.20	1.45	0.00	0.00	4.40	0.92
1.00	3.92	2.17	7.85	2.22	1.00	1.00	9.03	1.69
1.50	3.09	1.56	4.60	1.69	1.00	1.00	12.35	1.28
2.00	0.83	0.83	5.79	1.95	1.00	1.00	17.73	3.97
2.50	0.00	0.00	7.73	3.29	1.00	1.00	15.28	3.07
3.00	0.00	0.00	11.89	3.12	0.00	0.00	17.45	2.32
3.50	0.00	0.00	16.16	2.30	0.00	0.00	22.31	1.79
4.00	0.00	0.00	28.23	3.47	0.00	0.00	38.08	2.77
4.50	0.00	0.00	32.59	1.33	0.00	0.00	34.59	0.86
5.00	0.00	0.00	36.08	3.08	1.00	1.00	42.58	4.35
5.50	0.00	0.00	40.61	5.26	0.00	0.00	48.97	2.18
6.00	1.24	0.64	49.25	4.54	0.00	0.00	48.55	3.71
6.50	0.00	0.00	51.36	2.79	0.00	0.00	57.14	6.37
7.00	0.00	0.00	50.74	4.95	1.00	1.00	56.20	4.72
7.50	0.83	0.83	57.36	0.90	0.00	0.00	61.12	3.98

8.00	0.53	0.53	57.90	3.11	1.00	1.00	54.90	3.36
8.50	0.53	0.53	67.87	3.37	2.00	2.00	59.95	5.89
9.00	0.71	0.71	70.40	1.04	2.00	2.00	67.63	2.57
9.50	1.24	0.64	76.35	3.63	1.00	1.00	76.32	3.05
10.00	1.36	0.73	71.69	4.13	2.00	2.00	75.14	4.94
10.50	2.72	1.46	76.05	5.73	0.00	0.00	79.33	2.92
11.00	1.36	0.73	82.51	4.11	1.00	1.00	79.67	4.78
11.50	3.86	3.10	83.82	3.31	0.00	0.00	82.07	2.87
12.00	3.13	0.82	82.87	1.99	1.00	1.00	83.73	3.59

Table S36: Mean ± SEM evasion values for each time point.

	Hug-Gal4/ +, live *Pe*	**Hug > dome$^{\Delta}$CYT, live *Pe***
Minimum	49.25	48.55
25% Percentile	50.74	54.90
Median	57.36	57.14
75% Percentile	67.87	61.12
Maximum	70.40	67.63

Table S37: Shows median and whisker values represented by box plot in Fig 4.20B

Time [hours]	UAS-dome$^{\Delta}$CYT/ +, dead *Pe*		UAS-dome$^{\Delta}$CYT/ +, live *Pe*		ilp2 > dome$^{\Delta}$CYT, dead *Pe*		ilp2 > dome$^{\Delta}$CYT, live *Pe*	
	Mean	SEM	Mean	SEM	Mean	SEM	Mean	SEM
0.00	0.00	0.00	0.00	0.00	0.00	0.00	0.00	0.00
0.50	0.00	0.00	6.40	2.65	0.00	0.00	6.35	0.88
1.00	1.50	1.50	7.10	1.78	0.00	0.00	12.67	3.35
1.50	0.00	0.00	13.26	4.87	0.00	0.00	17.07	6.21
2.00	0.00	0.00	12.49	2.77	1.00	1.00	25.04	8.51
2.50	1.04	1.04	15.00	2.86	0.00	0.00	30.92	10.24
3.00	0.00	0.00	25.57	5.23	0.00	0.00	32.90	4.54
3.50	1.00	1.00	29.71	5.31	3.85	1.15	35.78	7.43
4.00	0.00	0.00	35.63	4.79	1.35	1.35	40.37	7.86
4.50	0.00	0.00	35.93	4.55	4.35	1.65	40.27	6.35
5.00	0.00	0.00	40.68	1.78	1.35	1.35	46.64	9.69
5.50	0.00	0.00	46.82	4.15	1.35	1.35	50.39	8.01
6.00	0.00	0.00	53.46	4.55	1.35	1.35	54.11	8.88
6.50	2.00	2.00	57.91	4.81	1.35	1.35	62.61	3.74
7.00	3.13	3.13	61.01	5.34	4.06	4.06	68.34	9.73
7.50	2.09	2.09	67.59	6.88	5.41	5.41	65.71	3.79
8.00	0.00	0.00	66.32	3.54	6.71	1.30	65.39	2.81
8.50	0.00	0.00	65.13	4.57	2.71	2.71	65.54	4.55
9.00	0.00	0.00	71.61	3.99	2.71	2.71	76.02	6.50
9.50	3.13	3.13	75.76	3.29	2.71	2.71	72.53	3.07
10.00	0.00	0.00	72.29	2.61	2.71	2.71	76.50	4.77
10.50	2.09	2.09	69.51	2.06	4.06	4.06	69.47	4.96
11.00	0.00	0.00	75.57	5.44	8.41	2.41	74.53	3.94
11.50	1.04	1.04	73.57	4.18	4.06	4.06	74.36	3.26
12.00	7.17	1.17	76.85	3.18	7.56	0.55	76.90	1.96

Table S38: Mean ± SEM evasion values for each time point.

	UAS-dome$^{\Delta}$CYT/ +, live *Pe*	dilp2 > dome$^{\Delta}$CYT, live *Pe*
Minimum	53.46	54.11

25% Percentile	57.91	62.61
Median	65.13	65.54
75% Percentile	67.59	68.34
Maximum	71.61	76.02

Table S39: Shows median and whisker values represented by box plot in Fig 4.22B

7.REFERENCES

Agaisse, H., Perrimon, N., Agaisse, H. and Perrimon, N. (2004) 'The roles of JAK/STAT signaling in Drosophila immune responses.', *Immunological reviews*, 198(1), pp. 72–82. doi: 10.1111/j.0105-2896.2004.0133.x.

Agaisse, H., Petersen, U. M., Boutros, M., Mathey-Prevot, B. and Perrimon, N. (2003) 'Signaling role of hemocytes in Drosophila JAK/STAT-dependent response to septic injury', *Developmental Cell*, 5(3), pp. 441–450. doi: 10.1016/S1534-5807(03)00244-2.

Akira, S., Uematsu, S. and Takeuchi, O. (2006) 'Pathogen Recognition and Innate Immunity', *Cell*, 124(4), pp. 783–801. doi: 10.1016/j.cell.2006.02.015.

Baganz, N. L. and Blakely, R. D. (2013) 'A dialogue between the immune system and brain, spoken in the language of serotonin', *ACS Chemical Neuroscience*, 4(1), pp. 48–63. doi: 10.1021/cn300186b.

Baines, R. a, Uhler, J. P., Thompson, a, Sweeney, S. T. and Bate, M. (2001) 'Altered electrical properties in Drosophila neurons developing without synaptic transmission.', *The Journal of neuroscience : the official journal of the Society for Neuroscience*, 21(5), pp. 1523–1531. doi: 21/5/1523 [pii].

Basset, A., Khush, R. S., Braun, A., Gardan, L., Boccard, F., Hoffmann, J. A. and Lemaitre, B. (2000) 'The phytopathogenic bacteria Erwinia carotovora infects Drosophila and activates an immune response.', *Proceedings of the National Academy of Sciences of the United States of America*, 97(7), pp. 3376–81. doi: 10.1073/pnas.070357597.

Bier, E. and Guichard, A. (2012) 'Deconstructing host-pathogen interactions in Drosophila', *Disease models & mechanisms*, 5, pp. 48–61. doi: 10.1242/dmm.000406.

Buchon, N., Broderick, N. A., Poidevin, M., Pradervand, S. and Lemaitre, B. (2009) 'Drosophila Intestinal Response to Bacterial Infection: Activation of Host Defense and Stem Cell Proliferation', *Cell Host and Microbe*. Elsevier Ltd, 5(2), pp. 200–211. doi: 10.1016/j.chom.2009.01.003.

Chandler, J. A., Lang, J. M., Bhatnagar, S. and Eisen, J. A. (2011) 'Bacterial Communities of Diverse Drosophila Species : Ecological Context of a Host – Microbe Model System', *PLoS Genetics*, 7(9). doi: 10.1371/journal.pgen.1002272.

Chiu, C. N., Rihel, J., Lee, D. A., Singh, C., Mosser, E. A., Chen, S., Sapin, V., Pham, U., Engle, J., Niles, B. J., Montz, C. J., Chakravarthy, S., Zimmerman, S., Salehi-Ashtiani, K., Vidal, M., Schier, A. F. and Prober, D. A. (2016) 'A Zebrafish Genetic Screen Identifies Neuromedin U as a Regulator of Sleep/Wake States', *Neuron*. Elsevier Inc., 89(4), pp. 842–856. doi: 10.1016/j.neuron.2016.01.007.

Clarke, T. B., Davis, K. M., Lysenko1, E. S., Zhou, A. Y., YuWeiser, Y. and N, J. (2010) 'Recognition of Peptidoglycan from the Microbiota by Nod1 Enhances Systemic Innate Immunity', *Nat Med*, 16(2), pp. 228–231. doi: 10.1038/nm.2087.Recognition.

Curtis, V. A. (2014) 'Infection-avoidance behaviour in humans and other animals', *Trends in Immunology*. Elsevier Ltd, 35(10), pp. 457–464. doi: 10.1016/j.it.2014.08.006.

Dantzer, R. (2001) 'Cytokine-induced sickness behavior: mechanisms and implications', *Ann N Y Acad Sci*, 933(33), pp. 222–234. doi: 10.1016/S0889-1591(02)00077-6.

Dantzer, R., Connor, J. C. O., Freund, G. G., Johnson, R. W. and Kelley, K. W. (2008) 'From inflammation to sickness and depression: when the immune system subjugates the brain', *Nat Rev Neuroscience*, 9(1), pp. 46–56. doi: 10.1038/nrn2297.From.

Dantzer, R. and Kelley, K. W. (2007) 'Twenty Years of Research on Cytokine-Induced Sickness Behavior', 21(2), pp. 153–160. doi: 10.1016/j.pestbp.2011.02.012.Investigations.

Farhan, A., Gulati, J., Große-Wilde, E., Vogel, H., Hansson, B. S. and Knaden, M. (2013) 'The CCHamide 1 receptor modulates sensory perception and olfactory behavior in starved Drosophila.', *Scientific reports*, 3, p. 2765. doi: 10.1038/srep02765.

Fosque, B. F., Sun, Y., Dana, H., Yang, C. T., Ohyama, T., Tadross, M. R., Patel, R.,

Zlatic, M., Kim, D. S., Ahrens, M. B., Jayaraman, V., Looger, L. L. and Schreiter, E. R. (2015) 'Neural circuits. Labeling of active neural circuits in vivo with designed calcium integrators', *Science*, 347(6223), pp. 755–760. doi: 10.1126/science.1260922.

Gershon, M. D. and Tack, J. A. N. (2007) 'The Serotonin Signaling System : From Basic Understanding To Drug Development for Functional GI Disorders', *Gastroenterology*, 132, pp. 397–414. doi: 10.1053/j.gastro.2006.11.002.

De Gregorio, E., Spellman, P. T., Tzou, P., Rubin, G. M. and Lemaître, B. (2002) 'The Toll and Imd pathways are the majors regulators of the immune response in Drosophila', *Embo Journal*, 21(11), pp. 2568–2579.

Harrison, D. A., Mccoon, P. E., Binari, R., Gilman, M. and Perrimon, N. (1998) 'Drosophila unpaired encodes a secreted protein that activates the JAK signaling pathway', *Genes and Development*, pp. 3252–3263.

Hart, B. L. (1988) 'Biological basis of the behavior of sick animals', *Neuroscience and Biobehavioral Reviews*, 12(2), pp. 123–137. doi: 10.1016/S0149-7634(88)80004-6.

Hedengren, M., Asling, B., Dushay, M. S., Ando, I., Ekengren, S., Wihlborg, M. and Hultmark, D. (1999) 'Relish, a central factor in the control of humoral but not cellular immunity in *Drosophila*.', *Molecular cell*, 4(5), pp. 827–37.

Hoffmann, J. A. and Reichhart, J.-M. (2002) 'Drosophila innate immunity: an evolutionary perspective', *Nature Immunology*, 3(2), pp. 121–126. doi: 10.1038/ni0202-121.

Hückesfeld, S., Peters, M. and Pankratz, M. J. (2016) 'Central relay of bitter taste to the protocerebrum by peptidergic interneurons in the Drosophila brain', *Nature Communications*, 7, p. 12796.

Huser, A., Rohwedder, A., Apostolopoulou, A. A., Widmann, A., Pfitzenmaier, J. E., Maiolo, E. M., Selcho, M., Pauls, D., von Essen, A., Gupta, T., Sprecher, S. G., Birman, S., Riemensperger, T., Stocker, R. F. and Thum, A. S. (2012) 'The Serotonergic Central Nervous System of the Drosophila Larva: Anatomy and Behavioral Function', *PLoS ONE*, 7(10). doi: 10.1371/journal.pone.0047518.

Jiang, H., Patel, P. H., Kohlmaier, A., Grenley, M. O., McEwen, D. G. and Edgar, B.

A. (2009) 'Cytokine/Jak/Stat Signaling Mediates Regeneration and Homeostasis in the Drosophila Midgut', *Cell*. Elsevier Ltd, 137(7), pp. 1343–1355. doi: 10.1016/j.cell.2009.05.014.

Kappler, C., Meister, M., Lagueux, M., Gateff, E., Hoffmann, J. A. and Reichhart, J. J. (1993) 'Insect immunity. Two 17 bp repeats nesting a xB-related sequence confer inducibility to the diptericin gene and bind a polypeptide in bacteria-challenged Drosophila', *The EMBO journal*, 12(4), pp. 1561–1568.

Kim, M., Qie, Y., Park, J. and Kim, C. H. (2016) 'Gut Microbial Metabolites Fuel Host Antibody Responses', *Cell Host Microbe*, 20(2), pp. 202–214. doi: 10.1016/j.chom.2016.07.001.Gut.

Kootte, R. S., Vrieze, A., Holleman, F., Zoetendal, E. G., Vos, W. M. De, Groen, A. K., Hoekstra, J. B. L., Stroes, E. S. and Nieuwdorp, M. (2012) 'The therapeutic potential of manipulating gut microbiota in obesity and type 2 diabetes mellitus', *Diabetes, Obesity and Metabolism*, 14, pp. 112–120. doi: 10.1111/j.1463-1326.2011.01483.x.

L. Weiss, A. Dahanukar, J. K. et al (2011) 'The Molecular and Cellular Basis of Bitter Taste in Drosophila', *Neuron*, 69(2), pp. 258–272. doi: 10.1016/j.neuron.2011.01.001.The.

Lanot, R., Zachary, D., Holder, F. and Meister, M. (2001) 'Postembryonic Hematopoiesis in Drosophila', *Developmental Biology*, 230(2), pp. 243–257. doi: 10.1006/dbio.2000.0123.

Lemaitre, B. (2015) 'Pseudomonas entomophila: A versatile bacterium with entomopathogenic properties', in *Pseudomonas: Volume 7: New Aspects of Pseudomonas Biology*. doi: 10.1007/978-94-017-9555-5_2.

Lemaitre, B. and Hoffmann, J. (2007) 'The Host Defense of Drosophila melanogaster', *Annual Review of Immunology*, 25, pp. 697–743. doi: 10.1146/annurev.immunol.25.022106.141615.

Lozupone, C., Stombaugh, J., Gordon, J. and Al, E. (2013) 'Diversity , stability and resilience of the human gut microbiota', 489(7415), pp. 220–230. doi: 10.1038/nature11550.Diversity.

Maurer, S., Wabnitz, G. H., Kahle, N. A., Stegmaier, S., Prior, B., Giese, T., Gaida, M. M., Samstag, Y. and Hänsch, G. M. (2015) 'Tasting Pseudomonas aeruginosa Biofilms: Human Neutrophils Express the Bitter Receptor T2R38 as Sensor for the Quorum Sensing Molecule N-(3-Oxododecanoyl)-l-Homoserine Lactone.', *Frontiers in immunology*, 6(July), p. 369. doi: 10.3389/fimmu.2015.00369.

Mayer, E. A. (2013) 'Gut feelings: the emerging biology of gut – brain communication', *Nat Rev Neuroscience*, 12(8). doi: 10.1038/nrn3071.Gut.

McCusker, R. H. and Kelley, K. W. (2013) 'Immune-neural connections: how the immune system's response to infectious agents influences behavior', *J Exp Biol*, 216(Pt 1), pp. 84–98. doi: 10.1242/jeb.073411.

Medzhitov, R., Schneider, D. S., Soares, M. P., Caldwell, R. M., Schafer, J. F., Compton, L. E., Patterson, F. L., Schafer, J., Råberg, L., Graham, A. L., Read, A. F., Råberg, L., Sim, D., Read, A. F., Read, A. F., Graham, A. L., Råberg, L., Schneider, D. S., Ayres, J. S., Kavaliers, M., Choleris, E., Agmo, A., Pfaff, D. W., Liberles, S. D., Rivière, S., Challet, L., Fluegge, D., Spehr, M., Rodriguez, I., Tizzano, M., Pradel, E., Zhang, Y., Lu, H., Bargmann, C. I., Cremer, S., Sixt, M., Kiesecker, J. M., Skelly, D. K., Beard, K. H., Preisser, E., Curtis, V., Barra, M. de, Aunger, R., Graham, A., Allen, J., Read, A., Casadevall, A., Pirofski, L. A., Ayres, J. S., Freitag, N., Schneider, D. S., Ayres, J. S., Schneider, D. S., Shinzawa, N., Richardson, C. E., Kooistra, T., Kim, D. H., Sun, J., Singh, V., Kajino-Sakamoto, R., Aballay, A., Ferreira, A., Balla, J., Jeney, V., Balla, G., Soares, M. P., Gozzelino, R., Jeney, V., Soares, M. P., Ferreira, A., Seixas, E., Pamplona, A., Larsen, R., Bente, D., Gren, J., Strong, J. E., Feldmann, H., Matzinger, P., Kamala, T., Balch, W. E., Morimoto, R. I., Dillin, A., Kelly, J. W., Kensler, T. W., Wakabayashi, N., Biswal, S., Walter, P., Ron, D., Foster, S. L., Hargreaves, D. C., Medzhitov, R., Durieux, J., Wolff, S., Dillin, A., Prahlad, V., Cornelius, T., Morimoto, R. I., Sapolsky, R. M., Romero, L. M., Munck, A. U., Pamplona, R., Costantini, D., Hart, B. L., Gromkowski, S. H., Yagi, J., Janeway, C. A., Ayres, J. S., Schneider, D. S., Playfair, J. H., Taverne, J., Bate, C. A., Souza, J. B. de, Schofield, L., Hewitt, M. C., Evans, K., Siomos, M. A., Seeberger, P. H., Peiris, J. S., Hui, K. P., Yen, H. L., Little, T. J., Shuker, D. M., Colegrave, N., Day, T., Graham, A. L., Tscherne, D. M., García-Sastre, A., Miller, M. R., White, A., Boots, M., Roy, B. A., Kirchner, J. W., Miller, R. A., Shaw, A. C., Joshi, S., Greenwood, H., Panda, A., Lord, J. M., Kurtz, C. C., Lindell, S. L., Mangino, M. J., Carey, H. V. and

Kenyon, C. J. (2012) 'Disease tolerance as a defense strategy.', *Science (New York, N.Y.)*, 335(6071), pp. 936–41. doi: 10.1126/science.1214935.

Melcher, C., Bader, R. and Pankratz, M. J. (2007) 'Amino acids, taste circuits, and feeding behavior in Drosophila: Towards understanding the psychology of feeding in flies and man', *Journal of Endocrinology*, 192(3), pp. 467–472. doi: 10.1677/JOE-06-0066.

Melcher, C. and Pankratz, M. J. (2005) 'Candidate gustatory interneurons modulating feeding behavior in the Drosophila brain', *PLoS Biology*, 3(9), pp. 1618–1629. doi: 10.1371/journal.pbio.0030305.

Meng, X., Wahlström, G., Immonen, T., Kolmer, M., Tirronen, M., Predel, R., Kalkkinen, N., Heino, T. I., Sariola, H. and Roos, C. (2002) 'The Drosophila hugin gene codes for myostimulatory and ecdysis-modifying neuropeptides', *Mechanisms of Development*, 117(1–2), pp. 5–13. doi: 10.1016/S0925-4773(02)00175-2.

Montell, C. (2009) 'A Taste of the Drosophila Gustatory Receptors', *Curr Opin Neurobiol*, 19(4), pp. 345–353. doi: 10.1016/j.conb.2009.07.001.A.

Nakazato, M., Hanada, R., Murakami, N., Date, Y., Mondal, M. S., Kojima, M., Yoshimatsu, H., Kangawa, K. and Matsukura, S. (2000) 'Central effects of neuromedin U in the regulation of energy homeostasis.', *Biochemical and biophysical research communications*, 277(1), pp. 191–194. doi: 10.1006/bbrc.2000.3669.

Nässel, D. R., Kubrak, O. I., Liu, Y., Luo, J. and Lushchak, O. V (2013) 'Factors that regulate insulin producing cells and their output in Drosophila', 4(September), pp. 1–12. doi: 10.3389/fphys.2013.00252.

Nässel, D. R. and Winther, Å. M. E. (2010) 'Drosophila neuropeptides in regulation of physiology and behavior', *Progress in Neurobiology*, 92(1), pp. 42–104. doi: 10.1016/j.pneurobio.2010.04.010.

Oldefest, M., Nowinski, J., Hung, C. W., Neelsen, D., Trad, A., Tholey, A., Grötzinger, J. and Lorenzen, I. (2013) 'Upd3 - An ancestor of the four-helix bundle cytokines', *Biochemical and Biophysical Research Communications*. Elsevier Inc., 436(1), pp. 66–72. doi: 10.1016/j.bbrc.2013.04.107.

Osman, D., Buchon, N., Chakrabarti, S., Huang, Y. T., Su, W. C., Poidevin, M., Tsai,

Y. C. and Lemaitre, B. (2012) 'Autocrine and paracrine unpaired signaling regulate intestinal stem cell maintenance and division', *J Cell Sci*, 125(Pt 24), pp. 5944–5949. doi: 10.1242/jcs.113100.

Park, J. and Kwon, J. Y. (2011) 'Heterogeneous Expression of Drosophila Gustatory Receptors in Enteroendocrine Cells', *PLoS ONE*, 6(12). doi: 10.1371/journal.pone.0029022.

Park, J., Lee, S. B., Lee, S. B., Kim, Y., Song, S., Kim, S., Bae, E., Kim, J. M., Shong, M. H., Kim, J. M. and Chung, J. K. (2006) 'Mitochondrial dysfunction in Drosophila PINK1 mutants is complemented by parkin', *Nature*, 441(7097), pp. 1157–1161. doi: 10.1038/nature04788.

Rajan, A. and Perrimon, N. (2012) 'Drosophila cytokine unpaired 2 regulates physiological homeostasis by remotely controlling insulin secretion', *Cell*, 151(1), pp. 123–137. doi: 10.1016/j.cell.2012.08.019.

Read, A. F., Graham, A. L. and Råberg, L. (2008) 'Animal Defenses against Infectious Agents : Is Damage Control More Important Than Pathogen Control ?', 6(12), pp. 2638–2641. doi: 10.1371/journal.pbio.1000004.

Ridley, E. V, Wong, A. C., Westmiller, S. and Douglas, A. E. (2012) 'Impact of the Resident Microbiota on the Nutritional Phenotype of Drosophila melanogaster', *PLoS ONE*, 7(5). doi: 10.1371/journal.pone.0036765.

Rubio-Godoy, M., Aunger, R. and Curtis, V. (2006) 'Serotonin - A link between disgust and immunity?', *Medical Hypotheses*, 68(1), pp. 61–66. doi: 10.1016/j.mehy.2006.06.036.

Schlegel, P., Texada, M. J., Miroschnikow, A., Schoofs, A., Peters, M., Schneider-mizell, C. M., Lacin, H., Hu, S., Li, F., Fetter, R. D., Truman, J. W., Cardona, A. and Pankratz, M. J. (2016) 'Synaptic transmission parallels neuromodulation in a central food-intake circuit', pp. 1–28. doi: 10.7554/eLife.16799.

Schoofs, A., Hückesfeld, S., Schlegel, P., Miroschnikow, A., Peters, M., Zeymer, M., Spieß, R., Chiang, A. S. and Pankratz, M. J. (2014) 'Selection of Motor Programs for Suppressing Food Intake and Inducing Locomotion in the Drosophila Brain', *PLoS Biology*, 12(6). doi: 10.1371/journal.pbio.1001893.

Schoofs, A., Hückesfeld, S., Surendran, S. and Pankratz, M. J. (2014) 'Serotonergic Pathways in the *Drosophila* Larval Enteric Nervous System', *Journal of Insect Physiology*. Elsevier Ltd, 69(June), pp. 118–125. doi: 10.1016/j.jinsphys.2014.05.022.

Shai, Y. (1999) 'Mechanism of the binding , insertion and destabilization of phospholipid bilayer membranes by K -helical antimicrobial and cell non-selective membrane-lytic peptides', *Biochimica et Biophysica Acta*, 1462.

Shakhar, K. and Shakhar, G. (2015) 'Why Do We Feel Sick When Infected- Can Altruism Play a Role?', *PLoS Biology*, 13(10), pp. 1–15. doi: 10.1371/journal.pbio.1002276.

Shanbhag, S. and Tripathi, S. (2009) 'Epithelial ultrastructure and cellular mechanisms of acid and base transport in the Drosophila midgut.', *The Journal of experimental biology*, 212(Pt 11), pp. 1731–1744. doi: 10.1242/jeb.029306.

Shreiner, A., Kao, J. and Young, V. (2015) 'The gut microbiome in health and in disease', *Curr Opin Gastroenteol*, 31(1), pp. 69–75.

Stensmyr, M. C., Dweck, H. K. M., Farhan, A., Ibba, I., Strutz, A., Mukunda, L., Linz, J., Grabe, V., Steck, K., Lavista-Llanos, S., Wicher, D., Sachse, S., Knaden, M., Becher, P. G., Seki, Y. and Hansson, B. S. (2012) 'A conserved dedicated olfactory circuit for detecting harmful microbes in drosophila', *Cell*. Elsevier Inc., 151(6), pp. 1345–1357. doi: 10.1016/j.cell.2012.09.046.

Sternberg, E. M. (2007) 'Neural regulation of innate immunity: a coordinated nonspecifichost response to pathogens', 6(4), pp. 318–328.

Surendran, S., Hückesfeld, S., Wäschle, B. and Pankratz, M. J. (2017) 'Pathogen-induced food evasion behavior in Drosophila larvae', pp. 1774–1780. doi: 10.1242/jeb.153395.

Tracey, K. J. (2009) 'Reflex control of immunity.', *Nature reviews. Immunology*, 9(6), pp. 418–428. doi: 10.1038/nri2566.

Tracey, K. J. (2010) 'Understanding immunity requires more than immunology.', *Nature immunology*, 11(7), pp. 561–4. doi: 10.1038/ni0710-561.

Veenstra, J. A. (2009) 'Peptidergic paracrine and endocrine cells in the midgut of the fruit fly maggot', *Cell and Tissue Research*, 336(2), pp. 309–323. doi: 10.1007/s00441-009-0769-y.

Vodovar, N., Vinals, M., Liehl, P., Basset, A., Degrouard, J., Spellman, P., Boccard, F. and Lemaitre, B. (2005) 'Drosophila host defense after oral infection by an entomopathogenic Pseudomonas species.', *Proceedings of the National Academy of Sciences of the United States of America*, 102(32), pp. 11414–9. doi: 10.1073/pnas.0502240102.

Wäschle, B. (2014) 'Central immunity and pathogen evasion behaviour of Drosophila larvae'.

Wikoff, W. R., Anfora, A. T., Liu, J., Schultz, P. G., Lesley, S. A., Peters, E. C. and Siuzdak, G. (2009) 'Metabolomics analysis reveals large effects of gut microflora on mammalian blood metabolites'.

Williams, E. K., Chang, R. B., Strochlic, D. E., Umans, B. D., Lowell, B. B., Liberles, S. D., Williams, E. K., Chang, R. B., Strochlic, D. E., Umans, B. D. and Lowell, B. B. (2016) 'Sensory Neurons that Detect Stretch and Nutrients in the Digestive System', *Cell*. Elsevier Inc., 166(1), pp. 209–221. doi: 10.1016/j.cell.2016.05.011.

Woting, A. and Blaut, M. (2016) 'The Intestinal Microbiota in Metabolic Disease', *Nutrients*, 8(202). doi: 10.3390/nu8040202.

Yano, J. M., Yu, K., Mazmanian, S. K., Hsiao, E. Y., Yano, J. M., Yu, K., Donaldson, G. P., Shastri, G. G., Ann, P., Ma, L., Nagler, C. R., Ismagilov, R. F., Mazmanian, S. K. and Hsiao, E. Y. (2015) 'Indigenous Bacteria from the Gut Microbiota Regulate Host Serotonin Biosynthesis', *Cell*. Elsevier Inc., 161, pp. 264–276. doi: 10.1016/j.cell.2015.02.047.

Zhang, X. and Zhang, Y. (2012) 'DBL-1 , a TGF- β , is essential for Caenorhabditis elegans aversive olfactory learning', 109(42), pp. 17081–17086. doi: 10.1073/pnas.1205982109.

Zhang, Y., Lu, H. and Bargmann, C. I. (2005) 'Pathogenic bacteria induce aversive olfactory learning in Caenorhabditis elegans', *Nature*, 438(7065), pp. 179–184. doi: 10.1038/nature04216.

Zhou, F., Rasmussen, A., Lee, S. and Agaisse, H. (2013) 'The UPD3 cytokine couples environmental challenge and intestinal stem cell division through modulation of JAK/STAT signaling in the stem cell microenvironment', *Developmental Biology*, 373(2), pp. 383–393. doi: 10.1016/j.ydbio.2012.10.023.